Sequential Modeling for Mortality Prediction in the ICU

by

Tejas G. Sundaresan

Submitted to the Department of Electrical Engineering and Computer Science
in partial fulfillment of the requirements for the degree of

Master of Engineering in Electrical Engineering and Computer Science

at the

MASSACHUSETTS INSTITUTE OF TECHNOLOGY

June 2017

Author .....
Department of Electrical Engineering and Computer Science
May 26, 2017

Certified by .....
Peter Szolovits
Professor of Computer Science
Thesis Supervisor

Accepted by .....
Christopher J. Terman
Chairman, Masters of Engineering Thesis Committee

Sequential Modeling for Mortality Prediction in the ICU

by

Tejas G. Sundaresan

Submitted to the Department of Electrical Engineering and Computer Science
on May 26, 2017, in partial fulfillment of the
requirements for the degree of
Master of Engineering in Electrical Engineering and Computer Science

Abstract

Severity of illness scores are commonly used in critical care medicine to guide treatment decisions and benchmark the quality of medical care. These scores operate in part by predicting patient mortality in the ICU using physiological variables including lab values, vital signs, and admission information. However, existing evidence suggests that current mortality predictors are less performant on patients who have an especially high risk of mortality in the ICU. This thesis seeks to reconcile this difference by developing a custom high risk mortality predictor for high risk patients in a process termed sequential modeling. Starting with a base set of features derived from the APACHE IV score, this thesis details the engineering of more complex features tailored to the high risk prediction task and development of a logistic regression model trained on the Philips eICU-CRD dataset. This high risk model is shown to be more performant than a baseline severity of illness score, APACHE IV, on the high risk subpopulation. Moreover, a combination of the baseline severity of illness score and the high risk model is shown to be better calibrated and more performant on patients of all risk types. Lastly, I show that this secondary customization approach has useful applications not only in the general population, but in specific patient subpopulations as well. This thesis thus offers a new perspective and strategy for mortality prediction in the ICU, and when taken in context with the increasing digitization of patient medical records, offers a more personalized predictive model in the ICU.

Thesis Supervisor: Peter Szolovits
Title: Professor of Computer Science

Acknowledgments

I would like to acknowledge the support and advice from many individuals that made this thesis possible.

I would first like to thank my research advisor, Prof. Peter Szolovits, for his continued support throughout my undergraduate and graduate studies at MIT. Prof. Szolovits has provided me countless points of advice and wisdom throughout my studies in medical informatics over the last couple of years and I am extremely grateful for all the times where he has taught me from his own extensive experiences in the field. I cannot thank him enough for inspiring me to find both a research and career interest within the intersection of healthcare and computer science.

I would also like to thank my collaborators on this research, Rodrigo Deliberato, Stephanie Ko, and Leo Anthony Celi from the MIT Lab for Computational Physiology. I've really enjoyed working with them and have learned a tremendous amount from them over the course of this research. This project would not have been possible without their insights and clinical intuition. Rodrigo and Stephanie also helped contribute written text and figures to the background and methods section of this thesis.

I would also like to thank other members of the MEDG group and the Lab for Computational Physiology at MIT for their time and support. It was a pleasure to work with them on this research and get to know them better over the course of working on this thesis.

I would like to thank my academic advisor, Prof. John Guttag, for his perspective and support throughout my undergraduate and graduate experience. I am extremely grateful for his advice on how to navigate the extensive academic opportunities at MIT.

Lastly, I would like to thank my family, including my mom, my dad, and my brother. I can't appreciate enough their unwavering support throughout my life and the impact they've had in helping me grow over the last 22 years.

Contents

List of Figures

List of Tables

Chapter 1

Introduction

The digitization of medical records over the last decade has enabled the development of more personalized and complex mortality models in the ICU. In this work, I seek to develop a multi-stage risk-based model for mortality prediction and validate it in a modern, multi-center ICU dataset.

1.1 Mortality Prediction in the ICU

The emergence of digital technologies to measure, transmit, store and analyze clinical information has enabled a renaissance in medical care. The modern hospital room is equipped with hundreds of sensors that rapidly measure changes in patient vital signs and send those values to an electronic health record (EHR); meanwhile, physicians and nurses meticulously document their clinical impression and recommendations for their patients, the results of lab tests they ordered via the EHR itself, and past medical history of the patient they learn via patient interviews. The hospital electronically measures overarching metrics about the patient stay and for billing purposes stores such key summary information in the EHR. Thus, these technologies have produced digital representations of episodes of patient care that provide a foundation of knowledge to learn from.

A data-driven approach to medical care has taken special root in critical care medicine. The Intensive Care Unit (ICU) is a complex, dynamic, and high-intensity medical environment: A 2011 study found that in a modern ICU, almost 250 ad hoc decisions, defined by the authors as "critical judgments...needed for a specific purpose at a precise moment", are made per day [1]. Often times, these decisions are extremely complex; observational interviews investigated how nurses administered sedatives in the ICU and found that nurses could identify almost 50 attributes and factors related to sedation administration [2].

Because ICU decisions are complex, multidimensional, and highly impactful, data-driven guidelines have been developed for physicians to follow in response to certain situations in the ICU. For example, in an England NHS-based study, a patient population treated with the "sepsis care bundle", a group of highly coordinated interventions spanning lab measurements, fluid introductions, physical treatment, and medication administration, showed a mortality rate more than half as low when compared to a population that did not receive the guideline [3]. Similar guidelines and protocols have been developed for a variety of tasks in the ICU, such as extubation [4], transfusion [5], cardiac arrest [6], and neurologic conditions [7].

At the basis of these protocols and guidelines, however, is an overall estimate of patient health upon arrival in the ICU. For a clinician, knowledge of whether a patient is critically ill could reshape or even disqualify a certain protocol entirely; in other words, such knowledge is essential for the numerous ad hoc decisions made in the ICU on a daily basis. Moreover, an assessment of the health state of a patient is critical in understanding the resources patients may require over their ICU stay and triaging care to certain patients over others. Ultimately, an intuition for patient health state is useful in evaluating medical care itself by examining whether the medical care improved the overall health state of the patient.

A patient's likelihood of mortality captures the notion of patient health state well; patients who are likelier to pass away in the ICU require more immediate attention from physicians and more medical resources. Moreover, mortality likelihood in the ICU can inform the ad hoc decision making by ICU healthcare professionals: patients who have a high risk of death would likely not be treated well with a protocol that does not address their core medical issue immediately. To this end, severity of illness scores such as APACHE IV (Acute Physiology and Chronic Health Evaluation) [8] and SAPS II (Simplified Acute Physiology Score) [9] have historically met the clinical need for an estimate of patient mortality risk early on after admission into the ICU. Both scores use readily available clinical information such as lab test values, vital signs, admitting diagnoses, and comorbidities to forecast the mortality risk of patients via logistic regression.

In this thesis, I seek to develop mortality models that take further advantage of the digitization of medical records and a risk-based approach to modeling. Building off the core features identified in APACHE, I hand-engineer features that leverage the high-resolution, temporal data obtained from in-hospital sensors and EHR systems that are especially useful for predicting mortality in patients who are at especially

high risk for mortality. Moreover, I will combine these mortality prediction techniques used for the high risk population with the canonical APACHE approach to develop a "sequential" multi-stage mortality technique. Lastly, I will then evaluate this "sequential" approach to mortality prediction on the mortality prediction tasks in the general population and specific population cohorts.

1.2 Thesis Overview

My thesis is organized as follows:

- Chapter 2 provides background information on severity of illness scores, examines in detail the APACHE score, and explains the sequential modeling approach.
- Chapter 3 discusses the Philips eICU-CRD dataset analyzed in this thesis and the data processing steps required to develop the mortality prediction algorithms.
- Chapter 4 details the development of a high-risk mortality predictor.
- Chapter 5 assesses the calibration and performance of the sequential modeling approach on the general patient population.
- Chapter 6 examines the performance of the sequential modeling approach on specific patient cohorts.
- Chapter 7 discusses my thesis in the context of the field of risk prediction in the ICU and motivates future directions for this research.

Chapter 2

Background

In this section, I will discuss severity of illness scores involved in mortality prediction, identify the criteria upon which such scores are evaluated, and then provide a hypothesis that a risk-based "sequential" approach to mortality prediction could meet such criteria well.

2.1 Severity of Illness Scores

Severity of illness (SOI) scores seek to numerically quantify how sick a patient is and often do so by estimating the probability of death for a presenting patient.

While there are several types of SOI scores, most scores consist of a numerical value representing a transformation of certain patient attributes to a score, which is then fitted with a logistic regression towards a classification task, such as mortality prediction [10]. A key attribute of a severity of illness score is the data it uses to compute the numerical score itself. Most SOI scores derive their predictions based on the data recorded in the first 24 hours of a patient stay. Afterwards, models are usually developed on a training data set of patients, complete with all attributes used in the model, and then are assessed on two metrics: discrimination and calibration. Discrimination represents the ability of a model to correctly identify patients who will die from those who won't, and is commonly measured by metrics for binary classification, such as AUC (area under the receiver operating characteristic curve). A model must also be well calibrated: the mortality probabilities it returns should be reasonably consistent with the underlying mortality probability distribution [10]. For example, in a well-calibrated model, we would expect 50% of the patients who have a predicted mortality probability around 50% to die in the ICU. A common method of assessing calibration is the Hosmer-Lemeshow test [11], which runs a chi-squared based calculation to test whether the model matches the results expected from perfect calibration.

Name	Data Used for Prediction
APACHE (Acute physiologic and chronic health evaluation)	First 24 hours after admission. 12 physiologic variables, combined with diagnosis, demographic, comorbidities, and ICU type.
SAPS (Simplified Acute Physiology Score)	First 24 hours after admission. 12 physiologic variables, age, admission type, acute diagnosis.
SOFA (Sequential Organ Failure Assessment Score)	First 24 hours after admission. Severity of illness based on organ dysfunction in six organ systems.
MPM (Mortality Probability Models)	First 24, 48, 72 hours after admission. Chronic conditions, vital signs, acute diagnosis, device variables (ventilation).

Table 2.1: Overview of Severity of Illness Scores [10]

Table 2.1 provides an overview of well-known severity of illness scores. Section 2.2 provides a detailed overview of one such score, APACHE IV [8].

2.2 The APACHE IV Severity of Illness Score

APACHE IV [8] is the 4th iteration of the Acute Physiology and Chronic Health Evaluation score and was developed in 2006 as a recalibration and improvement upon the APACHE III score model. Using data from about 131,000 ICU admissions sourced from 104 ICUs in 45 U.S. hospitals, the authors developed a mortality model with strong discriminative and calibrated performance. The model had an AUC of 0.88 for the prediction of hospital mortality on the validation population and had a Hosmer-Lemeshow p-value of 0.08 (where $p > 0.05$ indicates good calibration). In this section, we will go into detail regarding how the APACHE IV model was constructed and evaluated by Zimmerman, et al.

The study used admissions data from 131,000 ICU admissions collected from 2002 and 2003, of which 110,000 were analyzed because they did not meet the following exclusion criteria: admissions with patients who were less than 16 years of age, admissions that last less than 4 hours or more than 365 days, and admissions that were preceded by another ICU stay in the same hospitalization. Secondly, stays that did not include enough information to calculate the APS score, which is detailed next, were also excluded from the study.

For each patient, the authors calculated an integer "acute physiology score" from 0-252 from the following physiological measurements during the first 24 hours of the

admission: *pulse rate, mean blood pressure, temperature, respiratory rate, PaO2/FIO2 ratio, hematocrit, white blood cell count, creatinine, urine output, blood urea nitrogen, sodium, albumin, bilirubin, glucose, acid base abnormalities, and neurological abnormalities based on Glasgow Coma Score.* Each of these values is assigned a score value based on the most "abnormal" value for each category. For example, if the patient's heart rate is measured at 60 and 120 at different points within the first 24 hours, the value of 120 will be recorded as it deviates the most from the APACHE heart rate midpoint of 75 [13]. A heart rate of 120 adds 7 points to the APS Score [14] and the sum of these score values forms the APS score.

In addition, the APACHE IV score incorporates demographic, past history, and patient stay-related information. For example, it includes a splined age term, chronic health variables (AIDS, cirrhosis, hepatic failure, immunosuppression, lymphoma, leukemia or myeloma, metastatic tumor), length of stay before ICU admission, whether the patient is undergoing emergency surgery, whether the patient is receiving mechanical ventilation, a rescaled version of the Glasgow Coma Scale, and the admission source that preceded the ICU (such as floor, emergency room, other hospital, etc.). Lastly, the APACHE IV score considers the admitting diagnosis for each patient. The authors ascribed one of 430 diseases, injuries, and surgical procedures for each patient admission as the APACHE diagnosis code.

Using these variables as features for a multivariate logistic regression model, the authors demonstrated that the APACHE IV model was well-calibrated (Figure 2) and performed well on the mortality prediction task (AUC=0.88). The calibration curve in Figure 2-1 demonstrates that for all risk deciles, APACHE's predicted mortality rates are concordant with the validation set.

2.3 Limitations of Current Severity of Illness Scores

Severity of illness scores, however, are limited by the skewed nature of the datasets they are trained on. Up to half of intensive care patients in cohorts used to derive such scores are predicted to have a low risk of death (mortality risk $<10\%$) [8, 16-18]. This distribution is visible in Figure 2-1 in the validation set used to evaluate the APACHE IV model.

The over-presence of low risk individuals in the training set used to develop mortality models could result in poorer model calibration. While this miscalibration was not found in the APACHE IV paper, other studies of similar mortality models

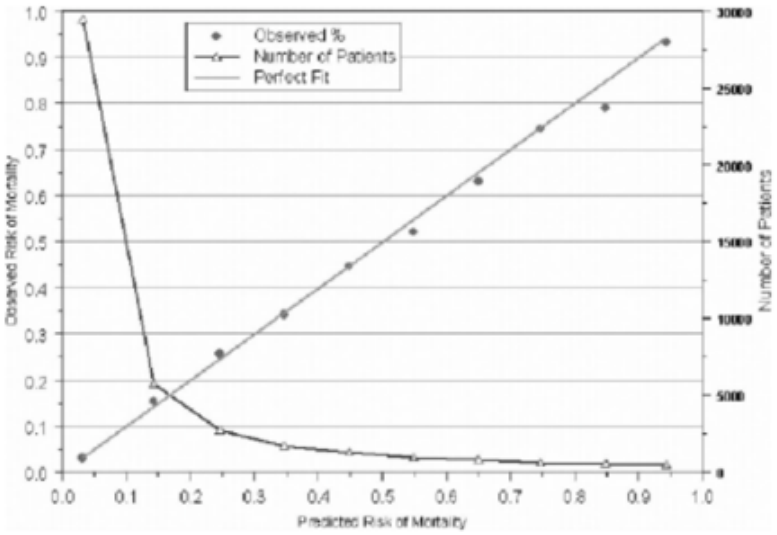

Figure 2-1: Calibration Curve of APACHE IV Classifier on Validation dataset. Image replicated from [8].

(models that rely on a similar feature set as that of APACHE IV), have shown impaired goodness-of-fit. In a cohort from the United Kingdom, the mortality ratios (observed:expected) of the low risk group are nearly twice as high compared to the higher risk group, as predicted by APACHE II and SAPS II [17]. Likewise, the MPM model was found to have a mortality ratio of 3.00 in the low risk population compared to 0.92 in the high risk population [18].

The difference in calibrations between low risk and high risk patients suggest that general mortality models might miss cohort-specific information useful in the mortality prediction task [17]. High risk patients are inherently physiologically different from low risk patients and might be modeled more accurately with a set of features that differ from those of SAPS and APACHE IV; for example, lactate levels are closely monitored in septic patients [19], an extremely high-risk condition, but are not globally diagnostic for most patients in the ICU.

Moreover, scores such as APACHE and SAPS utilize simple features that are less dependent on the hospital information systems, but the APACHE IV authors themselves postulated that future prognostic models would likely be more complex and tied more closely to the hospital information technology infrastructure [8]. Because current EHR systems can now process and store periodic measurements from hospital room sensors and record the results of lab tests during a patient stay in real-time, such data streams enable more complex mortality prediction models that can utilize the temporal trends and aggregate statistics in data in a manner especially relevant

for high risk patients, who are likely to be monitored the most during their stay. For example, whereas APACHE IV tracks heartrate as an APS variable, a more complex mortality model, as done in [44], could track trends in heart rate over time to, for example, detect compensation or decompensation episodes in severe sepsis.

Thus, this thesis is motivated by evidence that suggests that existing mortality models can be augmented by focusing specifically on developing additional features targeted at predicting mortality in high risk populations. To this end, this thesis centers on evaluating a sequential approach to risk prediction by developing a new risk prediction model only on the high risk subgroup of a large ICU cohort that uses these features.

2.4 Sequential Modeling: a multi-stage model of mortality

The bulk of this thesis evaluates the sequential modeling approach: the idea that mortality prediction could be thought of as a two-stage sequence (Figure 2-2).

1. First: use a canonical mortality predictor such as APACHE IV to predict patient mortality probability
2. Second: For patients deemed "high risk", then forecast their mortality using a custom high risk classifier using custom engineered features

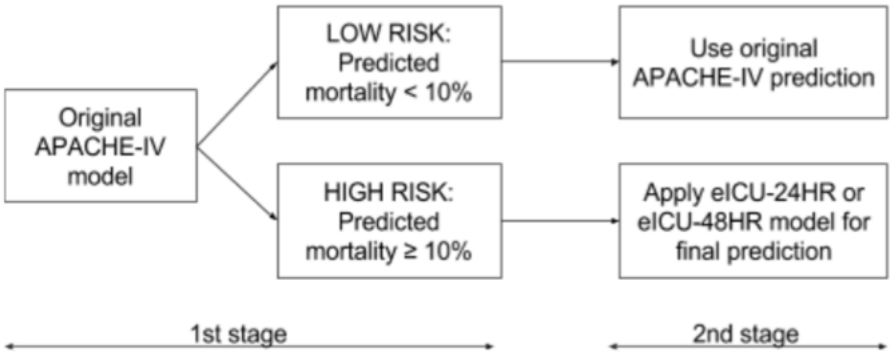

Figure 2-2: The Sequential Modeling Approach. Low Risk patients utilize the APACHE model, while High-Risk patients utilize a risk-specific mortality model. eICU-24HR and eICU-48HR refer to custom high risk models to be developed in this thesis.

A potential use case of this approach is as follows: a patient arrives in the ICU with an indication for sepsis and an APACHE probability of mortality of 35%. Such a pa-

tient is then evaluated with the custom eICU-24HR classifier, which includes features such as heart rate trend detection, where the patient is found to be in decompensated shock (indicated by blood pressure trends). The custom classifier provides a mortality risk estimate of 85%, greatly impacting the expected treatment plan formulated by the physician.

This sequential approach has the potential to provide an improvement upon both the discrimination and calibration of existing mortality models. The addition of high-risk specific features in the custom high risk model would better model conditions such as sepsis and cardiac arrest, and therefore obtain better predictive performance on the patient subpopulations that possess those admitting diagnosis. Moreover, existing APACHE features weights would be re-calibrated for the high risk patients in the custom high risk classifier. For example, in high risk patients, the GCS score could be especially diagnostic as high risk patients are likely to have low GCS scores. The high risk classifier would be able to learn a larger weight for the GCS score itself. Superior performance on high risk patients would further enhance the calibration of the model, fine-tuning risk probability predictions with a high risk subpopulation that is underrepresented in the development of canonical mortality prediction tools.

Further details regarding how the sequential model is evaluated can be found in Section 3.6, the results of which can be found in Chapter 5.

Chapter 3

Methods and Data Overview

The mortality models developed in this thesis were trained and validated on the Philips eICU Collaborative Research Dataset (eICU-CRD). This chapter discusses the data processing and modeling required to develop such models. I first provide background information and analysis on the eICU-CRD dataset, formalize the concepts of "high risk" and "low risk" patients within the study, and discuss the exclusion criteria used to identify the training and validation populations. Afterwards, I discuss how APACHE-specific features were processed and how custom high-risk features were constructed from the dataset. Lastly, I describe and motivate each of the logistic regression models trained as part of the study.

3.1 Philips eICU-CRD Data Overview

3.1.1 Background

The Philips eICU Collaborative Research Dataset [21] was released in 2017 by a joint collaboration between MIT and Philips Healthcare. It contains data on over 200,000 ICU stays collected over the last 10 years from over 250 hospitals via the Philips eICU platform [22].

The Philips eICU platform is a telehealth program for the intensive care unit that aims to achieve more efficient and effective ICU care in the US. It features an off-site 24/7 electronic monitoring system of an ICU overseen by medical professionals that enable clinics to provide more continuous care to patients in the ICU. Moreover, it couples this technology offering with several decision support and alerting features, such as a "sepsis alert", helping subscribing clinics offer higher quality medical care. The eICU program has been shown historically to result in an increased chance of survival in the ICU and a shorter length of stay [23].

Concept	Table Name in eICU-CRD	Description
Demographics	patient	Per-patient information
Lab Values	lab	Lab values for patients
Medications	medication	Prescribed medications for patients
Vital Signs	vitalsperiodic	Periodic vitals: vital signs that are measured regularly in an automated process (every 15 minutes usually)
Vital Signs	vitalsaperiodic	Aperiodic vitals: vital signs that are measured, usually with
Diagnoses	pasthistory	List of past medical history in a structured format.
Devices	respiratorycharting	Mechanical ventilation settings
Interventions	treatment	Treatment steps for patients, including transfusions
Fluid	intakeoutput	Tracks fluid inputs and output events for patients. Used to calculate the fluid balance for a patient.
APACHE score	apacheapsvar	Lists the variables used in the calculation of the APS score in APACHE
APACHE score	apachepredvar	Lists the variables used in the calculation of the APACHE score that are not APS variables
APACHE score	apachepatientresults	Provides the APACHE risk probabilities for patients from APACHE API

Table 3.1: Key tables used in the eICU-CRD Dataset [10]

To enable the tele-ICU concept, the Philips eICU program stores high-dimensional and feature-rich data about patients. Every patient admission in the ICU is identified by a "patientunitstayid", which links to various tables containing information labs, vital signs, medication prescriptions, and previous diagnoses. Table 3.1 summarizes key tables used in this analysis.

Sections 3.4 and 3.5 will discuss each of these tables in further detail with respect to how features were extracted from each table for mortality modeling.

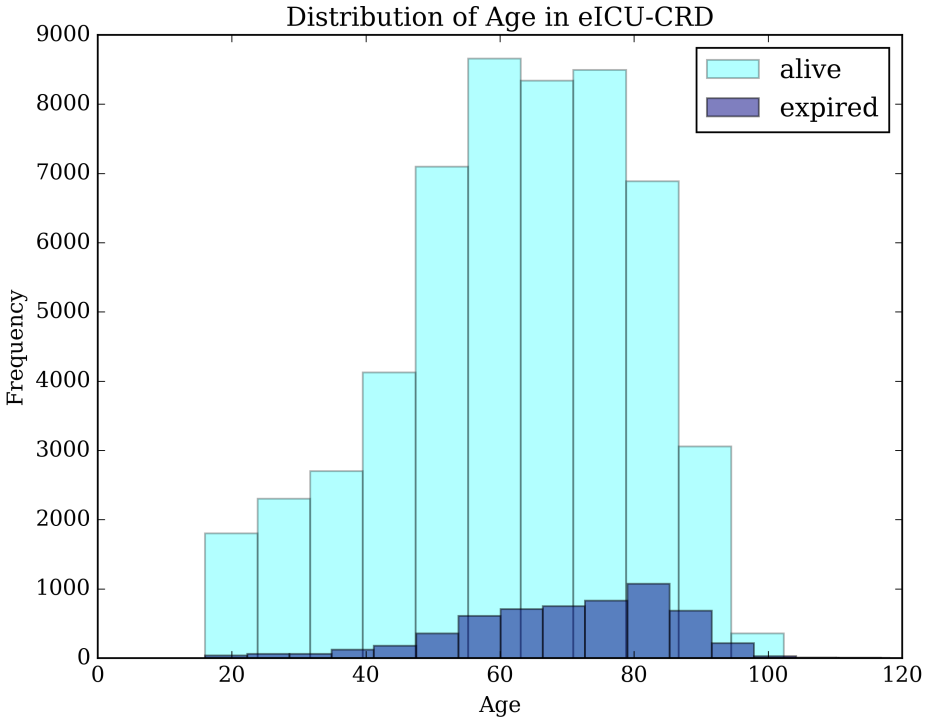

Figure 3-1: Distributions of Ages in Study Population, labeled by whether the patient survived the hospital stay ("alive") or did not ("expired").

3.1.2 Exploratory Analysis

The eICU-CRD dataset contained APACHE values for 63,000 patients of which 60,000 contained APACHE IV probability estimates. For these 60,000 patients, the global mortality rate was 9.6% and the average APACHE IV in hospital probability estimate was 12.4%. the APACHE IV probability estimates were sourced from the *predictedhospitalmortality* field supplied by and precomputed in the dataset by the APACHE API. The average age of all patients was 62.6 years, and there were 32,000 male patients and 27,000 female patients in the dataset. About 13,000 patients underwent mechanical ventilation.

Figure 3-1 shows the age distribution of patients in the dataset. We can notice that no patients below 16 years of age receive an APACHE IV score, consistent with clinical guidelines and indications for the score's use. The plots in this thesis were generated via matplotlib [24] and Google Sheets [25].

Patients in the dataset were ascribed 411 different APACHE diagnoses globally. Table 3.2 summarizes the top-10 most common diagnoses, along with their mortality

Diagnosis Name	Count	Predicted APACHE Mortality Rate	Actual Mortality Rate
AMI	3316	6.70%	4.50%
CVASTROKE	2265	18.90%	13.00%
S-CABG	2028	4.60%	1.20%
SEPSISPULM	1792	23.30%	22.40%
CHF	1615	13.10%	12.60%
RHYTHATR	1387	8.90%	6.00%
CARDARREST	1317	60.10%	53.50%
PNEUMBACT	1256	19.50%	17.00%
SEPSISUTI	1184	15.20%	14.60%
UNSTANGINA	1182	2.50%	3.00%

Table 3.2: Top 10 Most Common APACHE IV Diagnoses in eICU-CRD

rates and average predicted mortality probability sourced from APACHE.

Figure 3-2 depicts the distribution of APACHE in-hospital mortality probability estimates across the entire dataset. From this graph, we can see that our patient population is highly skewed towards low risk patients who receive a low probability estimate from the APACHE score. Figure 3-3 demonstrates the calibration of the dataset's APACHE hospital mortality predictions.

Table 3.2 and Figure 3-3 demonstrate that APACHE IV is not well-calibrated in the eICU-CRD dataset. For most conditions in Table 3.2, APACHE IV overestimates the mortality risk of patients. This trend is also seen in the calibration curve, which is positioned below that of a curve of perfect calibration. This indicates that APACHE's predicted mortality probabilities are larger than those observed in the dataset. Moreover, this difference is especially pronounced in patients who have larger APACHE risk estimate, an attribute of the calibration curve that is consistent with our earlier hypotheses that mortality models tend to be calibrated well to either the low risk or high risk populations, but not both (Section 2.3). At the same time, it is important to note that there are potential confounders that could also result in the overprediction of mortality. Advances in medical practices and technologies to treat especially high risk conditions, such as cardiac arrest and sepsis, made since 2006 could reduce the overall mortality of these conditions; the effect of these novel medical treatments would not be incorporated into the APACHE IV model's weights. Secondly, the eICU platform itself has been shown to improve mortality outcomes; the miscalibration seen above could be a visual representation of this effect.

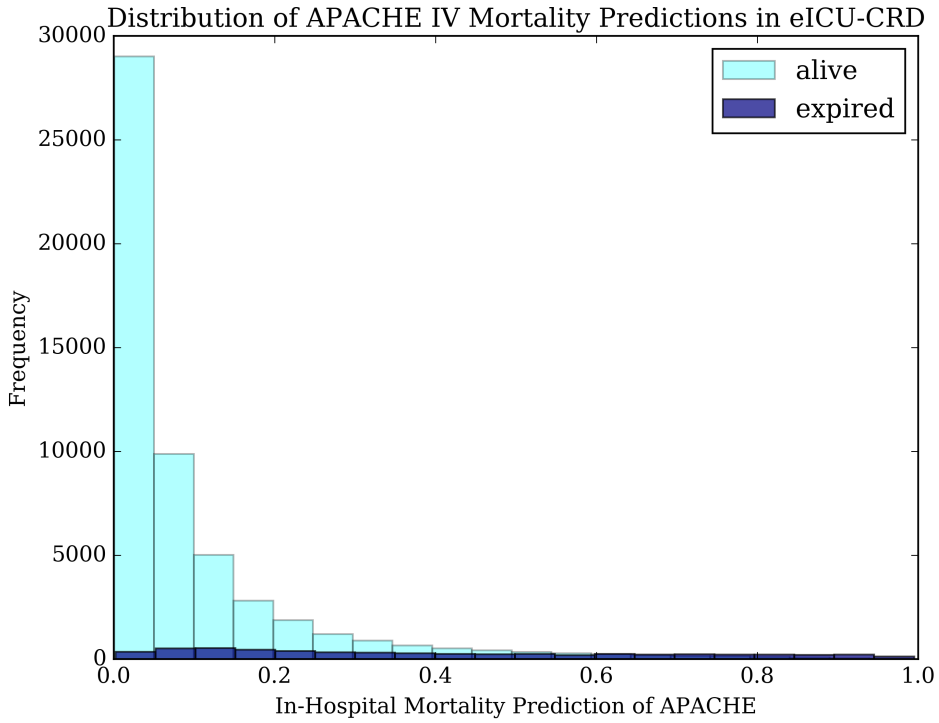

Figure 3-2: Distribution of APACHE probability estimates across the entire dataset, labeled by whether the patient survived the hospital stay ("alive") or did not ("expired").

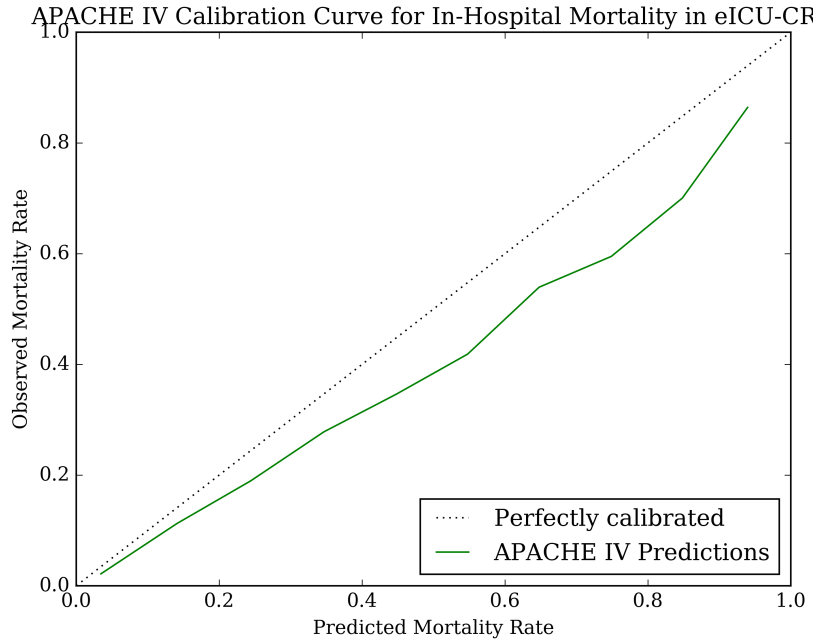

Figure 3-3: APACHE IV Calibration Curve in the eICU-CRD dataset

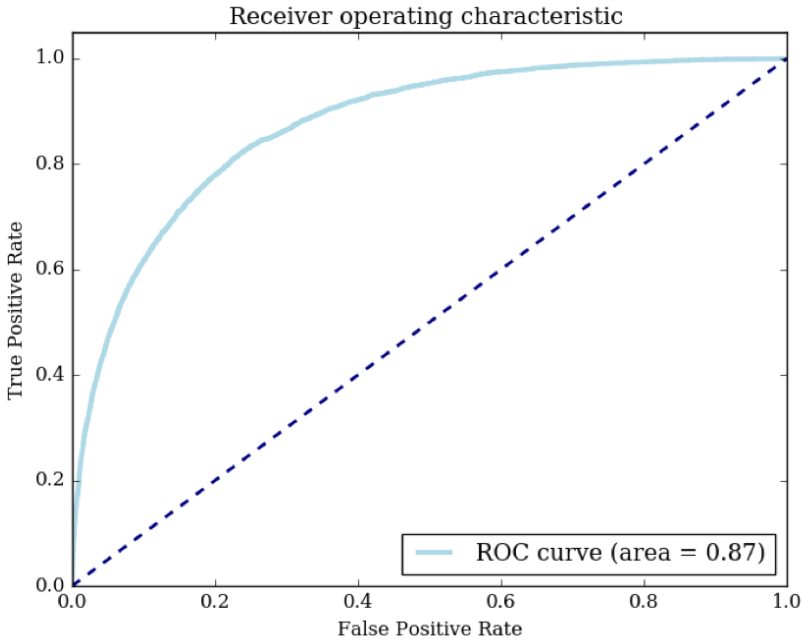

Figure 3-4: APACHE IV ROC Curve in the eICU-CRD dataset for the entire patient population

APACHE IV demonstrates robust global discrimination in eICU-CRD for the task of mortality prediction with an AUC of 0.87, consistent with the APACHE IV paper result of 0.88. The receiver operating characteristic curve is shown in Figure 3-4. However, the discriminative ability of APACHE IV is worse when considering high risk patient populations. For example, APACHE IV has an AUC of 0.66 on the 3600 patients in eICU-CRD who have an APACHE IV predicted mortality risk of greater than 50%. On the comparable low-risk population (patients with a predicted mortality risk of less than 50%), the model performs much better with an AUC of 0.83. The ROC curves for both values are detailed in Figures 3-5 and 3-6.

In summary, initial exploration of the eICU-CRD dataset suggests that the APACHE IV risk prediction model is less calibrated and less discriminative in the high risk patient subpopulation. At the same time, APACHE is globally discriminative and better calibrated on the low risk population, and this difference can be reconciled by the fact that the eICU-CRD patient population is skewed towards lower risk predictions by APACHE; while the performance on the high risk population is poor, the notably smaller number of high risk cases results in a minimal impact on global AUC. These results further motivate the sequential modeling approach, which I hypothesize can improve upon the 0.66 AUC found in the high risk cohort and obtain better discrimination and calibration in the process.

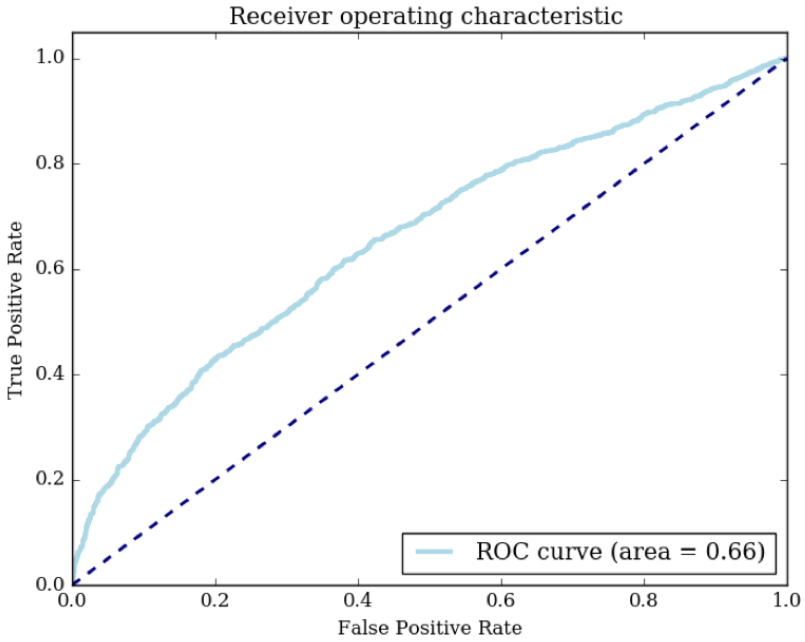

Figure 3-5: APACHE IV ROC Curve in the eICU-CRD dataset for high risk patients (APACHE probability $>$ 50%).

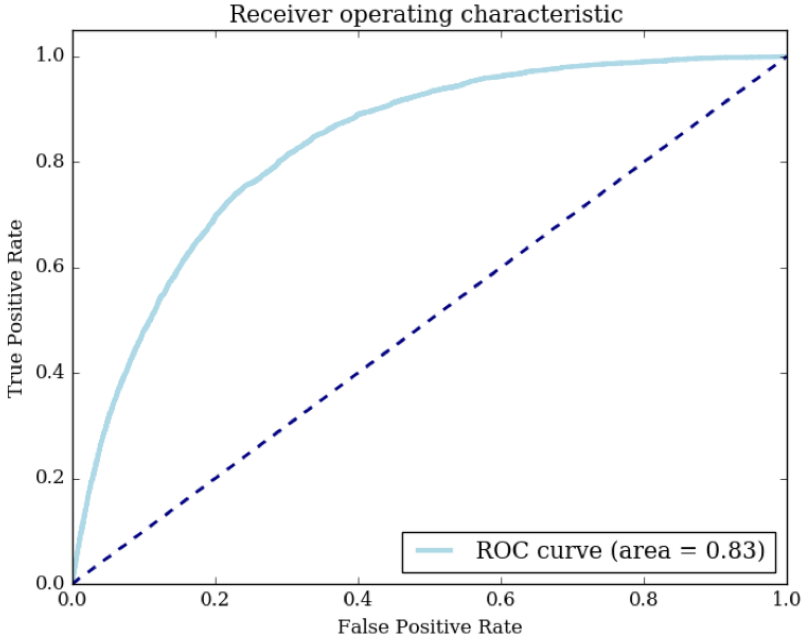

Figure 3-6: APACHE IV ROC Curve in the eICU-CRD dataset for low risk patients (APACHE probability $<$ 50%).

3.2 Patient Inclusion Criteria

To allow the analysis in thesis to closely resemble that of APACHE IV, I structured the exclusion criteria of the study to be concordant with that of APACHE IV. APACHE IV's exclusion criteria were as follows [8]:

1. Patients who are less than 16 years of age
2. Patient in the ICU as a result of burn injuries
3. Patients missing an APS score on day 1
4. Patients admitted after transplant operations except for hepatic and renal transplants
5. Multiple admissions from the same patient during a hospital stay
6. Patients admitted from another ICU during the same hospitalization
7. Patients with a length of stay >365 days.

Table 3.3 summarizes the impact of these exclusion criteria on our study population. It also discusses how each exclusion criterion was calculated in eICU. In the case where multiple exclusion criteria were met for a patient, we ascribed the exclusion criteria to a single criterion that matched the patient. In most cases, the exclusion criteria had been applied prior to the collection of APACHE data in the eICU, and therefore did not affect the study population as much as expected. For example, because the APACHE IV score is not indicated for patients under 16 years of age, we had close to zero patients less than 16 years old in the study population. Likewise, a missing APS score would result in a missing mortality prediction, patients with which were excluded in the beginning of the analysis. The resultant study population size was 59,574 patients.

Exclusion Criteria	Number of Patients Matched	How Computed in eICU
Missing APS	2155	acutephysiologyscore missing in apachepatientresults table
Age	69	age in patient table
Burn	17	Patient apacheadmissiondx contains ?burn?
LOS >365 days	4	Patient ICU hospitaldischargeoffset >365 days
LOS <4 hours	4	Patient ICU unitdischargeoffset <4 hours
Admitted after transplant	13	Patient apacheadmissiondx contains ?transplant?
Admitted from other ICU	0	Patient demographic table

Table 3.3: Exclusion Criteria in eICU-CRD used for study

3.3 Risk Stratification and Mortality Type Selection

A key question in this study is the definition of "high risk", or in other words, a risk threshold upon which we designate patients to use the custom high risk classifier in the sequential modeling approach. For example, the analysis in section 3.1 identified that at a risk threshold of 0.50 (50% mortality risk or higher), the APACHE IV score has an AUC of 0.66 on the high risk patients, patients with a predicted mortality of greater than the threshold of 0.50. However, one could imagine replicating the analysis at a variety of thresholds to obtain the following table and graph of AUC vs risk threshold, starting at a risk threshold set to the average mortality of the dataset (about 10%).

There are three main factors that affect the risk threshold selection:

1. Choosing a risk threshold that is too small would reduce the ability of a custom high-risk model to fit the underlying physiology of the high risk subpopulation well. When taken to the extreme for example, a very low risk threshold would face similar challenges to that of global severity of illness scores in calibration.

2. Choosing a risk threshold that is too high could result in a more difficult prediction task with less training data: For example, only 368 of the 60,000 patients

Risk Threshold	AUC for APACHE IV Predictions for Patients Above Risk Threshold
0.1	0.75
0.2	0.72
0.3	0.69
0.4	0.67
0.5	0.66
0.6	0.64
0.7	0.64
0.8	0.64
0.9	0.58

Table 3.4: AUC vs. Risk Threshold in the eICU-CRD Data

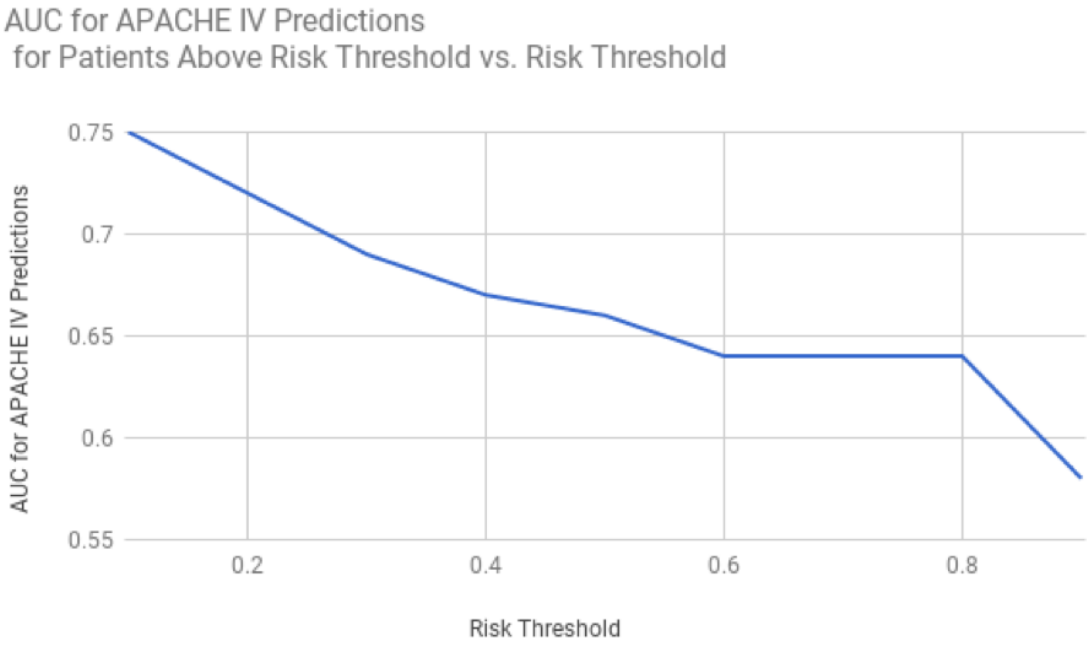

Figure 3-7: AUC vs. Risk Threshold in the eICU-CRD Data

in the study population have a predicted mortality probability of 0.9 or higher. It would be very difficult to learn a model from such few data points with the very high dimensional feature sets found in EHRs.

3. Choosing a risk threshold that is too high can impact the overall benefit the model provides in application and global AUC metrics. An improved classifier for only patients with a predicted mortality of greater than 90% would only improve performance on less than 0.5% of patients. The sequential model would in large part serve predictions similar to those of APACHE IV as this difference is minimal.

In this thesis, I will treat the risk threshold as an independent variable within a bounded range of 0.10-0.75. That is, I will experiment with different thresholds between 10% and 75% mortality risk in the evaluation of the custom high risk model and the sequential model to identify the threshold that provides the optimal balance of the three factors discussed above.

3.4 APACHE Feature Engineering

In addition to obtaining the APACHE IV prediction probabilities from the *apachepatientresults* table, we extracted the APACHE IV variables from the eICU dataset for not only the custom high risk classifier, but also several control classifiers discussed in Section 3.6.

3.4.1 APS Variables

The APACHE IV APS variables were sourced from the *apacheapsvar* table. The eICU-CRD dataset stores each APS variable in its raw format (i.e heartrate as 92), and therefore, to replicate the value assignment to each value made by APACHE, I converted each raw value to its APS value using the logic from an APACHE IV calculator [15]. Missing APS values were assumed to be normal and therefore received an APS value of 0.

The intuition behind each conversion is two-fold:

1. The APS value should capture meaningful deviations from normal for a certain lab test or physiological measurement. Deviating slightly from normal should not receive a positive APS value as such deviations are likely due to person-by-person variation in the vital sign rather than a clinical abnormality.

2. The APS value should capture bi-directional abnormality. In the ICU, an elevated or reduced heartrate are both indicative of physiological abnormality, and thus should both have a positive APS value. A linear transformation of the raw vital sign would not provide a positive APS value in both cases.

Table 3.5 summarizes the conversion logic used for each APS variable, which closely follows the APACHE guidelines.

APS Variable	Conversion Logic
Pulse (bpm)	<39: 8 40-49: 5 50-99: 0 100-109: 1 110-119: 5 120-139: 7 140-154: 13 155+: 17
MABP - mean arterial blood pressure (mmHg)	<39: 23 40-59: 15 60-69: 7 70-79: 6 80-99: 0 100-119: 4 120-129: 7 130-139: 9 140+: 10
Temperature (C)	<33: 30 33-33.4: 16 33.4-33.9: 14 34.0-34.9: 8 35.0-35.9: 2 36-39.9: 0 40+: 2
Respiratory Rate (rpm)	<6: 17 6-11: 8 12-13: 7 14-24: 0 25-34: 0 35-39: 9 40-49: 11 50+: 18
PaO2 (%)	<50: 14 50-70: 5 70-79: 2 80+: 0
Hematocrit (%)	<41: 3 41-49: 0 49+: 3
WBC count (count/nL)	<1.0: 19 1.0-2.9: 5 3.0-19.9: 0 20.0- 24.9: 1 25.0+: 5
Creatinine (mg/dL)	<1.4: 0 >1.4: 10
Urine Output (mL)	<400: 15 400-600: 8 600-899: 7 900-1499: 5 1500-1999: 4 2000-3999: 0 4000+: 1
Blood urea nitrogen (mg/dL)	<17: 0 17-19: 2 20-39: 7 40-79: 11 80+: 12
Sodium (mEq/L)	<120: 3 120-134: 2 135-154: 0 155+: 4
Albumin (g/dL)	<2.0: 11 2.0-2.4: 6 2.5-4.4: 0 4.5+: 4
Bilirubin (mg/dL)	<2.0: 0 2.0-2.9: 5 3.0-4.9: 6 5.0-7.9: 9 8.0+: 16
Glucose (mg/dL)	<40: 8 40-59: 9 60-199: 0 200-349: 3 350+: 4
Acid Base (pH, pCO2)	See below
Glasgow Coma Scale	See below

Table 3.5: APACHE APS Variable Conversion Logic

The Acid Base and GCS conversions to APS scores required slightly more involved calculations, summarized in Python code below.

```
def acid_base_aps(pco2, ph):
      if ph < 7.2 and pco2 < 50:
            return 12
      else:
            return 4
      if ph < 7.35 and pco2 < 30:
            return 9
      if ph < 7.3 and pco2 < 40:
            return 6
      if ph < 7.3 and pco2 < 50:
            return 3
      if ph < 7.3:
            return 2
      if ph < 7.50 and pco2 < 30:
            return 5
      if ph < 7.50 and ph >= 7.45 and pco2 >= 30 and pco2 < 35:
            return 0
      if ph < 7.45 and ph >= 7.30 and pco2 >= 30 and pco2 < 45:
            return 0
      if ph < 7.45 and ph >= 7.30 and pco2 >= 45:
            return 1
      if ph < 7.50 and ph >= 7.45 and pco2 >= 35 and pco2 < 45:
            return 2
      if ph < 7.50 and ph >= 7.45 and pco2 >= 45:
            return 12
      if ph >= 7.50 and pco2 >= 40:
            return 12
      if ph >= 7.60 and pco2 <= 25:
            return 0
      if ph >= 7.50 and pco2 <= 25:
            return 3
      if ph >= 7.50 and pco2 >= 25:
            return 3
      return 0
```

Figure 3-8: Acid Base Conversion Logic

```
def gcs_aps(eyes, motor, verbal):
      if eyes == 1:
            if verbal == 1:
                  if motor == 5 or motor == 6:
                        return 16
                  elif motor == 4 or motor == 3:
                        return 33
                  else:
                        return 48
            else:
                  if motor == 3 or motor == 4:
                        return 24
                  else:
                        return 29
      else:
            if verbal == 5:
                  if motor == 6:
                        return 0
                  else:
                        return 3
            elif verbal == 4:
                  if motor == 6:
                        return 3
                  if motor == 5:
                        return 8
                  else:
                        return 13
            elif verbal == 3 or verbal == 2:
                  if motor == 6:
                        return 10
                  if motor == 5:
                        return 13
                  if motor == 4 or motor == 3:
                        return 24
                  else:
                        return 29
            else:
                  if motor >= 5:
                        return 15
                  if motor >= 3:
                        return 24
                  else:
                        return 29
            return 0
```

Figure 3-9: GCS Conversion Logic

3.4.2 APACHE Variables (APACHE Predvar)

Each of the APACHE prediction variables were extracted from the *apachepredvar* table of the eICU-CRD dataset.

Variable	Extraction Process
Age	The eICU-CRD table would label patients above the age of 89 with a flag >89 instead of including their age. I set the age of these patients to 90. Age term not splined as done in APACHE IV.
Comorbidities	Binary indicator variables present in apachepredvar for AIDS, hepatic failure, lymphoma, metastatic cancer, leukemia, immunosuppression, diabetes, and cirrhosis.
Ventilation	Binary indicator variable present in the ventday1 field
Admit Source	Present in predvar table: binarized to a one-hot vector representing the admitsource
Pre-ICU LOS	Used var03hspxlos field in predvar
Emergency Surgery	If elective surgery field was 0 and the admitdiagnosis was surgery related (prefixed with an "S-"), then labeled as 1.
Thrombolytics	Only set for patients with AMI diagnosis. Binary indicator present in predvar field.
GCS	From apacheapsvar table.
UnableGCS	If GCS not present, label as unable to obtain.

Table 3.6: APACHE Non-APS Variable Conversion Logic

3.4.3 APACHE Diagnosis

Lastly, the diagnoses were extracted from the admit diagnosis field of the apachepredvar table. The diagnoses were then transformed into a one-hot vector of length about 430 that contained a single indicator for the admit diagnosis for the patient.

3.5 High-risk Feature Engineering

While the APACHE IV features were extracted from eICU-CRD for all patients, I also extracted per-patient features from other tables in eICU-CRD to develop the custom high risk classifier. Each of these features were extracted for "high risk"

patients: because the high risk threshold outlined in Section 3.3 was at minimum 0.10, I extracted these features for all patients with an APACHE-predicted mortality risk of 10% or greater. The extracted features are summarized in Table 3.7.

Category	**Features Extracted**
Demographics	Age, BMI, height, gender, weight
Admission data	Source of admission ICU admission diagnosis (based on APACHE)
Laboratory data (trajectory, mean, worst value)	Blood gases: PaO2, pH, base excess, bicarbonate, Hematology: hematocrit, hemoglobin, lymphocytes, neutrophils, platelets, white cell count Electrolytes: calcium, chloride, magnesium, phosphate, sodium Biochemistry: albumin, amylase, bilirubin, blood urea nitrogen, B-natriuretic peptide, creatine phosphokinase, creatinine, lactate, lipase, troponin I/T Coagulation: PT/INR, fibrinogen
Vital Sign data (trajectory, mean, worst value)	Heart rate, temperature, SaO2, Respiratory rate, diastolic, systolic, ETCO2 Urine output and Fluid balance, Glasgow coma scale
Comorbidities (Yes/No)	All comorbidities necessary for APACHE and CHARLSON [26] score: AIDS, cerebrovascular disease, congestive heart failure, chronic kidney disease, connective tissue disease, COPD, dementia, diabetes with end organ damage, diabetes without end organ damage, hemiplegia, hypertension, leukaemia, liver disease, lymphoma, metastatic tumour, myocardial infarction, peptic ulcer disease, peripheral vascular disease, chronic pulmonary disease, renal disease, tumour without metastasis
Treatment (Yes/No)	Drugs: antiarrhythmics, antibiotics, lasix, sedatives, vasopressors Blood products: blood, platelets, cryoprecipitate, plasma
Devices (Yes/No, Attributes: Mean)	Pacemaker, IABP Ventilation: yes/no, tracheostomy size, plateau pressure, PEEP, FIO2, tidal volume, tidal volume/body weight
Thrombolytics	Only set for patients with AMI diagnosis. Binary indicator present in predvar field.
GCS	From apacheapsvar table.
UnableGCS	If GCS not present, label as unable to obtain.

Table 3.7: Summary of High Risk Features Extracted from Dataset

Key: BMI: Body Mass Index; ICU: intensive care unit; APACHE: Acute Physiology and Chronic Health Evaluation; PaO2: partial pressure arterial oxygen; IABP: intraaortic balloon pump; PEEP: positive end expiratory pressure: FIO2: fraction of inspired oxygen; ETCO2: end tidal CO2; COPD: chronic obstructive pulmonary disorder

3.5.1 Demographics

While the age used the analysis was the same as that found used in Section 3.4, I additionally extracted height, gender, and weight from the *patient* table in eICU-CRD. Afterwards, a BMI-like statistic was computed by calculating $weight/(height^2)$ as an additional feature.

3.5.2 Admissions

The admit source and admit diagnosis were the same as that used by APACHE. The only modification was that in the high risk cohort, I only considered 30 common diagnoses instead of all 430 APACHE diagnoses as in the high risk subpopulation, most diagnoses did not have a significant presence in the population.

3.5.3 Laboratory Values

For the high risk classifier, I sought to enhance the feature engineering of lab values in two steps. First, I incorporated additional lab values not previously used in the APACHE score. Secondly, I included several temporal and nonlinear transformations on the lab values themselves.

The additional lab values used in this analysis were: *bicarbonate, chloride, calcium, magnesium, pt inr, hco3, base excess, ionized calcium, lactate, troponin i, troponin t, amylase, lipase, platelets, hemoglobin, phosphate, cpk, bnp, fibrinogen, neutrophil count, lymphocyte count*. I also extracted the raw values from lab tests used as part of the APACHE APS score. These tests were: *sodium, creatinine, bun, wbc, albumin, ph, bilirubin*, and *hematocrit*.

Each lab value was obtained from the *lab* table in eICU-CRD. Consistent with the APACHE IV approach of only using data from the first 24 hours of the patient stay, all lab results within the first 24 hours of the patient stay (identified by labresultoffset) for each of the lab tests above were extracted from eICU-CRD. Often times, patients would have multiple lab results within this time period for a given test, enabling additional analyses such as temporal trends.

For each series of lab data for a given test, we computed three different sets of features:

1. A single data point representative of the lab test result
2. A set of trendlines identifying changing patterns in the dataset
3. A set of indicators that conveyed how "abnormal" a lab score is.

To choose a single data point that captured the lab test result, I either chose the clinically "worst" value or the average value across all results for a lab test within the first 24 hours. For labs not included in the APACHE IV score, I used the "worst" score (either a maximum or minimum based on the lab test, as indicated by a collaborating physician), and for labs that were included in the APACHE IV score, I used the average value of those lab scores, as the "worst" score was already contained within the APACHE APS value for that lab. Table 3.8 includes a discussion of which lab score was used as the "worst" lab score for each lab test.

For each lab test where there were at least 2 separate measurements, I computed 8 different trendline features between the first half and second half of the data. In other words, if there were 2 unique measurements, I would compare the first with the second to generate the trendline. If there were 8 measurements, I would then compare the average of the first four measurements with the average of the last four measurements, thereby reducing the sensitivity of the feature to single lab measurements. Note that often times, I would apply a nonlinear transformation to the trendline slopes in a similar fashion to that of the APS score calculation to capture its effects in either direction (positive or negative). Without this transformation, the linear model could only learn the effects of a single direction of slope, as it has to assign a single sign to the weight associated with the slope itself.

1. *Time-scaled-slope*: The time-scaled slope of the lab measurement (measuring the change in lab value per min)
2. *Raw-trend-negative*: The negative slope between the first two halves of the set of measurements. If the slope is positive, the value is 0. This feature, when taken in conjunction with raw-trend-positive would enable the model to learn whether the presence of a trend, regardless of whether the trend is positive or negative, is indicative of potential mortality.
3. *Raw-trend-positive*: The positive slope between the first two halves of the set of measurements. If the slope is negative, the value is 0.

4. *Trend-negative*: Slope of the lab measurement after the lab measurements are normalized by the population average and standard deviation. 0 if positive.

5. *Trend-negative-presence*: Binary indicator of whether trend-negative has a negative slope or not.

6. *Trend-positive*: Slope of the lab measurement after the lab measurements are normalized by the population average and standard deviation. 0 if negative.

7. *Trend-positive-presence*: Binary indicator of whether trend-positive has a positive slope or not

8. *From-default*: Slope of the measurements after the measurements are normalized by the "default" lab value for a given lab test. Default lab tests are found in Table 3.8.

To further mimic the APACHE APS scoring process, we compiled a list of "normal" ranges for the lab tests in the analysis and developed a series of indicators of whether the worst or average lab value (the single data point feature obtained for the lab test) was abnormal or not.

1. *Is-abnormal*: Whether the value falls outside the normal range for this test.

2. *Is-low*: Whether the value is lower than the lowest value in the normal range for this test.

3. *Is-low-by*: By how much the value is lower than the lowest value in the normal range for this test.

4. *Is-high*: Whether the value is higher than the higher value in the normal range for this test.

5. *Is-high-by*: By how much the value is higher than the highest value in the normal range for this test.

Table 3.8 contains the normal ranges for each of these lab values. These values were sourced from [27-35].

Lastly, missing lab values were substituted with a default lab value and zeroes for all trend and abnormality scores. For example, patients without a platelets measurement were given a value of 300 for the lab test single data point value and 0 for all other values.

Lab Name	Default Value	Normal Range	"Worst" Value
bicarbonate	25 mmol/L	22-29	Min
chloride	100 mmol/L	98-107	Min
calcium	9.5 mg/dL	8.6-10	Min
magnesium	1.9 mg/dL	1.6-2.6	Min
pt_inr	1	0.9-1.2	Max
hco3	25 mmol/L	22-29	Min
base_excess	0 mEq/L	-2-3	Min
lactate	1.0 mmol/L	0.5-2.2	Max
troponin_i	0 ng/L	0-0.1	Max
troponin_t	0 ng/L	0-0.1	Max
amylase	50 U/L	27-131	Max
lipase	50 U/L	23-300	Max
platelets	300 count/mcL	130-400	Min
hemoglobin	140 g/L	140-180	Min
phosphate	3 mg/dL	2.7-4.5	Min
cpk	150 U/L	22-190	Max
bnp	300 pg/mL	100-400	Max
fibrinogen	300 mg/dL	200-400	Min
neutrophil	5 countx10^3/mm3	2-8	Avg
lymphocyte	2 x10^3/uL	1-5	Avg
sodium	140 mEq/L	135-145	Avg
creatinine	0.9 mg/dL	0.7-1.3	Avg
bun	19 mg/dL	7-20	Avg
wbc	9 (count/nL)	4.5-11	Avg
albumin	4.5 g/dL	3.9-5.1	Avg
bilirubin	1.1 mg/dL	0.5-1.5	Avg
ph	7.4	7.35-7.45	Avg
hct	45 %	40-50%	Avg

Table 3.8: Default/Normal Ranges and Worst Values for Lab Values

3.5.4 Vital Signs

Trend related features for vital signs were developed from the following vital signs: heart rate, temperature, SaO2, blood pressure measurements, and respiratory rate, in addition to the vital sign APS scores used in the APACHE APS computation. Secondly, I computed the fluid balance for every patient as an additional feature.

Vital sign trend features followed a similar pattern to the 8 lab-based trend features constructed per lab test and were sourced through two tables, the *vitalsperiodic* and *vitalsaperiodic* tables in eICU-CRD. Vitalsperiodic contained periodic vital sign measurements recorded at 15 minute intervals for the systolic and diastolic blood pressure, sao2, etco2, temperature, heartrate, and respiration rate. Vitalsaperiodic contained irregular measurements of blood pressure that were also used in this study. I labeled blood pressure measurements from vitalsaperiodic with the "noninvasive" tag because they were likely sourced in a noninvasive manner in the clinic itself.

The default values used for each vital sign measurement are summarized in Table 9 below. Unlike in the feature engineering for the lab result data, I did not compute abnormality ranges for vital signs as this information is likely already captured in the APACHE APS computation. The average value was used the "worst" value in each vital sign; each vital sign, especially those periodically measured every 15 minutes, had numerous data points per patient; an averaging of the vital signs results would reduce the sensitivity of the feature towards rare sensor errors.

Vital Sign	**Default Value**	**"Worst Value"**
Noninvasive systolic	120 mmHg	Avg
Noninvasive diastolic	70 mmHg	Avg
Invasive systolic	120 mmHg	Avg
Invasive systolic	70 mmHg	Avg
SaO2	99 %	Avg
ETCO2	40 %	Avg
Temperature	98.5 F	Avg
Heart rate	60 bpm	Avg
Respiratory Rate	20 rpm	Avg

Table 3.9: Default Values and Worst Values for Vital Signs

Fluid balance is a strong prognosticator of overall health [36] and a commonly examined diagnostic in the ICU. Patients who have imbalanced fluid output or input

could suffer from electrolyte imbalance or dehydration, which in turn could impair kidney and cardiovascular function, and thus patients who either lose a lot of fluid in the ICU or have reduced urine output or other methods of fluid excretion are at risk. Fluid balance was calculated in the eICU-CRD using the *intakeoutput* table; each entry in the table contributes a "nettotal" to the patients overall fluid level. For each patient, we calculated the fluid balance by computing the cumulative sum of all fluid inputs or outputs within the first 24 hours.

3.5.5 Comorbidities

In addition to the comorbidities considered by the APACHE score, I computed the Charlson Comorbidities [26] for each high risk patient. The Charlson Comorbidity is an index that uses the binary presence or absence of around 20 conditions in patients as a predictor of mortality. Each condition is given an integer point score ranging from 1 to 6, the sum of which provides an estimate of 10-year survival. For example, 5 points on the index provides a 21% estimated 10-year survival whereas 6 points on the index provides a 2% estimated 10-year survival [37].

Each of the Charlson Comorbidities were extracted from the *pasthistory* table in eICU-CRD by examining the pasthistorypath for each condition. The table below summarizes the condition:pasthistorypath mappings used to ascribe each condition to a high risk patient. However, because these pathhistorypaths are not fully structured fields that correspond to the Charlson Comorbidities, there is likely error in ascribing these conditions to patients. Each of these comorbidities corresponded to a single binary indicator feature ascribed to a high risk patient for modeling.

Charlson Comorbidity	Pasthistorypath
Myocardial Infarction	%notes/Progress Notes/Past History/Organ Systems/Cardiovascular (R)/Myo%
Congestive Heart Failure	%notes/Progress Notes/Past History/Organ Systems/Cardiovascular (R)/Congestive%
Peripheral Vascular Disease	%peripheral%
TIA	%neurologic/tia(s)%
Dementia	%neurologic/dementia%
COPD	%copd%
Connective Tissue Disease	%rheumatic%
Peptic Ulcer Disease	%peptic%
Mild Liver Disease	%cirrhosis/biopsy% %cirrhosis/clinical diagnosis%
Uncomplicated Diabetes	%diabetes% NOT %renal failure%/ %renal insu%
Diabetes with End Organ Damage	%diabetes% AND %renal failure%/ %renal insu%
Renal Disease	%renal failure% / %renal insu%
Hemiplegia	%stroke%
Tumor without Metastasis	%cancer/cancer% %cancer therapy%
Leukemia	%hematologic malignancy/leukemia%' '%hematologic malignancy/all%' '%hematologic malignancy/cml%' '%hematologic malignancy/aml%' %hematologic malignancy/cll%
Lymphoma	%hematologic malignancy/non-hodgkins lymphoma% %hematologic malignancy/ hodgkins disease%
Severe Liver Disease	%cirrhosis/varices% %cirrhosis/ugi bleeding% %cirrhosis/coma% %cirrhosis/jaundice% %cirrhosis, encephalopathy% %cirrhosis/ascites%
AIDS	%aids%
Metastatic Cancer	%cancer/metastases% %metast%

Table 3.10: Assignment of Pasthistorypaths to Charlson Comorbidities

3.5.6 Treatment

Intervention-related features were developed to indicate whether the patient was on certain types of medication or received certain types of blood product related interventions. For each of these features, we extracted a binary indication of whether the

patient received a medication or blood transfusion within the first 24 hours of the patient stay, as shown in Table 11. Medication information was extracted from the *medication* table, whereas blood transfusion related information was sourced from the *treatment* table.

Vasopressors	**Table Source and Field Name**	**Query Strings**
Sedatives	eicu.medication.drugname	%fentanyl%, %midazolan%, %propofol%, %diprivan%
Vasopressors	eicu.medication.drugname	%norepinephrine%, %vasopressin%, %dobutamine%, %dopamine%, %epinephrine%, %milrinone%
Antiarrhythmic	eicu.medication.drugname	%amiodorone%
Diuretics	eicu.medication.drugname	%lasix%, %furosemide%
Antibiotics	eicu.medication.drugname	%aminoglycoside%, %carbapenem%, %clindamycin%, %linezolid%, %macrolide%, %metronidazole%, %monobactam%, %penicillin%, %quinolone%, %sulfonamide%, %vancomycin%
Blood transfusion	eicu.treatment.treatmentstring	%prbc%
Platelets transfusion	eicu.treatment.treatmentstring	%platelet%
Fresh Frozen Plasma Transfusion	eicu.treatment.treatmentstring	%fresh frozen plasma%
Cryoprecipitate Transfusion	eicu.treatment.treatmentstring	%cryoprecipitate%

Table 3.11: Assignment of Query Strings to Interventions

3.5.7 Device Usage and Attributes

I extracted multiple features related to the medical devices a patient might be using, including pacemakers, intra-aortic balloon pumps (IABPs), and mechanical ventilation. Because high risk patients tend to undergo mechanical ventilation, I also

extracted various device settings related to the ventilator to provide further prognostic information that conveyed, for example, the strength of ventilation provided to the patient.

The use of pacemakers and IABPs were extracted as a binary indicator variable by the treatmentstring field in the treatment table to the following query strings: `%implantation of heart pacemaker%`, `%temporary or external pacemaker%`, and `%intraaortic balloon pump%`.

I extracted the values for each mechanical ventilation setting from the *respiratorycharting* table by matching the respiratorychartvaluelabel field to the specific setting. Afterwards, I averaged each setting across the entire patient stay for use a feature in the mortality prediction task.

3.5.8 Expanding the Analysis to 48h

While APACHE IV only leverages features obtained within the first 24 hours of an ICU stay, a high-risk focused predictive model could benefit greatly from the additional information gained between hours 24-48 of an ICU stay. Hours 24-48 capture the patient response to initial treatment on the first day, and this response is in many cases not grounded in information accessible in the first 24 hours of an ICU stay. For example, a study of the MPM II model found that the model, when calibrated at 24 hours, showed poor calibration and discrimination at the 48hr and 72hr time points [38].

Thus, in addition to developing a high-risk feature set that uses the first 24 hours of patient data to predict mortality in high risk patients, I additionally developed a similar feature set derived from the first 48 hours of patient data, retaining the same exclusion criteria and feature extraction processes. Key additions to the feature extraction process while obtaining features from the first 48 hours of the patient stay are summarized below:

1. *Demographics*: Because the demographics features are not time dependent, the same features used in the 24 hour period were applicable for the 48 hour period.

2. *Admission data*: Because the admission features were extracted only at admission, the same features calculated for the 24 hour period were applicable for the 48 hour period.

3. *Laboratory data*: The features extracted for the 24 hour period were replicated for the 24-48 hour period and the global 0-48 hour period. In other words,

"worst" values were additionally chosen for the 24-48 hour period and the global 0-48 hour period. Likewise, trend values were calculated within the 24-48 hour period, and the entire 0-48 hour period.

4. *Comorbidities*: Because the Charlson Comorbidities relate to conditions diagnosed prior to the admission itself, the same features used in the 24 hour period were applicable for the 48 hour period.

5. *Treatment*: I additionally record the binary presence of a medication or transfusion treatment in the first 48 hours. For example, if a patient receives a sedative in the first 24 hours, then the patients 24hr and 48hr sedative_presence feature will be 1. If a patient receives a sedative at hour 36, the sedative_presence_24h feature will be 0 but the sedative_presence_48h feature will be 1.

6. *Devices*: In addition to the 24 hour features calculated for ventilation, the same features will be averaged over the 0-48 hour time period.

To summarize, the 48 hour feature set includes all features calculated in the 24 hour feature set, and has additional features that utilize data in hours 24-48 of the ICU stay. Moreover, both custom feature sets (24 hour and 48 hour) include all the features in the APACHE IV feature set. The 24 hour feature set has 661 features, whereas the 48 hour feature set has 1217 features. The APACHE IV feature set has 462 features.

3.6 Model Development

Using eICU-CRD based feature sets, the extractions of which were detailed in Sections 3.4 and 3.5, I developed several Logistic Regression models as detailed in Table 3.12. This section will discuss each model and motivate the reasons for its construction.

Each model was implemented using L2 Regularized Logistic Regression and was trained on its respective feature set using a 70-30 training / testing split and feature normalization prior to training. Logistic Regression implementation used is that of scikit-learn [20], a well-known Python machine learning library. Models were trained for 100-200 steps using Stochastic Average Gradient Descent. Models were evaluated using AUROC and calibration analysis.

Model	Description
APACHE	APACHE Probabilities sourced from apachepatientresults table
APACHE-All	APACHE features recalibrated on eICU-CRD patients (retrained weights)
APACHE-HR	APACHE features recalibrated on high risk eICU-CRD patients (retrained weights)
eICU-24h-HR	APACHE features and extracted features within the first 24h trained on all high risk patients
eICU-48h-HR	APACHE features and extracted features within the first 48h trained on all high risk patients
Combined-24h	A ?Sequential model? where if pt <10% risk, then APACHE used, otherwise eICU-24h-HR
Combined-48h	A ?Sequential model? where if pt <10% risk, then APACHE used, otherwise eICU-48h-HR

Table 3.12: Models Developed from the eICU-CRD features in this thesis.

APACHE: APACHE represents the canonical implementation of the APACHE IV prediction model as implemented in the Philips eICU platform. The APACHE predictions are obtained from the apachepatientresults table directly and were calculated by the APACHE API *in situ*.

APACHE-All: APACHE-All involves recalibrating the weights of APACHE features on the eICU-CRD dataset. The feature engineering detailed in Section 3.4 follows the APACHE IV feature extraction process closely. While there are some small differences between feature sets (for example, lack of splining of the age term), the feature set of 3.4 is likely very close to what the APACHE API receives when calculating patient mortality risk. However, as discussed in Section 3.1, the Philips eICU dataset demonstrated an over prediction of mortality by the APACHE, resulting in a poorer calibration than found in the APACHE IV paper. APACHE-All is a retrained version of the APACHE features; we would expect this classifier to be better calibrated to the dataset than the canonical APACHE classifier.

APACHE-HR: APACHE-HR was developed by recalibrating the weights of APACHE features on the high risk patients in the eICU-CRD dataset. It is similar to APACHE-All and differs only on the training population (high risk vs. all patients). APACHE-HR will indicate the ability of the APACHE features to fit the high risk population after recalibration.

eICU-24h-HR: eICU-24h-HR is a custom high risk classifier developed using the feature set constructed in Section 3.5. The feature set includes all APACHE features and additionally includes the engineered features used for the high risk population. It is trained exclusively on the high risk population (the same population that APACHE-HR) is trained on. Comparing eICU-24h-HR with the results from APACHE-HR will demonstrate the marginal value of the engineered features in Section 3.5.

Combined-24h: Combined-24h is a "sequential" model that follows the architecture described by Figure 2-2 (Section 2.4). Given an input risk threshold, it uses the APACHE classifier if the patient?s APACHE IV risk prediction is lower than the risk threshold, and uses eICU-24h-HR for high risk patients.

Combined-48h: Combined-48h is a "sequential" model that similarly follows the architecture described by Figure 3 (Section 2.4). Given an input risk threshold, it uses the APACHE classifier if the patient?s APACHE IV risk prediction is lower than the risk threshold, and uses eICU-48h-HR for high risk patients.

The models above enable the study to test the "sequential modeling" hypothesis. Chapter 4 discusses the creation and evaluation of the eICU-24h-HR and eICU-48h-HR model. By comparing its performance with that of the baseline APACHE model and a recalibrated APACHE-HR model, I demonstrate that the additional features developed in Section 3.5 enable eICU-24h-HR and eICU-48h-HR to better fit the high risk population. Next, in Chapter 5, I show that the combined classifiers, Combined-24h and Combined-48h are able to outperform the baseline results from APACHE. Lastly, in Chapter 6, I demonstrate that in specific physiologically significant cohorts of patients, eICU-24h-HR and Combined-24h are able to outperform APACHE predictions in those cohorts.

Chapter 4

Development of the eICU High Risk Classifiers

Both eICU-24h-HR and eICU-48h-HR outperformed APACHE baselines and controls for all high risk thresholds between 0.1 and 0.75. Section 4.1 compares the discriminative abilities for each of the high risk classifiers, while Section 4.2 compares their calibration to the high risk cohort in the dataset. Lastly, in Section 4.3, I examine the feature weights learned in each of the high risk models to suggest why they might perform better in the high risk patient population.

4.1 High Risk Threshold-Based Results

Table 4.1 summarizes the performance (AUC) of the high risk classifiers on the high risk patient cohort as a function of the risk threshold. Each AUC was calculated as the average of three trials (which involved three randomly generated training-validation set splits from the global dataset), the standard deviations of which are in parentheses.

High Risk Threshold	Number of Patients in Training Set	APACHE	APACHE-HR	eICU-24h-HR	eICU-48h-HR
0.1	13821	0.752 (.005)	0.754 (.005)	0.813 (.003)	0.822 (.003)
0.15	9936	0.727 (.004)	0.726 (.010)	0.782 (.008)	0.807 (.007)
0.2	7666	0.710 (.003)	0.722 (.010)	0.772 (.008)	0.797 (.001)
0.25	6053	0.700 (.009)	0.722 (.005)	0.767 (.004)	0.782 (.001)
0.3	5001	0.686 (.009)	0.693 (.003)	0.757 (.010)	0.781 (.012)
0.35	4172	0.678 (.012)	0.695 (.021)	0.749 (.003)	0.778 (.005)
0.4	3521	0.675 (.014)	0.699 (.004)	0.753 (.003)	0.772 (.015)
0.45	2999	0.653 (.016)	0.685 (.012)	0.732 (.008)	0.759 (.013)
0.5	2546	0.640 (.007)	0.691 (.010)	0.735 (.003)	0.756 (.016)
0.55	2145	0.658 (.031)	0.664 (.015)	0.741 (.017)	0.746 (.006)
0.6	1798	0.639 (.002)	0.662 (.009)	0.717 (.020)	0.730 (.006)
0.65	1467	0.618 (.030)	0.648 (.014)	0.716 (.012)	0.708 (.017)
0.7	1193	0.621 (.016)	0.646 (.011)	0.668 (.008)	0.722 (.024)
0.75	928	0.641 (.015)	0.616 (.011)	0.702 (.051)	0.714 (.006)

Table 4.1: High Risk Models Developed from the eICU-CRD features in this thesis.

Figure 4-1 depicts this table visually to show dependence of the high risk classifier performance on the high risk threshold as a line graph. Figures 4-2 and 4-3 provide the ROC curves the four classifiers trained on the first 24 hours of patient data in the ICU (APACHE, APACHE-HR, APACHE-All, and eICU-24h-HR) at two separate high risk thresholds, 0.10 and 0.50.

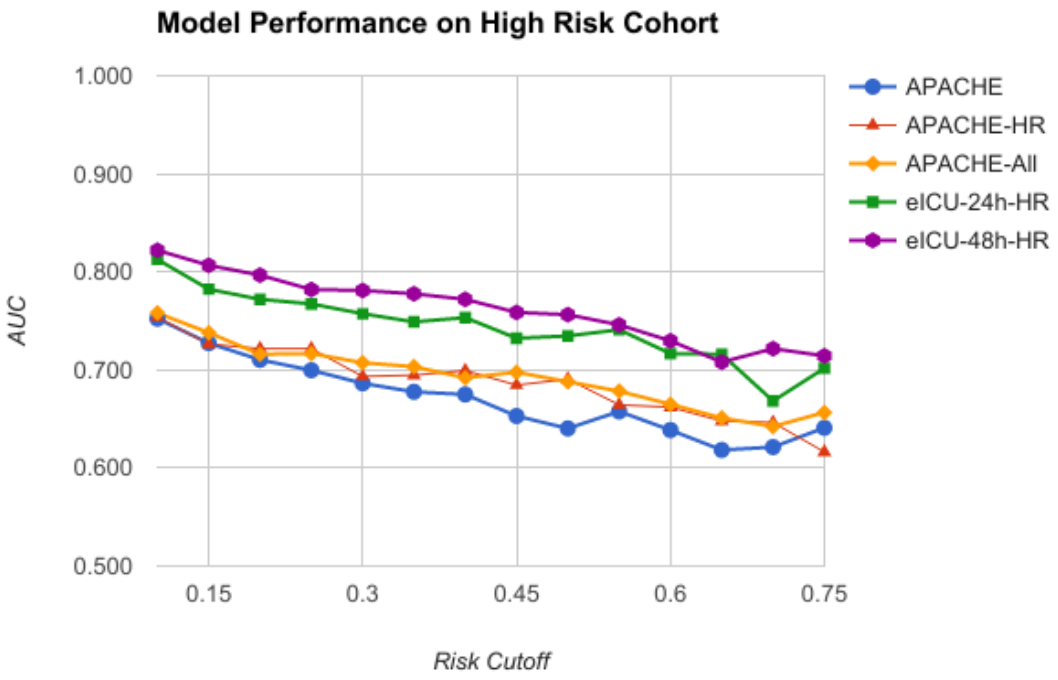

Figure 4-1: High Risk Classifier Performance By High Risk Threshold

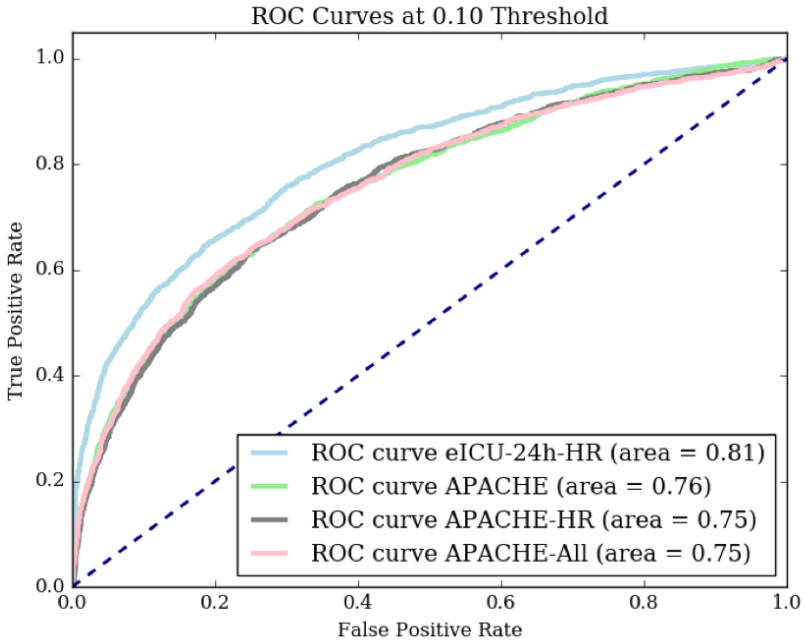

Figure 4-2: ROC Curves at a High Risk Threshold of 0.10

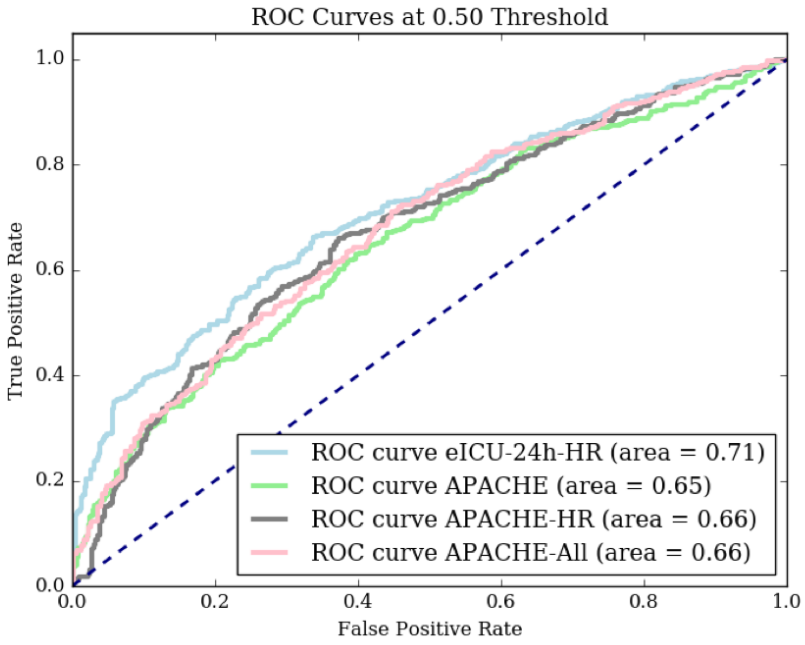

Figure 4-3: ROC Curves at a High Risk Threshold of 0.50

Overall, the custom high risk classifiers performed significantly better than their APACHE counterparts. At a 0.10 high risk threshold, eICU-24h-HR has an AUC

of 0.812 and eICU-48h-HR has an AUC of 0.822 compared to AUCs of 0.754, 0.758, and 0.752 from APACHE-HR, APACHE-All, and APACHE respectively. Moreover, this trend continues throughout the tested risk thresholds from 0.10 to 0.75, with eICU-48h-HR slightly outperforming eICU-24h-HR and both custom classifiers outperforming all APACHE baselines. At the same time, Table 4-1 demonstrates increased AUC standard deviations as the risk threshold is increased: this is likely due to much smaller training and testing sizes at higher risk thresholds, making it less reliable to compare model performances at those thresholds.

The fact that the custom classifiers, eICU-24h-HR and eICU-48h-HR, are able to perform better than their high-risk APACHE counterparts suggests that the features engineered in Section 3.5 capture meaningful prognosticators of mortality that are overlooked by the current APACHE feature set. Specifically, both custom classifiers perform better than recalibrating APACHE features to the eICU-CRD dataset and also recalibrating APACHE features to high risk patients within the eICU-CRD dataset. Furthermore, the results indicate that even a high risk threshold of 0.10 is enough to warrant secondary customization of the mortality model via a custom high risk classifier with high risk features.

Interestingly, APACHE-HR and APACHE-All performed relatively similarly on the high risk cohort. My earlier hypothesis would have suggested that even retraining (and thereby recalibrating) APACHE-IV on the high risk cohort would improve its performance on the high risk cohort; however, the results demonstrate that any improvement APACHE-HR showed when compared to canonical APACHE IV score was likely due to a recalibration to the Philips eICU-CRD dataset as a whole rather than a recalibration to the physiological nuances of the high risk population. This result also supports that the APACHE feature set does not represent the physiology of a high risk patient completely.

Lastly, the downward trends in each classifier's performance as the risk threshold increases is consistent with the results found in Section 3.1. Each model has hundreds of features to train, but as the risk threshold increases, less data is available for the model to train its features with: for example, at a risk threshold of 0.75, the model is trained with less than 1,000 patients. In addition, high risk patients are "high risk" for a multitude of reasons and conditions, and a larger training set would be able to accommodate all the different risk modes a patient may fall under. A smaller training set would not capture all modes of risk that could be found in the validation set.

4.2 High Risk Calibration

Figure 4-4 depicts the calibration curves for each of the 24hr classifiers evaluated in Section 4.1. Each calibration curve was generated only from patients that met the risk threshold (in this case, had an APACHE mortality risk of greater than 10%), and thus the calibration curves are truncated in the beginning. The APACHE IV, sourced from the APACHE classifier, calibration curve discussed in Section 3.1 is shown in green on the image.

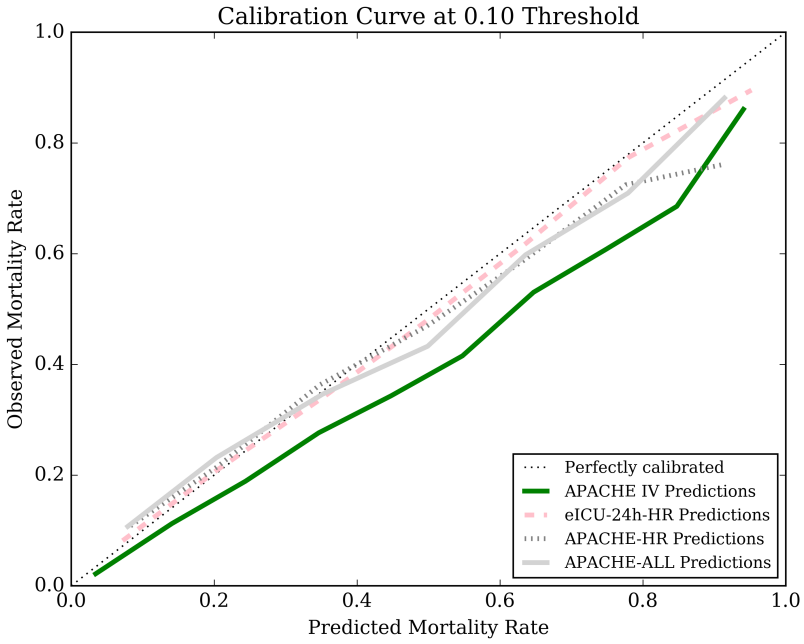

Figure 4-4: Calibration Curve for High Risk Classifiers

A visual inspection of the calibration curves shows that all three curves that were trained on eICU-CRD demonstrate better calibration when compared to the baseline APACHE values sourced from the apachepatientresults table. This is likely the case because each classifier was retrained on the data in eICU-CRD, and was thus able to model potential changes in mortality rates as a result of the eICU platform itself or as a result of the advances in medical care reducing mortality rates for certain conditions. The calibration strengths between APACHE-HR and APACHE-All are likely similar for the same reasons both classifiers performed equally well in the discrimination task discussed in Section 4.1: the differences in the high risk population are not captured as well by the APACHE feature set. It seems that the eICU-24h-HR classifier is the most calibrated of all the mortality models in the Figure 14. For example, in the high risk regions of the calibration curve (where predicted mortality

is highest), it lies closest to the "perfect" calibration curve.

These results are further supported by Hosmer-Lemeshow goodness-of-fit tests for each model. Using the hoslem function and the Package *ResourceSelection* [39], we computed the H-L statistics for each model in *R*, summarized by Table 4.2.

Model	**C-Statistic**	**Degrees of Freedom**	**P-Value**
APACHE-All	141.05	8	<2e-16
APACHE-HR	62.141	8	2.00E-10
APACHE	140.59	8	<2e-16
eICU-24h-HR	53.3	8	9.00E-09

Table 4.2: Hosmer-Lemeshow Test Results for High Risk Calibration

The Hosmer-Lemeshow test seeks to accept the null hypothesis that there is no meaningful difference between a line of perfect calibration and a calibration in question. Thus, calibration curves with a p-value of 0.05 or greater are said to be "well-calibrated". The p-values themselves are computed from the degrees of freedom and the chi-squared statistic.

The Hosmer-Lemeshow C-Statistic is smallest for the eICU-24h-HR model, which is consistent with our earlier visual analysis that suggests it is better calibrated than the other models. At the same time, all models are shown to be poorly calibrated by the Hosmer-Lemeshow test. Interestingly, the APACHE-HR model has an almost equal C-Statistic, especially when compared to APACHE-All. This is likely due to the fact that a majority of the sample size in the calibration curve is located in the lower risk regions of the curve: thus, although the curves are concordant in higher risk thresholds, the APACHE-HR's relatively proximity to perfect calibration allows it to have a lower C-statistic.

4.3 Feature Inspection

Lastly, I examined the Top 25 largest (in magnitude) beta values associated with features in the eICU-24h-HR and eICU-48h-HR models to provide a potential explanation on why both models are able to better fit the high risk population.

4.3.1 Betas of eICU-24h-HR at 0.10 Threshold

feature	high_coef
raw_heartratetime_scaled_slope_24h	-0.4381116749
age	0.4346858815
raw_sao2_trend_neg_24h	-0.2863309715
gcs_aps	0.2749182956
ventday1	0.2439719728
admitsource_1	-0.2423298045
adj_gcs	0.2331826556
raw_sao2_trend_pos_24h	0.2072460171
mv_fio2_24h	0.2044287917
diag_CVASTROKE	0.1972846975
platelets_24h_is_low_by	0.1935466283
raw_heartrate_trend_neg_presence_24h	-0.1872668128
diag_CARDARREST	0.1824073049
diag_ICH	0.1794139669
temperature_aps	0.1759291846
unable_gcs	0.1632902035
raw_heartrateraw_trend_neg_24h	0.1594274995
raw_ph_24h_is_low_by	-0.1560873298
admitsource_4	0.155585972
raw_creatinine_24h_is_high	0.1528072596
pulse_aps	0.148451886
calcium_24h_is_low_by	0.1362912168
vasopressors_bin_24h	0.1360236644
raw_creatinine_24h_is_low_by	0.1356836865
troponin_i_24h_is_high	0.1336640364

Table 4.3: Top 25 Feature Weights for the eICU-24h-HR model when trained on a risk threshold of 0.10

The logistic betas follow an expected pattern. Features like age, gcs_aps, and ventday1 (patient received ventilation treatment on the first day) have large weights within the APACHE score itself and are highly correlated with mortality. Moreover, certain high risk diagnoses such as CARDARREST and CVASTROKE receive highly positive beta values, indicating that they are positively correlated with mortality. Analysis in Section 3.1 demonstrated that both diagnoses had mortality rates within eICU-CRD of 60% and 20% respectively. Admit_source1 has a largely negative beta value: ac-

cording to the APACHE User Foundations Guide [13], Admit_source1 corresponds to another hospital; patients arriving in the ICU from another hospital, where they could have received care previously, are likely to be in a better health state than those arriving through other sources, such as the floor [40].

Interestingly, a number of eICU-24h-HR specific features receive Top-25 magnitude beta values, and this supports the result that the eICU-24h-HR is able to model high-risk physiological nuances that APACHE is unable to. For example, the largely negative beta assigned raw_heartratetime_scaled_slope_24h might find that decreases in heart rate, such as those seen near in cardiac arrest, are strongly correlated with mortality. The fact that raw_sao2_trend_neg_24h has a largely negative beta value and raw_sao2_trend_pos_24h has a largely positive beta value suggests that an increase in sao2 is correlated with mortality: while this might not be physiologically intuitive, it might be a surrogate for medical procedures like mechanical ventilation, which is correlated with mortality. Accordingly, mv_fio2_24h is a feature that receives a very high beta value.

4.3.2 Betas of eICU-48h-HR at 0.10 Threshold

The overarching patterns in which features are most important in the eICU-48h-HR model follow that of the eICU-24h-HR model closely. For example, many feature importances, such as those of age, gcs, ventilation, admitsource_1, are shared between the two classifiers.

However, the 48 hour features might explain the slightly better performance obtained by the 48h classifier. The feature raw_heartratetime_scaled_slope_48h could find the same decreases in heart rate that are correlated with mortality over a longer time span. In addition, the vasopressors_bin_48h feature, which indicates that the patient had received vasopressors over the first 0-48 hours, are likely indicative of an adverse blood pressure condition in the patient, such as that of septic shock.

feature	high_coef
age	0.4182880361
raw_heartratetime_scaled_slope_24h	-0.4182246687
raw_heartratetime_scaled_slope_48h	-0.3437232557
raw_sao2_trend_neg_24h	-0.3164562885
gcs_aps	0.2547864841
adj_gcs	0.2447833242
raw_sao2_trend_pos_24h	0.2401448675
raw_sao2raw_trend_neg_48h	-0.2198420638
ventday1	0.2138186249
raw_sao2_trend_pos_48h	0.2083905423
platelets_24h_is_low_by	0.1852721765
raw_sao2_trend_neg_48h	-0.1673404568
vasopressors_bin_48h	0.1655460438
unable_gcs	0.165110415
raw_sodium_48h	0.1594565824
diag_CVASTROKE	0.1566705426
admitsource_1	-0.1559160505
diag_ICH	0.1537210176
chloride_48h	-0.1511943901
raw_creatinine_24h_is_high	0.1483552512
pulse_aps	0.1475160821
diag_S-CABG	-0.146697249
troponin_i_24h_is_high	0.1464784967
metastaticcancer	0.1412570285
raw_sodium_inverse_effect_48h	-0.1408620904

Table 4.4: Top 25 Feature Weights for the eICU-48h-HR model when trained on a risk threshold of 0.10.

Chapter 5

Development of the Sequential Model

The Combined-24h and Combined-48h slightly outperformed APACHE baselines on the entire population for some high risk thresholds between 0.1 and 0.75. Section 5.1 compares the discriminative abilities of each model with respect to the APACHE baselines, while Section 5.2 examines the calibration of both models on the validation dataset from eICU-CRD used to evaluate each model.

5.1 High Risk Threshold-Based Results

Table 5.1 summarizes the AUC scores of each classifier on the validation set derived from the entire patient population. As discussed in Section 2.4, the AUC of the Combined-24h model for example, given a high risk threshold T, is calculated by computing the combined AUC of the baseline APACHE values (APACHE model, sourced from APACHE API) and the predicted mortality probabilities obtained from the eICU-24h-HR model on all patients whose baseline APACHE risk probability is greater than T. The AUC values for APACHE and APACHE-All are independent of this high risk threshold as the latter involves only recalibration on the entire dataset, and this independence is seen in Table 5.1. Each AUC was calculated as the average three trials, the standard deviations of which are in parentheses.

Figure 5-1 demonstrates the high risk threshold dependence of each model. Figures 5-2 and 5-3 provide the confusion matrices for each model at a high risk threshold of 0.10 and 0.50 respectively. Each confusion matrix was computed by considering any predicted mortality risk of greater than 0.5 to be a prediction of mortality, and any predicted mortality less than 0.5 to be a prediction of survival. Figures 5-4 and 5-5 contain the ROC curves for each model at those two respective thresholds.

High Risk Threshold	APACHE	APACHE-All	Combined-24h	Combined-48h
0.1	0.873 (.001)	0.870 (.001)	0.880 (.001)	0.882 (.001)
0.15			0.876 (.004)	0.872 (.004)
0.2			0.871 (.006)	0.866 (.004)
0.25			0.869 (.004)	0.863 (.001)
0.3			0.865 (.002)	0.858 (.008)
0.35			0.868 (.001)	0.855 (.005)
0.4			0.867 (.003)	0.859 (.003)
0.45			0.866 (.003)	0.859 (.002)
0.5			0.867 (.005)	0.859 (.002)
0.55			0.857 (.003)	0.857 (.002)
0.6			0.862 (.004)	0.858 (.005)
0.65			0.863 (.002)	0.861 (.003)
0.7			0.867 (.004)	0.858 (.006)
0.75			0.866 (.003)	0.864 (.001)

Table 5.1: High Risk Threshold-Based Results for Models on Validation Set of Entire Patient Population

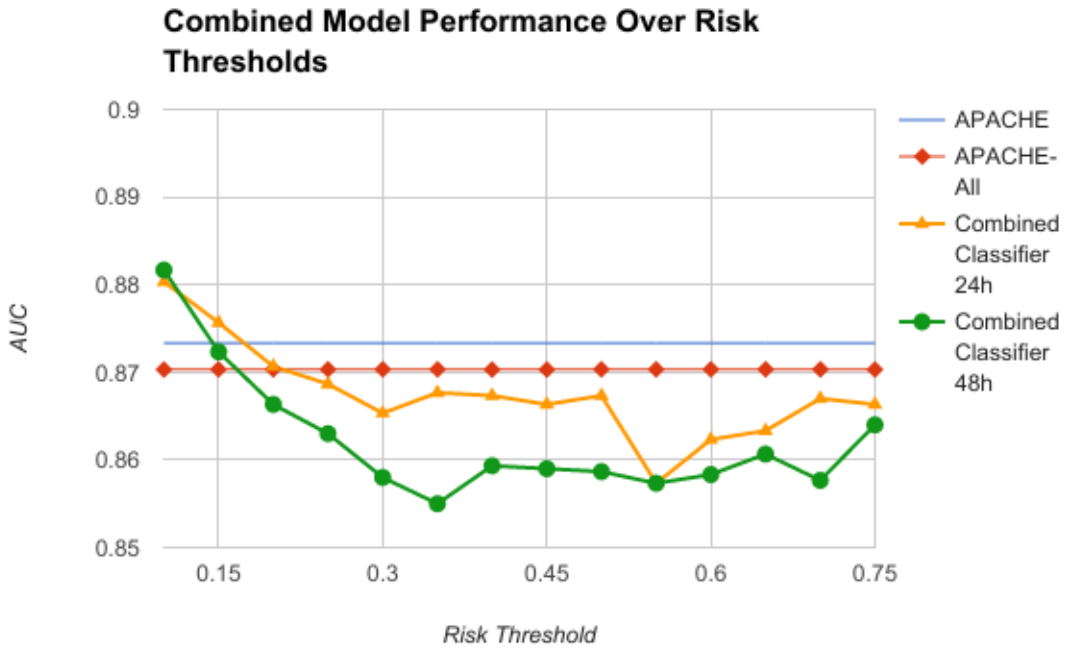

Figure 5-1: Sequential Model Performance Across All High Risk Thresholds for Validation Set.

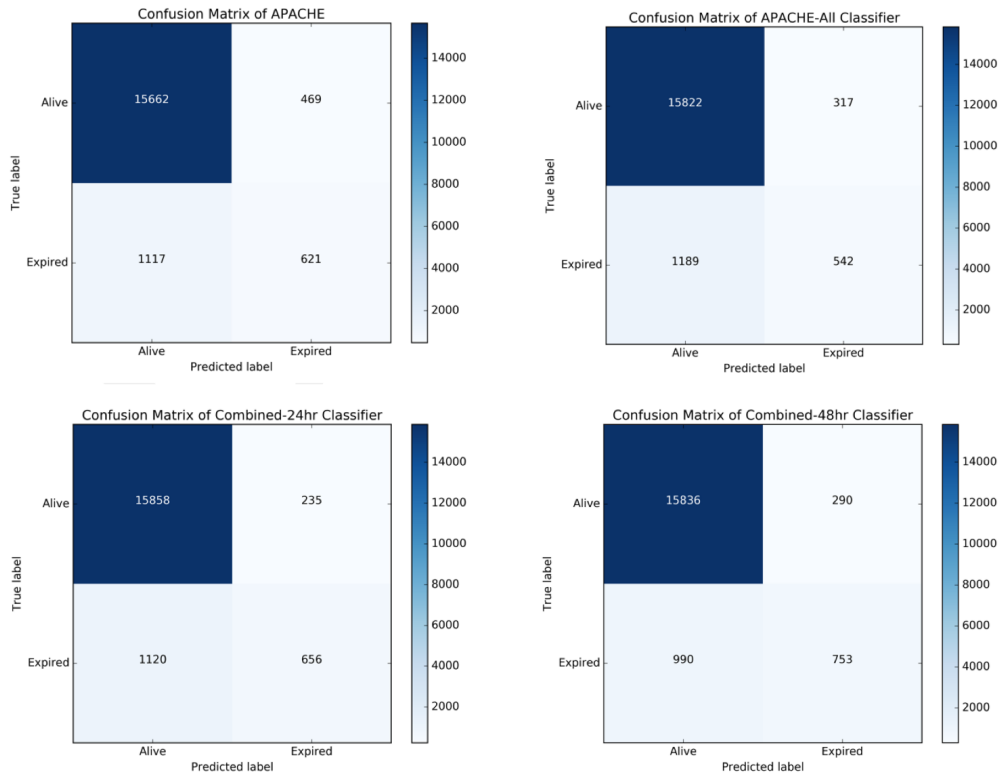

Figure 5-2: Confusion Matrices for Each Model When Prediction Threshold Set to 50% and High Risk Threshold is 10%

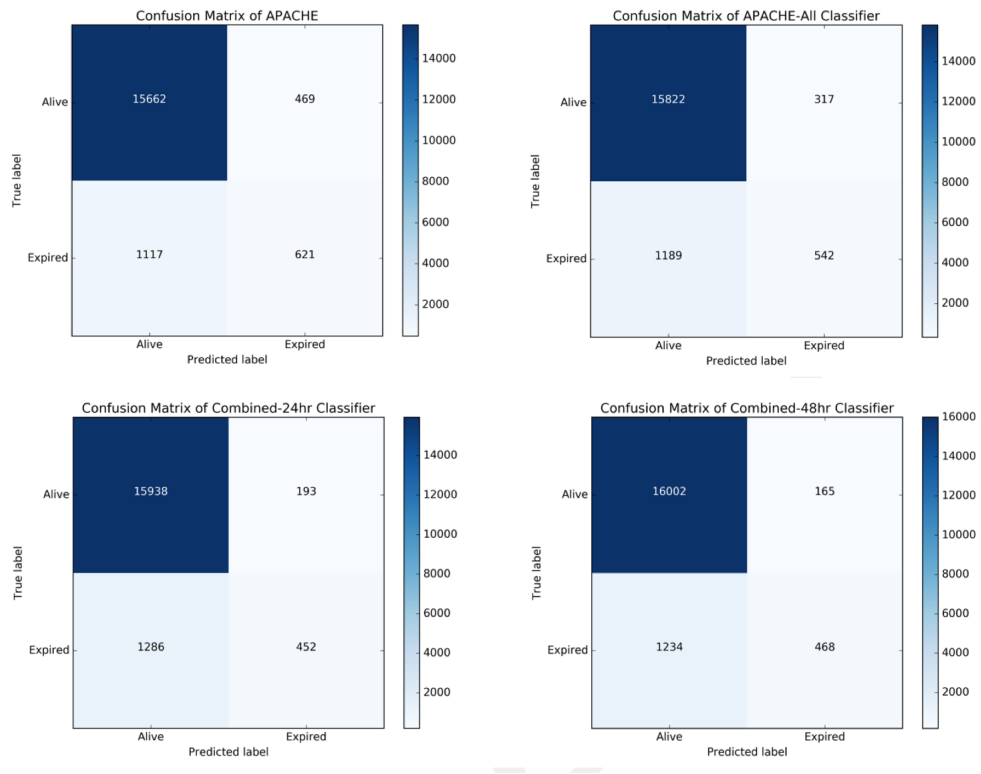

Figure 5-3: Confusion Matrices for Each Model When Prediction Threshold Set to 50% and High Risk Threshold is 50%

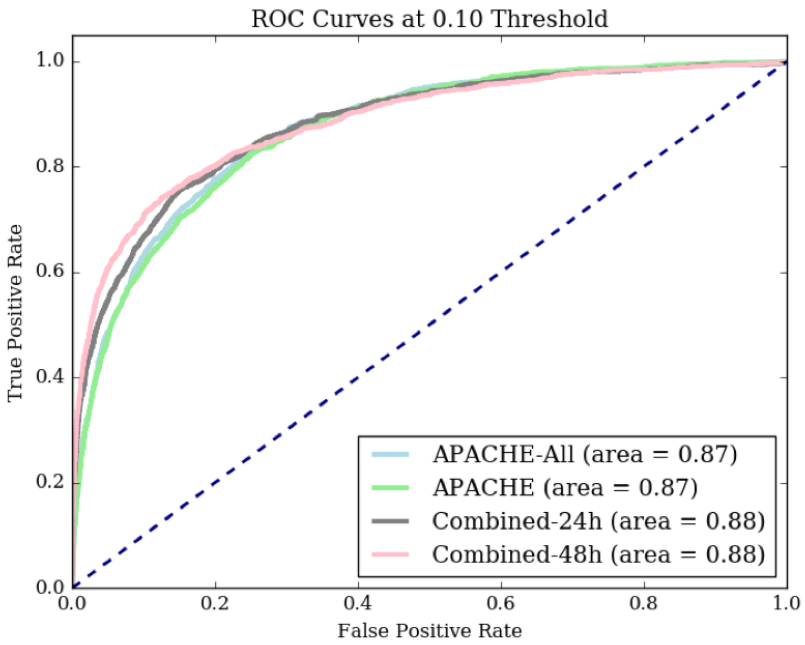

Figure 5-4: ROC Curves for Each Model When High Risk Threshold Set to 10%

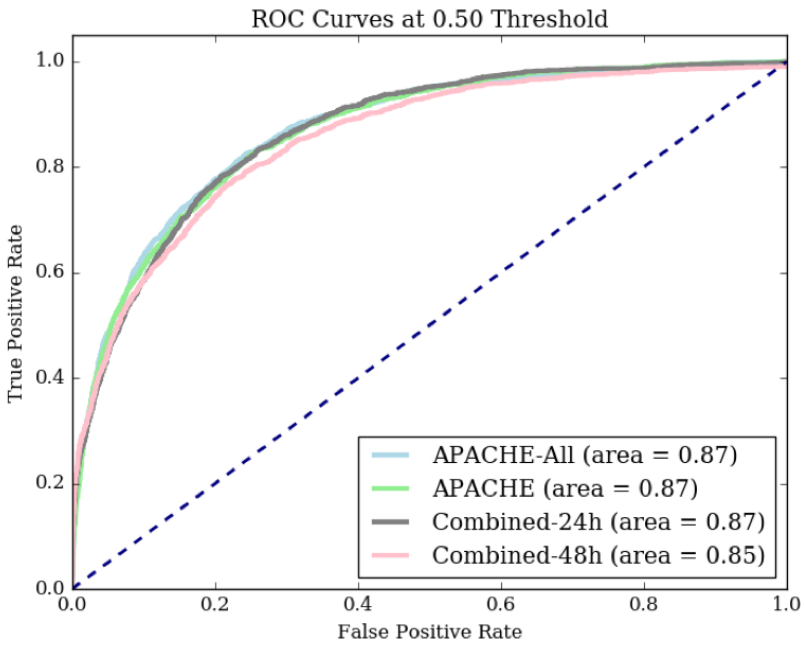

Figure 5-5: ROC Curves for Each Model When High Risk Threshold Set to 50%

Overall, the sequential modeling approach did not perform as well as anticipated in the mortality prediction task and was partially successful in improving upon the results of APACHE. At a high risk threshold of 0.10, both the Combined-24hr and Combined-48hr outperformed the APACHE IV score and APACHE-All, a recalibration of the APACHE IV score on the entire dataset. However, beginning at high risk thresholds above 0.20, both constructed classifiers underperform compared to their APACHE counterparts. Moreover, the additional features found in Combined-48hr, even though they contributed to an improved performance in eICU-48hr-HR model, seemed to have a negligible or somewhat deleterious effect on global classifier performance. Figures 5-4 and 5-5 depict the ROC curves in two contrasting situations. In Figure 5-4, where the high risk thresholds were 0.10, the sequential models (Combined-24h and Combined-48h) outperformed the APACHE based models. Figure 5-5 shows the ROC curves at a high risk threshold of 0.50, where the APACHE models outperformed the sequential models instead.

The confusion matrices shown in Figures 5-2 and 5-3 provide partial evidence for why Combined-24h and Combined-48h have a lower AUC overall despite performing with a higher AUC for high risk patients. In the 0.10 high risk threshold, at a decision point at 0.50, Combined-24h has sensitivity (TP / (TP + FN)) of 656 / (656 + 1120) = 37% and a specificity (TN / (TN + FP)) of 15858 / (15858 +235)= 98.5%. In the 0.50 threshold, however, these values are 26% and 98.8% respectively because

the model incorporates the custom model's underpredicted mortality: with the 0.50 risk threshold, the model is not as able to detect expired patients, and thus, there are fewer false positives and more false negatives. This lower prediction of mortality could stem from the fact that the 50% high risk classifier was only trained on a much smaller number of patients, and this model likely underpredicted mortality within its validation population. This error would penalize the combined model's AUC with more false negatives. At the same time, this suggests that the 50% high risk classifier is calibrated well to the higher risk regions as it tends to avoid overpredicting mortality in high risk patients as done by the base APACHE IV implementation.

The confusion matrices indicate that the 0.10 high risk threshold combined models have an improved false positive and false negative profile, and hence larger AUC, when compared to APACHE and APACHE-All. Suggesting why the 0.10 high risk threshold combined models perform better than those of other risk thresholds is grounded in the three tradeoffs of the high risk threshold selection discussed in Section 3.4 and replicated below:

1. Choosing a high risk threshold that is too small would reduce the ability of a custom high-risk model to fit the underlying physiology of the high risk subpopulation well. When taken to the extreme for example, a very low risk threshold would face similar challenges to that of global severity of illness scores in calibration. *The performance of the 0.1 high risk threshold eICU-24h-HR when compared to that of APACHE suggests that the 0.1 probability and above cohort is structurally meaningful enough to learn high-risk specific feature relationships.*

2. Choosing a high risk threshold that is too high could result in a more difficult prediction task with less training data: For example, only 368 of the 60,000 patients in the study population have a predicted mortality probability of 0.9 or higher. It would be very difficult to learn a model from such few data points with the very high dimensional feature sets found in EHRs. *The 0.1 high risk threshold results in a training cohort of sufficient size. The 0.5 high risk threshold cohort results in a training set of about 2500 patients. In comparison, the 0.1 high risk threshold cohort results in a training set of more than 13,000 patients, which is extremely useful because of the high-dimensionality of the feature set. The 0.5 high risk threshold model is unable to learn feature relationships that enable reductions in both false negative and false positives as well as the 0.1 risk threshold classifier.*

3. Choosing a high risk threshold that is too high can impact the overall benefit the model provides in application and global AUC metrics. An improved classifier

for only patients with a predicted mortality of greater than 90% would only improve performance on less than 0.5% of patients. The sequential model would in large part serve predictions similar to those of APACHE IV as this difference is minimal. *The 0.1 high risk threshold is large enough such that the improved performance also affects the global AUC across the entire dataset.*

Thus, these results suggest that 0.1 is a good candidate for the high risk threshold of the sequential modeling approach.

5.2 Global Calibration

Next, I assessed the calibration of the 0.1 high risk threshold Combined-24h and Combined 48h models in a methodology similar to that contained in Section 4.2. Visualizing the calibration curves of each model and computing the Hosmer-Lemeshow statistic suggests that the Combined models at a high risk threshold of 0.10 are better calibrated than the APACHE and APACHE-All models.

Figure 5-6 contains the calibration curve of each model. As a reference, Figure 5-7 is also provided, which contains the calibration curve of the Combined-24h and Combined-48h models trained on a higher risk threshold, 0.50. Table 5.2 contains the Hosmer-Lemeshow test results for the calibration curves in Figure 5-6.

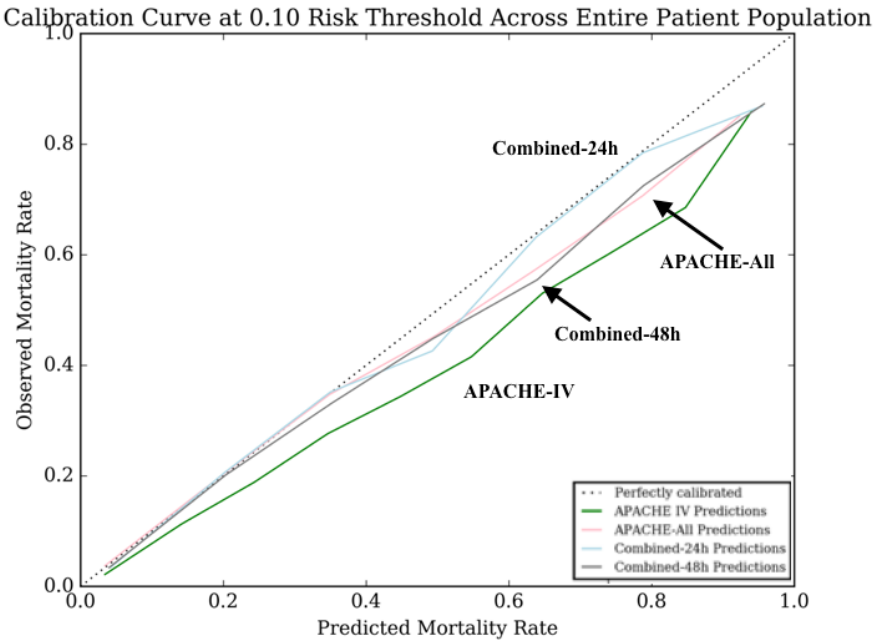

Figure 5-6: Calibration Curves for Sequential Predictors When 0.10 Risk Threshold is Used

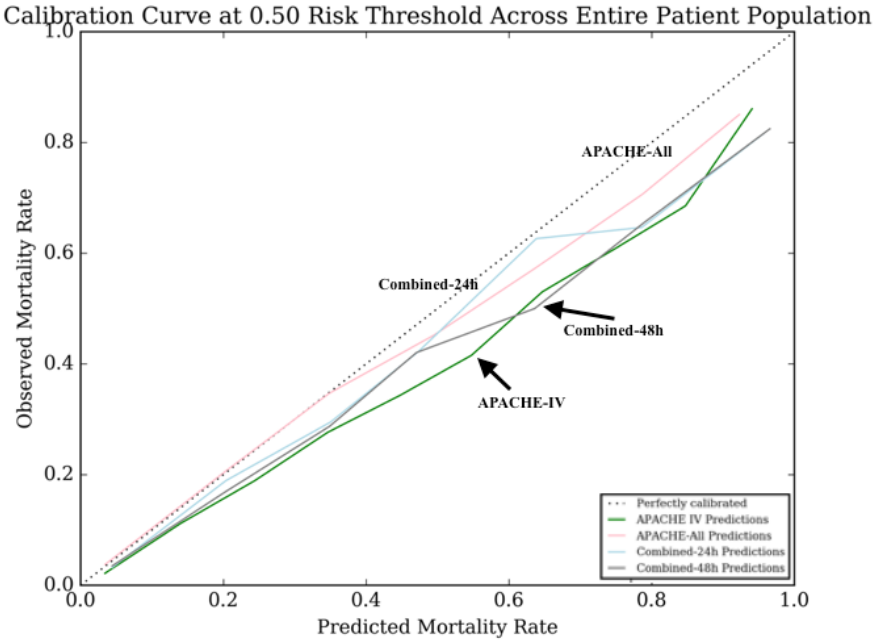

Figure 5-7: Calibration Curves for Sequential Predictors When 0.50 Risk Threshold is Used

Model	C-Statistic	Degrees of Freedom	P-Value
APACHE	141.05	8	<2e-16
APACHE-All	41.419	8	1.74E-06
Combined-24h	30.705	8	0.0001
Combined-48h	44.55	8	4.48E-07

Table 5.2: Hosmer-Lemeshow Test Results for Sequential Models at 0.10 Risk Threshold

The results above strongly support that the Combined-24h and Combined-48h classifiers, when developed using a high risk threshold of 0.10, are better calibrated than the APACHE baseline. Visual inspection of Figure 5-6 shows that the pink Combined-24h line is tied closely to the line of perfect calibration, and this is confirmed by the Hosmer-Lemeshow C-Statistic. While the test p-value itself indicates that there are meaningful deviations from the perfect calibration line, the C-Statistic for the Combined-24h model is the lowest of all models. The Combined-48h has comparable visual and H-L performance to APACHE-All, a recalibrated version of the APACHE features. This was unexpected because the Combined-48h model has significantly better discriminative performance: a potential hypothesis for why this may occur is based on the fact that the differences in both calibration lines from the perfect line occur in the higher risk areas of the curve. While APACHE-All might not have the feature set to capture all the nuances of high risk patients, the Combined-48h might not have enough sample size from those high risk thresholds to learn weights for a feature set of high-dimensionality, and is thus more reliant on patients in lower risk thresholds to help learn the weights for each feature. Lastly, Figure 5-7 demonstrates that the 0.50 high risk threshold Combined models are not well calibrated when compared to APACHE and APACHE-All.

Chapter 6

Cohort Specific Sequential Modeling

While Chapter 5 detailed the evaluation of the Combined-24hr and Combined-48hr models on a validation set developed from the entire eICU-CRD dataset, Chapter 6 discusses the sequential modeling approach applied within specific patient subpopulations. For patient subpopulations, I not only compute the combined model performance, but also examine the beta values for select subpopulations learned by the high risk classifier to generate an intuition for why specific high risk modeling would be useful for the subpopulation.

Table 6.1 summarizes the results from this study for various tested patient subpopulations. AUC values were obtained in triplicate with standard deviations of each AUC value in parenthesis, as done in previous sections. The columns of the table are as follows:

- Criteria: the specific logic applied to each patient to identify whether they are part of the subpopulation or not. For example, "Age $>$ 70" demonstrates a patient subpopulation of all patients in the study that are above 70 years old.
- Total Number: the total number of patients who match the criteria
- High Risk Number: the number of patients who match the criteria and also have a baseline APACHE mortality prediction of greater than 10% (and are thus "high risk")
- APACHE Performance on High Risk Patients: The baseline APACHE AUC on all patients in the subpopulation who are also high risk.
- eICU-24h-HR Performance on High Risk Patients: The eICU-24h-HR (trained only on patients within the subpopulation) AUC on all patients in the subpopulation who are also high risk.

- APACHE Performance on All Patients: The APACHE baseline AUC calculated on all the patients in the validation set, which is comprised of any patient risk level within the subpopulation.
- APACHE-ALL Performance on All Patients: The APACHE-All performance on the same validation set.
- Combined-24hr Performance: The Combined-24hr classifier performance with a high risk threshold of 0.10 on the same validation set.

Criteria	**Total No.**	**High Risk No.**	**APACHE on High Risk**	**eICU-24h-HR on High Risk**	**APACHE on All**	**APACHE-ALL on All**	**Combined-24hr**
Age >70	21924	11117	0.731 (.006)	0.792 (.005)	0.815 (.005)	0.815 (.005)	0.825 (.004)
Ventday1 = 1	13353	8208	0.747 (.006)	0.799 (.003)	0.835 (.003)	0.834 (.004)	0.846 (.002)
GCS_aps >5	14804	10362	0.776 (.007)	0.812 (.008)	0.841 (.002)	0.841 (.004)	0.848 (.002)
Pulse_aps >0	37919	14837	0.761 (.012)	0.800 (.007)	0.867 (.002)	0.868 (.002)	0.872 (.001)

Table 6.1: Results of Subpopulation Sequential Modeling

6.1 Age > 70 Top 25 Beta Values

feature	high_coef
diag_LOWGIBLEED	0.5797079776
amylase_24h	0.4799743024
calcium_24h	0.4652606185
plateletsraw_trend_neg_24h	0.4572197363
base_excessraw_trend_pos_24h	-0.4360061305
diag_S-CABG	0.432407427
calciumraw_trend_neg_24h	0.3772361759
metastaticcancer	0.3487893351
lipaseraw_trend_pos_24h	-0.3073908629
lipasetime_scaled_slope_24h	-0.3065337186
magnesiumtime_scaled_slope_24h	0.3020232832
pao2raw_trend_pos_24h	0.2873012975
troponin_i_24h	0.2788968788
total_troponin_24h	0.263862191
platelets_24h	-0.2620499552
diag_TRAUMHEAD	0.2356818188
lipase_24h	-0.2244354341
diag_CHF	-0.217074506
bicarbonatetime_scaled_slope_24h	-0.2031720306
calciumtime_scaled_slope_24h	0.202695306
hco3time_scaled_slope_24h	0.2021048574
diag_SEPSISPULM	0.1991832502
troponin_traw_trend_neg_24h	0.1974175373
ionized_calciumraw_trend_neg_24h	0.1958337551
raw_wbcraw_trend_neg_24h	0.187619073

Table 6.2: Top Beta Values for Age > 70 Subpopulation

The first subpopulation tested with the sequential modeling approach was that of the elderly population, with age > 70. As age is strongly correlated with mortality and accordingly has a large weight in the APACHE IV score, the elderly population is an especially high-risk cohort. The eICU-24h-HR classifier outperforms the APACHE baseline by 0.06 and the Combined-24h classifier, which uses the eICU-24h-HR high risk model for high risk patients, slightly outperforms the APACHE baseline on the entire subpopulation by 0.01. Interestingly, the beta values learned by the eICU-24h-HR differ from those learned in Section 4.3.1 on the general patient population.

For example, while age was the second highest weight feature in the latter, age as a feature does not appear in the top 25 features for the age-specific high risk classifier. Instead, diagnoses related to or correlated with old age appear with higher weights, such as GI Bleeding [41] and metastatic cancer. Furthermore, the reliance of the model on pancreatic measurements, such as lipase and amylase, suggests that such values are especially diagnostic for the elderly population. However, it is important to note that the elderly subpopulation is still likely a high variance one: there likely exist various different disease conditions and mortality modes within the population, and thus certain feature weights assigned by the model would be very similar to those assigned in the general population.

6.2 Ventday1=1 Top 25 Beta Values

feature	high_coef
magnesiumraw_trend_pos_24h	-0.8292389169
pao2_24h	0.7419987901
diag_S-VALVAO	0.6678395967
admitsource_4	0.6628255659
platelets_24h	-0.5847570716
total_troponin_24h	0.4022225269
admitsource_3	0.3904773615
diag_RHYTHATR	0.3882971204
amylaseraw_trend_pos_24h	-0.3600695383
admitsource_1	-0.3585181905
troponin_traw_trend_neg_24h	0.3544459631
total_troponintime_scaled_slope_24h	0.3401291838
diag_TRAUMHEAD	0.3399515793
diag_UGIBLEED	-0.3371160185
phosphate_24h	0.3001720339
cirrhosis	0.2881357117
ventday1	0.2863836099
diag_CHF	0.2857412491
hemoglobinraw_trend_neg_24h	0.2780089725
diag_PNEUMBACT	-0.2714051436
diag_ODSEDHYP	-0.2713190882
pt_inr_24h	-0.2570360664
magnesiumraw_trend_neg_24h	0.25633363
pao2raw_trend_pos_24h	0.2505776283
diag_S-CABG	0.2486541176

Table 6.3: Top Beta Values for Ventilated Subpopulation

The ventilated subpopulation, like that of age > 70, is a large and diverse one, and as also seen in the age subpopulation, the Combined-24h model obtains a slightly better discriminative performance in the ventilated subpopulation. Several of the high beta features in the model are associated with either ventilation or medical processes that indicate ventilation. For example, open heart procedures such as diag_SVALVAO (aortic valve replacement) commonly receive elective ventilation [42]. The overall pao2 of the patient within the first 24 hours was also diagnostic, interestingly with higher pao2 levels correlating with mortality: this might be due to the fact that patients who

receive stronger ventilation dosages, which thereby increase pao2, are likely at higher risk for mortality. In addition, admitsource_3 and admitsource_4, which correspond to the ER and hospital floor respectively, are positively associated with mortality. This is consistent with a previously conducted study [40]. Lastly, magnesium levels are negatively associated with mortality, suggesting that patients with lower serum magnesium are at risk. This is consistent with another study that found that patients with lower levels of magnesium were more likely to receive ventilation [43].

6.3 GCS APS > 5 Top 25 Beta Values

feature	high_coef
pao2_24h	-0.5544354888
lymphoma	0.4674164563
cpk_24h	0.4589916617
admitsource_3	-0.4430483347
diag_SEPSISUTI	0.403786319
admitsource_6	0.3979028502
bnp_24h	0.3899335738
pao2raw_trend_neg_24h	-0.3789104684
ionized_calcium_24h	0.3771504977
diag_ODSEDHYP	0.3726630308
age	0.3694230177
plateletsraw_trend_pos_24h	-0.3645141403
base_excessraw_trend_pos_24h	-0.3257475175
pao2time_scaled_slope_24h	0.3159328012
diag_CARDARREST	-0.3108017055
admitsource_4	0.2930995309
hemoglobin_24h	0.2703031815
hco3raw_trend_pos_24h	-0.2565664934
cirrhosis	0.2464028761
diag_PNEUMBACT	0.2418052133
raw_sodiumraw_trend_neg_24h	0.238730896
raw_bun_24h	-0.2344270767
troponin_i_24h	0.2340149184
plateletstime_scaled_slope_24h	-0.2318239007
platelets_24h	0.2315938671

Table 6.4: Top Beta Values for GCS APS > 5 Subpopulation

The GCS_aps > 5 subpopulation selects for patients who have some form of medium to severe altered mental status. GCS is a central APS variable that receives a large weight in the APACHE score computation and abnormalities in the GCS score are well-correlated with mortality. As found in the previously analyzed subpopulation, the Combined-24h model performed slightly better than its APACHE analogues. Interestingly, while in the ventilated population the pao2 was positively associated with mortality, in the GCS_aps > 5 subpopulation, the feature is negatively associated with mortality. This could be due to the fact that in the ventilated population, a higher pao2 level is associated with stronger treatment, while in the GCS_aps > 5 subpopulation, a higher pao2 level is more indicative of general patient health and not necessarily ventilation. Secondly, admitsource_6 (admission from the same ICU or Operating Room after surgery) has a higher beta value than previously seen in other subpopulations: this is consistent with the notion that many patients after surgery are unconscious or immobile, and thus would have an elevated GCS_aps score.

6.4 Interpretation of the Logistic Betas

However, it is important to note the impact of feature correlation on the logistic betas. Some of the differences in the beta values assigned to each feature within each subpopulation is likely due to stochasticity in the logistic regression training process. For example, a feature like fio2 (level of oxygenation) is only present if the patient is mechanically ventilated (ventday1), and thus both terms are highly correlated. If the model was looking to use whether a patient was ventilated or not as a feature and it had already learned the weight for ventday1, then the fio2 feature provides no marginal benefit in the prediction task: in the same way, if fio2 was learned first, then ventday1 would not offer any new information. Moreover, the model could learn a partial weight for each feature so that when taken together, both features are able to convey the presence of mechanical ventilation with the weight necessary for the concept in the prediction task. Thus, when examining and analyzing the logistic betas, while it is meaningful to discuss general trends and positive and negative correlations with the end mortality prediction task, the raw values of each feature weight are likely have high variance.

Nevertheless, these results suggest that subpopulations of high risk patients have meaningful structure. The sequential modeling approach, Combined-24h, outperformed APACHE baselines and the APACHE-All control in each subpopulation. Inspection of the logistic betas used in the high risk prediction task demonstrate subpopulation-based weight learning for each model, supporting the notion that the sequential model learns meaningful relationships between certain features and the

mortality outcome in a subpopulation-specific manner.

Chapter 7

Conclusion

This thesis detailed the creation of a sequential model for in-hospital mortality prediction in the ICU by developing a two-stage prediction process. First, patients would be designated as high risk or low risk. Second, mortality would be predicted as follows: for low risk patients, patient mortality prediction probabilities are the same as APACHE. For high risk patients, patient mortality prediction probabilities were obtained from a custom high-risk trained classifier called eICU-24h-HR or eICU-48h-HR.

Chapters 4-6 provide evidence to answer key implementation details for how such a two-stage prediction process would work:

1. Are the additional features extracted in Section 3.5 able to enhance the model?s discriminative ability for high risk patients?
2. What high risk threshold, if any, is best for creating a custom high risk classifier?
3. What is the overall impact on *discrimination* of this secondary customization to the APACHE model?
4. What is the overall impact on *calibration* of this secondary customization to the APACHE model?
5. Is "high risk" vs. "low risk" the only subcohort split that is enhanced by this approach?

Section 7.1 details the results of the thesis in the context of these five questions. Section 7.2 addresses the limitations of the thesis and future work that the thesis motivates. Lastly, Section 7.3 discusses how the results of the thesis could impact physician workflow and risk prediction in the ICU.

7.1 Summary of Results

First, in Chapter 4, two high risk classifiers were developed, eICU-24h-HR and eICU-48h-HR, that both outperformed the APACHE baseline predictor and the recalibrated APACHE-All model. This supports the earlier hypothesis that there are additional features not contained in the APACHE logic that are useful for predicting mortality in high risk patients, some of which are captured by eICU-24h-HR and eICU-48h-HR. The analysis in Chapter 5 helped provide guidance on the implementation of the sequential modeling approach. A risk threshold of 0.10 in the Combined-24h and Combined-48h outperformed the APACHE and APACHE-All predictions, whereas others did not; this helped identify 0.10 as the "optimal" threshold within this study, and this choice was validated by both examining the relative abilities of each classifier to predict mortality in a discriminative and calibrated way. The 0.10 risk threshold Combined-24h classifier was not only moderately more discriminative than APACHE and APACHE-all but seemed also much better calibrated, as indicated by visual inspection of the calibration curve and the Hosmer-Lemeshow test. Lastly, the results in Chapter 6 show that the sequential modeling approach could be successfully applied to subcohorts of the general population in eICU-CRD. Thus, in summary, this thesis supports the hypothesis that a two-stage risk-based cohort method of mortality prediction can enhance both the discrimination and calibration of a mortality model.

7.2 Limitations and Future Work

However, this thesis is limited by two main factors that motivate future work within the field: a limited dataset size and interpretability.

A larger dataset should enable the high risk classifiers, especially those that leverage the high-dimensional 48hr feature set, to obtain better performance. The eICU-CRD contained 60,000 admissions with APACHE related information, but only 3,000 of these admissions had APACHE risk predictions of 0.50 or higher. Accordingly, we saw poorer performance in the custom high risk classifiers when the higher risk threshold was increased. With a larger data set, there could be enough samples even within the high risk thresholds above 0.50, resulting in more robust training for the eICU-24h-HR and eICU-48h-HR models. We could thus expect that the drop off in model performance as the risk threshold increases will be dampened. With this additional dataset, we could also expect less noise in the results in Figures 4-1 and 5-1, which depict the linear trends of model performance over the various risk thresholds. Moreover, we could see the same effects on the calibration curves, which also visually depict this noise.

A larger dataset would also enable more nuanced cohort-specific models. The subcohorts in Chapter 6 are somewhat general, each selecting more than 10-15% of the study population. In contrast, a larger dataset could enable much more focused sequential models. Attempts to perform diagnosis based sequential modeling, such as selecting only patients who present with the CARDARREST condition, were unsuccessful in the eICU-CRD dataset due to low sample size. With a larger dataset, however, more parsimonious cohort selection could identify even more subpopulation-specific feature relationships than currently found in Chapter 6.

A second key limitation of this study is the intrepretability of the features learned by each model. The construction of over 1000 features for the high risk prediction task allows the model to capture more nuances of the population but at the same time makes it much harder to understand. For example, there might be little clinical intuition for why a feature such as "platelets_trend_neg_presence24h" might have a higher weight than "platelets_trend_neg_raw_slope48h" in a high risk model and moreover, due to the highly correlated nature of such features and the stochasticity of the training process, the logistic regression introduces randomness to the weights for each feature. Thus, two high risk models that obtain very similar performance characteristics might leverage very different feature subsets of the overall 24 hour and 48 hour feature sets constructed in Section 3.5. When contrasted to APACHE, which uses a limited and less correlated feature set of only easy to intuit variables, the high risk models are thus much more of a black box.

In addition, there exist additional avenues of future work. I did not evaluate high risk classifier performance or sequential model performance on high risk thresholds below 0.10 or above 0.75, but such risk thresholds could also be tested. Second, I could look into adding low-risk specific features to augment those of APACHE, and thus the sequential modeling approach could use, for the low risk population, a custom classifier as well. Lastly, I could look into expanding the feature set more, including interaction terms between various features to find non-linear modes in the ICU, such as the treatment response to a vasopressor for a septic patient.

7.3 The Sequential Modeling Approach in the ICU

The sequential modeling approach offers a new perspective on mortality prediction in the ICU. Traditional severity of illness scores have focused on simpler feature sets that could apply to a wide range of patients. With the increased digitization of the patient medical record and the emergence of TeleICU services like that of Philips eICU, more

detailed machine learning models are empowered to provide personalized recommendations on a variety of in-hospital prediction tasks. This suggests that the sequential modeling approach developed in this thesis is feasible in the ICU itself. Physicians could receive the mortality estimate from Combined-24h after 24 hours simultaneously with the APACHE score, and additionally could receive input from Combined-48h at the 48 hour point in the admission. Furthermore, cohort-specific sequential modeling is feasible in today's ICU. For example, if a CARDARREST sequential model shows much greater performance when compared to APACHE, then physicians could request mortality predictions from a CARDARREST-specific Combined-24h model for any patients presenting with cardiac arrest. Thus, the results of thesis have useful applications in the current ICU workflow and could be significantly enhanced with future work.

Chapter 8

References

[1] Lundgren-Laine H, Kontio E, Perttila J, Korvenranta H, Forsstrom J, Salantera S. Managing daily intensive care activities: An observational study concerning ad hoc decision making of charge nurses and intensivists. Critical Care. 2011;15(4):R188. doi:10.1186/cc10341.

[2] Aitken, L. M., Marshall, A. P., Elliott, R. and McKinley, S. (2009), Critical care nurses' decision making: sedation assessment and management in intensive care. Journal of Clinical Nursing, 18: 36-45. doi:10.1111/j.1365-2702.2008.02318.x

[3] Gao F, Melody T, Daniels DF, Giles S, Fox S. The impact of compliance with 6-hour and 24-hour sepsis bundles on hospital mortality in patients with severe sepsis: a prospective observational study. Critical Care. 2005;9(6):R764-R770. doi:10.1186/cc3909.

[4] Esteban, et al. Extubation Outcome after Spontaneous Breathing Trials with T-Tube or Pressure Support Ventilation. American Journal of Respiratory and Critical Care Medicine. 1996; doi: 10.1164/ajrccm.156.2.9610109.

[5] Hebert, et al. A Multicenter, Randomized, Controlled Clinical Trial of Transfusion Requirements in Critical Care. N Engl J Med 1999; 340:409-417. doi: 10.1056/NEJM199902113400601.

[6] Peberdy, et al. Part 9: Post-Cardiac Arrest Care. Circulation. 2010;122:S768-S786, originally published October 17, 2010. Retrieved May 24, 2017 from http://circ.ahajournals.org/content/122/18_suppl_3/S768.

[7] Acute Stroke Protocol. Boston Medical Center. Retrieved May 24, 2017 from https://www.bmc.org/stroke-and-cerebrovascular-center/medical-professionals/acute-stroke-protocol.

[8] Zimmerman JE, Kramer AA, McNair DS, Malila FM. Acute Physiology and Chronic Health Evaluation (APACHE) IV: hospital mortality assessment for today's critically ill patients. Crit Care Med. 2006;34(5):1297-1310.

[9] Le Gall J, Lemeshow S, Saulnier F. A New Simplified Acute Physiology Score (SAPS II) Based on a European/North American Multicenter Study. JAMA. 1993;270(24):2957-2963. doi:10.1001/jama.1993.03510240069035

[10] Rapsang AG, Shyam DC. Scoring systems in the intensive care unit: A compendium. Indian Journal of Critical Care Medicine: Peer-reviewed, Official Publication of Indian Society of Critical Care Medicine. 2014;18(4):220-228. doi:10.4103/0972-5229.130573.

[11] Hosmer, D. W. and Lemeshow, S. A goodness-of-fit test for the multiple logistic regression model. Communications in Statistics, A10, 1043-1069 (1980).

[12] Bouch, Christopher and Thompson, Jonathan. Severity scoring systems in the critically ill. Continuing Education in Anaesthesia, Critical Care & Pain (2008). doi:10.1093/bjaceaccp/mkn033.

[13] Manganaro, L and Stark, M. APACHE Foundations User Guide. Cerner Corporation. (c) 2010.

[14] Apache IV Calculator. N.p., n.d. Web. Retrieved May 24, 2017 from http://intensivecarenetwork.com/Calculators/Files/Apache4.html.

[15] APACHE IV Calculator Based on Knaus WA, Wagner DP, Draper EA, Zimmerman JE. The APACHE III prognostic system: risk prediction of hospital mortality for critically ill hospitalized adults. Chest 1991; 100:1619-1636.

[16] Lemeshow S, Teres D, Klar J, Avrunin JS, Gehlbach SH, Rapoport J. Mortality Probability Models (MPM II) based on an international cohort of intensive care unit patients. JAMA. 1993;270(20):2478-2486.

[17] Beck DH, Smith GB, Taylor BL. The impact of low-risk intensive care unit admissions on mortality probabilities by SAPS II, APACHE II and APACHE III. Anaesthesia. 2002; 57(1):21-26.

[18] Rowan KM, Kerr JH, Major E, McPherson K, Short A, Vessey MP. Intensive Care Society's Acute Physiology and Chronic Health Evaluation (APACHE II) study in Britain and Ireland: a prospective, multicenter, cohort study comparing two methods for predicting outcome for adult intensive care patients. Crit Care Med. 1994;22(9):1392-1401.

[19] Lee SM, An WS. New clinical criteria for septic shock: serum lactate level as new emerging vital sign. Journal of Thoracic Disease. 2016;8(7):1388-1390. doi:10.21037/jtd.2016.05.55.

[20] Scikit-learn: Machine Learning in Python, Pedregosa et al., JMLR 12, pp. 2825-2830, 2011.

[21] MIT Lab for Computational Physiology. (n.d.). EICU Collaborative Research Database. Retrieved May 24, 2017 from http://eicu-crd.mit.edu/about/eicu/.

[22] eICU Program. Philips Healthcare. Retrieved 24 May 2017 from http://www.usa.philips.com/healthcare/product/HCNOCTN503/eicu-program-telehealth-for-the-intensive-care-unit.

[23] Lilly CM, et al. A Multi-Center Study of ICU Telemedicine Reengineering of Adult Critical Care. CHEST. 2014 Mar 1; 145(3): 500-7

[24] Hunter, J. D. Matplotlib: A 2D graphics environment. Computing In Science & Engineering 9, pp. 90 - 93. Retrieved May 24, 2017 from https://matplotlib.org/.

[25] Google Sheets - create and edit spreadsheets online, for free. (n.d.). Retrieved May 24, 2017, from https://www.google.com/sheets/about/.

[26] Charlson, Mary E.; Pompei, Peter; Ales, Kathy L.; MacKenzie, C. Ronald (1987). A new method of classifying prognostic comorbidity in longitudinal studies: Development and validation. Journal of Chronic Diseases. 40 (5): 373-83. doi:10.1016/0021-9681(87)90171-8

[27] Duh, S., and Cook, J. D. (2015, August 15). LABORATORY REFERENCE RANGE VALUES. Retrieved May 23, 2017, from http://www.stedmansonline.com/webFiles/Dict-Stedmans28/APP17.pdf.

[28] Mayo Clinic Medical Laboratories. (n.d.). Test ID: TPNT Troponin T, Serum. Retrieved May 24, 2017, from http://www.mayomedicallaboratories.com/test-catalog/Clinical and Interpretive/82428

[29] Mayo Clinic. (2015, May 08). Low hemoglobin count. Retrieved May 24, 2017, from http://www.mayoclinic.org/symptoms/low-hemoglobin/basics/definition/sym-20050760

[30] The Myositis Foundation. (2015, January). Blood Tests. Retrieved May 24, 2017, from http://www.myositis.org/learn-about-myositis/diagnosis/blood-tests

[31] Cleveland Clinic. (2016, October). B-type Natriuretic Peptide (BNP) Blood Test. Retrieved May 24, 2017, from https://my.clevelandclinic.org/health/articles/b-type-natriuretic-peptide-bnp-bloodtest

[32] Medical Definition of Absolute neutrophil count. (n.d.). Retrieved May 24, 2017, from http://www.medicinenet.com/script/main/art.asp?articlekey=20030

[33] Mayo Clinic Staff. (2016, June 15). Lymphocytosis. Retrieved May 24, 2017, from http://www.mayoclinic.org/symptoms/lymphocytosis/basics/definition/sym-20050660

[34] Mayo Clinic Staff. (2016, July 02). Blood urea nitrogen (BUN) test. Retrieved May 24, 2017, from http://www.mayoclinic.org/tests-procedures/blood-urea-nitrogen/details/results/rsc-20211280

[35] Chen, Y. (2015, January 27). WBC count. Retrieved May 24, 2017, from https://medlineplus.gov/ency/article/003643.htm

[36] Scales K, Pilsworth J (2008) The importance of fluid balance in clinical practice. Nursing Standard. 22, 47, 50-57. Date of acceptance: June 12 2008.

[37] Charlson, M. (n.d.). Charlson Comorbidity Index (CCI). Retrieved May 24, 2017, from https://www.mdcalc.com/charlson-comorbidity-index-cci

[38] Lemeshow S, et al. Mortality probability models for patients in the intensive care unit for 48 or 72 hours: a prospective, multicenter study. Critical Care Medicine. 1994. Sep;22(9):1351-8.

[39] Lele, Subhash R., Keim, Jonah L., and Solymos, Peter. (2017, Feb 28) Package ResourceSelection. Retrieved May 24, 2017 from https://cran.r-project.org/web/packages/ResourceSelection/ResourceSelection.pdf.

[40] Datta A, Kar A, Ahmed A. Source of ICU admission: does it really matter? Critical Care. 2015;19(Suppl 1):P562. doi:10.1186/cc14642.

[41] Ghassemi KA, Jensen DM. Lower GI Bleeding: Epidemiology and Management. Current gastroenterology reports. 2013;15(7):10.1007/s11894-013-0333-5. doi:10.1007/s11894-013-0333-5.

[42] Jayalakshmi, T., Punnose, V., Kumar, A.S. et al. Ventilatory support following open heart surgery. Indian J Thorac Cardiovasc Surg (1985) 4: 28. doi:10.1007/BF02664081

[43] Guo, Su-Er, et al. The Relationship of Magnesium and Phosphorus to Mechanical Ventilation and Mortality in the Chronically Critically Ill. Midwest Nursing Research Society Conference. (2011)

[44] Hug CW, Szolovits P. ICU Acuity: Real-time Models versus Daily Models. AMIA Annual Symposium Proceedings. 2009;2009:260-264.

Appendix A

Feature Set Features

List of All Features Used in APACHE Feature Set

age
aids
hepaticfailure
lymphoma
metastaticcancer
leukemia
immunosuppression
cirrhosis
ventday1
admitsource_0
admitsource_1
admitsource_2
admitsource_3
admitsource_4
admitsource_5
admitsource_6
admitsource_7
admitsource_8
emergencysurg
preiculos
diagnosis
thrombolytics
unable_gcs
adj_gcs
pulse_aps
mabp_aps
temperature_aps
resp_aps
pao2_aps
hematocrit_aps
wbc_aps
creatinine_aps
urine_aps
bun_aps
sodium_aps
albumin_aps
bilirubin_aps
glucose_aps
acid_base_aps
gcs_aps
diag_AMI
diag_SEPSISPULM
diag_CHF
diag_CVASTROKE
diag_DKA
diag_S-CABG
diag_SEPSISUTI
diag_RHYTHATR
diag_PNEUMBACT
diag_CARDARREST
diag_EMPHYSBRON
diag_UNSTANGINA
diag_UGIBLEED
diag_COMA
diag_M-RESOTHER
diag_SEIZURES
diag_ICH
diag_RESPARREST
diag_SEPSISUNK
diag_LOWGIBLEED
diag_ARENFAIL
diag_UNKGIBLEED
diag_SEPSISGI
diag_HYPERTENS
diag_RHYTHCON
diag_S-CAROTEND
diag_PULMEMBOL
diag_S-VALVAO
diag_ODSEDHYP
diag_TRAUMHEAD
diag_SEPSISCUT
diag_CP-UNK
diag_PNEUMOTHER
diag_SEPSISOTH
diag_ACIDBASE
diag_HYPOVOLEM
diag_SDH
diag_S-CRANNEO
diag_S-GIOBSTRX
diag_RHYTHVEN
diag_M-CAROTHER
diag_S-GIPERFOR
diag_ODOTHER
diag_S-LUNGCA
diag_PNEUMASPIR
diag_ODSTREET
diag_DRUGWITHD
diag_S-AAANEUR
diag_AIROBSTRX
diag_PLEUREFFUS
diag_ASTHMA
diag_M-NEUROTH
diag_OTH_MI
diag_ODANALG
diag_STABANGINA
diag_PANCRITIS
diag_NEURONEO
diag_ANEMIA
diag_ARTHROMBUS
diag_S-SPINDECO
diag_ARDS
diag_SAH/IANEUR

diag_ODALCOH
diag_S-CHOLANGI
diag_S-LGINTCA
diag_S-CABGAOV
diag_GIOBSTRX
diag_S-SPINFUS
diag_TRHEADMULT
diag_DVT
diag_HYPOGLYCEM
diag_M-VASOTHER
diag_DHNKA
diag_M-GIOTHER
diag_CARDIOMYOP
diag_CELLULITIS
diag_S-TRAUMEXT
diag_ODDEPRES
diag_HEPENCEPH
diag_S-NEUOTHER
diag_LUNGCA
diag_S-CELLINFX
diag_S-FEMPGRAF
diag_S-ORTHOTH
diag_CARDSHOCK
diag_S-GIOTHER
diag_S-SDH
diag_S-VALVMR
diag_S-VALVMI
diag_ANAPHYLAX
diag_ENCEPHALOP
diag_ACUHEPFAIL
diag_TRHEADFACE
diag_DISAANEUR
diag_S-PLEURDIS
diag_PNEUMOTHOR
diag_M-MENOTHER
diag_TRAUMCHEST
diag_S-CAROTHER
diag_GIPERFORAT
diag_RESLUNGDIS
diag_PULMONHEM
diag_S-SAH/ICA
diag_TRHEADEXTR
diag_HEMORRHAGE
diag_S-GICOMPL
diag_S-VASOTHER
diag_TRCHESTMUL
diag_S-AFEMGRAF
diag_TRAUMEXTR
diag_TRAUMSPINE
diag_TRHEADCHES
diag_RENINFX
diag_S-GIOTHCA
diag_VARICBLEED
diag_PERICEFFUS
diag_M-GUOTHER
diag_TRHEADSPIN
diag_ETOHWITHD
diag_ATELECTAS
diag_S-RESOTHER
diag_S-PANCRECA
diag_S-TOTALHIP
diag_S-GENOTHER
diag_ATYPCHSTPA
diag_S-LARTRACA
diag_OTHERANEUR
diag_MENINGITIS
diag_S-TAANEUR
diag_COAGULOP
diag_S-GIVASISC
diag_S-ICH
diag_S-ENDOTHER
diag_S-THROMBWA
diag_TRCHESTABD
diag_S-TRANSPHE
diag_TRSPINMULT
diag_SAH/AVMAL
diag_S-THOROTH
diag_S-NEPHRNEO
diag_S-HERNIA
diag_S-PERIEFFU
diag_PERITOHEM
diag_S-DIVERTIC
diag_S-CABGREDO
diag_S-OTHGRAFT
diag_S-RESPINFX
diag_TRCHESTEXT
diag_S-CONDXMAP
diag_S-CRANCOMP
diag_S-APPENDIX
diag_S-OTHANEUR
diag_S-CSECTION
diag_PNEUMVIRAL
diag_S-VALVAM
diag_S-ORASINCA
diag_S-KIDTRAN
diag_S-TRACHEOT
diag_TRAUMABD
diag_CHOLANGIT
diag_S-HYSTERCA
diag_PREHEMMON
diag_S-AVMALFOR
diag_S-OBESITY
diag_S-CABGWOTH
diag_S-FRXOTHER
diag_S-BURRHOLE
diag_S-GIFISTAB
diag_S-CABREVAL
diag_S-SHUNTS
diag_M-MUSOTHER
diag_CP-GASTRO
diag_M-NMUSOTH
diag_S-BRAINBIO
diag_S-FEMFGRAF
diag_OHYDROCEPH
diag_S-THYROID
diag_S-CABGMVR
diag_S-TRAUMPEL
diag_S-AICD
diag_S-OBNEPHRO
diag_TRAUMFACE
diag_S-ESOPHCA
diag_S-TRAUMHEA
diag_S-AMPUTATN
diag_M-TRAUMOTH
diag_S-LIVTRAN
diag_S-TOTALKNE
diag_TRCHESTSPI
diag_GIABSCYST
diag_S-CRANERVE
diag_S-TRAUMABD
diag_S-EMBWANES
diag_S-SPINNEO
diag_S-SPLEEN
diag_ENDOCARDIT
diag_S-SPINEOTH
diag_HEMATOMAS
diag_TRABDMULT
diag_S-VASCOMPL
diag_TREXTRMULT
diag_TRFACEMULT
diag_RHABDOMYO
diag_S-HIATALH
diag_INFLAMBOWD
diag_THROMBOCYT
diag_TRSPINEXTR
diag_S-GIABSCYS
diag_WEANVENT
diag_NEURABSCES
diag_S-CYSTNEO
diag_TRAUMPELV
diag_RENALOBST
diag_S-TAANEUDI
diag_S-OTHINFX
diag_S-SKINOTH
diag_S-TREXTMUL
diag_S-HYSTFIB
diag_GIVASINSUF
diag_S-AAANEUUP
diag_S-STOMACCA
diag_S-ESOPHOTH

diag_MYASTHENIA
diag_S-LUNGBIOP
diag_GUILLIANBS
diag_S-CHESTMAL
diag_DIVERTIC
diag_PRIMHYPERT
diag_RENALBLEED
diag_DRUGTOXIC
diag_S-COSMETIC
diag_PERITAMPON
diag_S-CARDCOMP
diag_S-BENTUMOR
diag_S-CABGMIV
diag_S-TRABMULT
diag_SEPSISGYN
diag_COLONRECCA
diag_S-TRCHABD
diag_S-SUPROSCA
diag_SLEEPAPNEA
diag_ENCEPHALIT
diag_S-STEREOPR
diag_M-HEMOTHER
diag_HYPOTHERM
diag_TRPELVMULT
diag_PERITONIT
diag_CP-MUSCLSK
diag_PERICARDIT
diag_S-CRANINFX
diag_S-TRHEMULT
diag_S-CABGDVAL
diag_S-DIALGRAF
diag_S-AAANEUDI
diag_TRSPINFACE
diag_S-SKINGRAF
diag_NEUTROPEN
diag_S-SPINCOMP
diag_TRABDEXTR
diag_S-NEPHROTH
diag_S-THORREDU
diag_CP-RESP
diag_TRCHESTFAC
diag_OTHERGICA
diag_SICKLECELL
diag_S-LGIBLEED
diag_S-THROMWOA
diag_S-UGIBLEED
diag_CARDCOMP
diag_HEMOTHORAX
diag_S-PANCREAT
diag_PANCYTOPEN
diag_S-OBSTROTH
diag_TRHEADABD
diag_EPIHEMATOM
diag_PANCREATCA
diag_S-MASTECT
diag_POSTPARHEM
diag_S-SEIZURE
diag_S-SMINTCA
diag_S-AILGRAFT
diag_TREXTRFACE
diag_S-TRABEXTR
diag_S-SLEEPAPN
diag_TRPELVEXTR
diag_S-VENTRIC
diag_S-FACIAL
diag_S-CSFLEAK
diag_S-OOPHOREC
diag_HEPRENSYN
diag_PRE-ECLAMP
diag_S-INFBOWDI
diag_RENALNEO
diag_PNEUMFUNG
diag_S-CVTUMOR
diag_S-EPIHEMA
diag_S-PERICARD
diag_S-CARDASD
diag_AML
diag_LARYNXCA
diag_TRHEADPELV
diag_S-TRAUMFAC
diag_TRCHESTPEL
diag_S-ADRENAL
diag_S-VALVTRI
diag_S-OBSTRNEO
diag_TRABDPELV
diag_S-TRCHMULT
diag_S-TRCHEXTR
diag_S-CABGROTH
diag_S-METENOTH
diag_S-TRHEEXTR
diag_S-PERITON
diag_S-TRAUMOTH
diag_S-GIBLEOTH
diag_S-PELVEXEN
diag_S-TRAUMCHE
diag_S-TRAUMSPI
diag_HYPERSTORM
diag_ESOPHAGCA
diag_NONHODGLYM
diag_SMOKEINHAL
diag_BLOODREACT
diag_S-TURBPH
diag_S-CYSTOTH
diag_S-CABGMINI
diag_S-GASTROST
diag_S-TRHEFACE
diag_S-TRPELEXT
diag_PNEUMPARAS
diag_S-SPINDEV
diag_S-PARATHYR
diag_HYPERTHERM
diag_TRABDSPINE
diag_S-EMBWOANE
diag_TRPELVSPIN
diag_S-REMGRAFT
diag_S-TRFACMUL
diag_ORALCA
diag_HYPOTHYMYX
diag_ADDISON
diag_S-TREXTFAC
diag_S-TRSPIMUL
diag_S-ECTOPIC
diag_S-THESOPCA
diag_ALL
diag_S-HEMOTHER
diag_S-TRABPELV
diag_S-TRHECHES
diag_KIDNEYTRAN
diag_TRABDFACE
diag_S-CARCONG
diag_NEARDROWN
diag_STOMACHCA
diag_S-REPBLAD
diag_POISON
diag_HEATSTROKE
diag_S-SPBPH
diag_S-BPFISTUL
diag_S-TRPELMUL
diag_S-PORTSHUN
diag_ALS
diag_S-TURCA
diag_S-VALVPULM
diag_S-VARBLEED
diag_S-TRSPIEXT
diag_CLL
diag_NTCOMA
diag_SEPARTHRIT
diag_TRACHCA
diag_S-TAANEURU
diag_S-TRHEABD
diag_S-DILWANES
diag_PEPULCER
diag_S-RENGRAFT
diag_S-DILWOANE
diag_S-THYPARA
diag_S-VENANEUR
diag_S-BULLECT
diag_S-TRHESPIN
diag_S-VENAFILT
diag_LIVERTRAN

diag_LEUKOTHER
diag_S-VASCANAS
diag_S-CARDVSD
diag_CRANEPALSY
diag_S-RUPOVCYS
diag_THYROIDNEO
diag_CML
diag_S-CABGVALV
diag_S-TRCHFACE
diag_MIXEDCTDIS
diag_S-PELVREL
diag_S-TRABFACE
diag_ADRENNEO
diag_SYSTLUPUS
diag_HODGKINLYM
diag_S-TRABSPIN
diag_RHARTHRIT
diag_S-TRCHSPIN
diag_VASCULITIS
diag_S-LYMPHDIS
diag_S-CAPD
diag_TRPELVFACE
diag_S-PVENSHUN
diag_S-ORCHIECT
diag_S-TRSPIFAC
diag_MYOCONTUS
diag_S-TRCHPELV
diag_S-TRHEPELV
diag_S-LYMPHDSX
diag_PAPMUSCLE
diag_S-NONHODGL
diag_S-TRPELSPI
diag_S-PERITLAV
diag_S-PELVEXM
diag_VIRALMYOSI
diag_S-HODGKINL
diag_SCLERODERM
diag_S-TRPELFAC
diag_S-VENACLIP
diag_S-SYMPATH

List of All Features Used in 48 Hour Feature Set

diag_AMI
diag_SEPSISPULM
diag_CHF
diag_CVASTROKE
diag_DKA
diag_S-CABG
diag_SEPSISUTI
diag_RHYTHATR
diag_PNEUMBACT
diag_CARDARREST
diag_EMPHYSBRON
diag_UNSTANGINA
diag_UGIBLEED
diag_COMA
diag_M-RESOTHER
diag_SEIZURES
diag_ICH
diag_RESPARREST
diag_SEPSISUNK
diag_LOWGIBLEED
diag_ARENFAIL
diag_UNKGIBLEED
diag_SEPSISGI
diag_HYPERTENS
diag_RHYTHCON
diag_S-CAROTEND
diag_PULMEMBOL
diag_S-VALVAO
diag_ODSEDHYP
diag_TRAUMHEAD
age
aids
hepaticfailure
lymphoma
metastaticcancer
leukemia
immunosuppression
cirrhosis
ventday1
admitsource_0
admitsource_1
admitsource_2
admitsource_3
admitsource_4
admitsource_5
admitsource_6
admitsource_7
admitsource_8
emergencysurg
preiculos
diagnosis
thrombolytics
unable_gcs
adj_gcs
pulse_aps
mabp_aps
temperature_aps
resp_aps
pao2_aps
hematocrit_aps
wbc_aps
creatinine_aps
urine_aps
bun_aps
sodium_aps
albumin_aps
bilirubin_aps
glucose_aps
acid_base_aps
gcs_aps
bicarbonate_24h
chloride_24h
calcium_24h
magnesium_24h
pt_inr_24h
hco3_24h
base_excess_24h
ionized_calcium_24h
lactate_24h
troponin_i_24h
troponin_t_24h
total_troponin_24h
amylase_24h
lipase_24h
platelets_24h
hemoglobin_24h
phosphate_24h
pao2_24h
fio2_24h
cpk_24h
bnp_24h
fibrinogen_24h
neutrophil_24h
lymphocyte_24h
raw_sodium_24h
raw_creatinine_24h
raw_bun_24h
raw_wbc_24h
raw_albumin_24h
raw_ph_24h
raw_bilirubin_24h
raw_hct_24h
bicarbonate_48h
chloride_48h
calcium_48h
magnesium_48h
pt_inr_48h
hco3_48h
base_excess_48h
ionized_calcium_48h
lactate_48h
troponin_i_48h
troponin_t_48h
total_troponin_48h
amylase_48h
lipase_48h
platelets_48h
hemoglobin_48h
phosphate_48h
pao2_48h
fio2_48h
cpk_48h
bnp_48h
fibrinogen_48h
neutrophil_48h
lymphocyte_48h
raw_sodium_48h
raw_creatinine_48h
raw_bun_48h
raw_wbc_48h
raw_albumin_48h
raw_ph_48h
raw_bilirubin_48h
raw_hct_48h
bicarbonatetime_scaled_slope_24h
chloridetime_scaled_slope_24h
calciumtime_scaled_slope_24h
magnesiumtime_scaled_slope_24h
pt_inrtime_scaled_slope_24h
hco3time_scaled_slope_24h
base_excesstime_scaled_slope_24h
ionized_calciumtime_scaled_slope_24h
lactatetime_scaled_slope_24h
troponin_itime_scaled_slope_24h
troponin_ttime_scaled_slope_24h
total_troponintime_scaled_slope_24h
amylasetime_scaled_slope_24h
lipasetime_scaled_slope_24h
plateletstime_scaled_slope_24h
hemoglobintime_scaled_slope_24h
phosphatetime_scaled_slope_24h
pao2time_scaled_slope_24h

fio2time_scaled_slope_24h
cpktime_scaled_slope_24h
bnptime_scaled_slope_24h
fibrinogentime_scaled_slope_24h
neutrophiltime_scaled_slope_24h
lymphocytetime_scaled_slope_24h
raw_sodiumtime_scaled_slope_24h
raw_creatininetime_scaled_slope_24h
raw_buntime_scaled_slope_24h
raw_wbctime_scaled_slope_24h
raw_albumintime_scaled_slope_24h
raw_phtime_scaled_slope_24h
raw_bilirubintime_scaled_slope_24h
raw_hcttime_scaled_slope_24h
bicarbonatetime_scaled_slope_48h
chloridetime_scaled_slope_48h
calciumtime_scaled_slope_48h
magnesiumtime_scaled_slope_48h
pt_inrtime_scaled_slope_48h
hco3time_scaled_slope_48h
base_excesstime_scaled_slope_48h
ionized_calciumtime_scaled_slope_48h
lactatetime_scaled_slope_48h
troponin_itime_scaled_slope_48h
troponin_ttime_scaled_slope_48h
total_troponintime_scaled_slope_48h
amylasetime_scaled_slope_48h
lipasetime_scaled_slope_48h
plateletstime_scaled_slope_48h
hemoglobintime_scaled_slope_48h
phosphatetime_scaled_slope_48h
pao2time_scaled_slope_48h
fio2time_scaled_slope_48h
cpktime_scaled_slope_48h
bnptime_scaled_slope_48h
fibrinogentime_scaled_slope_48h
neutrophiltime_scaled_slope_48h
lymphocytetime_scaled_slope_48h
raw_sodiumtime_scaled_slope_48h
raw_creatininetime_scaled_slope_48h
raw_buntime_scaled_slope_48h
raw_wbctime_scaled_slope_48h
raw_albumintime_scaled_slope_48h
raw_phtime_scaled_slope_48h
raw_bilirubintime_scaled_slope_48h
raw_hcttime_scaled_slope_48h
bicarbonateraw_trend_neg_24h
chlorideraw_trend_neg_24h
calciumraw_trend_neg_24h
magnesiumraw_trend_neg_24h
pt_inrraw_trend_neg_24h
hco3raw_trend_neg_24h
base_excessraw_trend_neg_24h
ionized_calciumraw_trend_neg_24h
lactateraw_trend_neg_24h
troponin_iraw_trend_neg_24h
troponin_traw_trend_neg_24h
total_troponinraw_trend_neg_24h
amylaseraw_trend_neg_24h
lipaseraw_trend_neg_24h
plateletsraw_trend_neg_24h
hemoglobinraw_trend_neg_24h
phosphateraw_trend_neg_24h
pao2raw_trend_neg_24h
fio2raw_trend_neg_24h
cpkraw_trend_neg_24h
bnpraw_trend_neg_24h
fibrinogenraw_trend_neg_24h
neutrophilraw_trend_neg_24h
lymphocyteraw_trend_neg_24h
raw_sodiumraw_trend_neg_24h
raw_creatinineraw_trend_neg_24h
raw_bunraw_trend_neg_24h
raw_wbcraw_trend_neg_24h
raw_albuminraw_trend_neg_24h
raw_phraw_trend_neg_24h
raw_bilirubinraw_trend_neg_24h
raw_hctraw_trend_neg_24h
bicarbonateraw_trend_neg_48h
chlorideraw_trend_neg_48h
calciumraw_trend_neg_48h
magnesiumraw_trend_neg_48h
pt_inrraw_trend_neg_48h
hco3raw_trend_neg_48h
base_excessraw_trend_neg_48h
ionized_calciumraw_trend_neg_48h
lactateraw_trend_neg_48h
troponin_iraw_trend_neg_48h
troponin_traw_trend_neg_48h
total_troponinraw_trend_neg_48h
amylaseraw_trend_neg_48h
lipaseraw_trend_neg_48h
plateletsraw_trend_neg_48h
hemoglobinraw_trend_neg_48h
phosphateraw_trend_neg_48h
pao2raw_trend_neg_48h
fio2raw_trend_neg_48h
cpkraw_trend_neg_48h
bnpraw_trend_neg_48h
fibrinogenraw_trend_neg_48h
neutrophilraw_trend_neg_48h
lymphocyteraw_trend_neg_48h
raw_sodiumraw_trend_neg_48h
raw_creatinineraw_trend_neg_48h
raw_bunraw_trend_neg_48h
raw_wbcraw_trend_neg_48h
raw_albuminraw_trend_neg_48h
raw_phraw_trend_neg_48h
raw_bilirubinraw_trend_neg_48h
raw_hctraw_trend_neg_48h
bicarbonateraw_trend_pos_24h
chlorideraw_trend_pos_24h
calciumraw_trend_pos_24h
magnesiumraw_trend_pos_24h
pt_inrraw_trend_pos_24h
hco3raw_trend_pos_24h
base_excessraw_trend_pos_24h
ionized_calciumraw_trend_pos_24h
lactateraw_trend_pos_24h
troponin_iraw_trend_pos_24h
troponin_traw_trend_pos_24h
total_troponinraw_trend_pos_24h
amylaseraw_trend_pos_24h
lipaseraw_trend_pos_24h
plateletsraw_trend_pos_24h
hemoglobinraw_trend_pos_24h
phosphateraw_trend_pos_24h
pao2raw_trend_pos_24h
fio2raw_trend_pos_24h
cpkraw_trend_pos_24h
bnpraw_trend_pos_24h
fibrinogenraw_trend_pos_24h
neutrophilraw_trend_pos_24h
lymphocyteraw_trend_pos_24h
raw_sodiumraw_trend_pos_24h
raw_creatinineraw_trend_pos_24h
raw_bunraw_trend_pos_24h
raw_wbcraw_trend_pos_24h
raw_albuminraw_trend_pos_24h
raw_phraw_trend_pos_24h
raw_bilirubinraw_trend_pos_24h
raw_hctraw_trend_pos_24h
bicarbonateraw_trend_pos_48h
chlorideraw_trend_pos_48h
calciumraw_trend_pos_48h
magnesiumraw_trend_pos_48h
pt_inrraw_trend_pos_48h
hco3raw_trend_pos_48h
base_excessraw_trend_pos_48h
ionized_calciumraw_trend_pos_48h
lactateraw_trend_pos_48h
troponin_iraw_trend_pos_48h
troponin_traw_trend_pos_48h
total_troponinraw_trend_pos_48h
amylaseraw_trend_pos_48h
lipaseraw_trend_pos_48h
plateletsraw_trend_pos_48h
hemoglobinraw_trend_pos_48h
phosphateraw_trend_pos_48h
pao2raw_trend_pos_48h

fio2raw_trend_pos_48h
cpkraw_trend_pos_48h
bnpraw_trend_pos_48h
fibrinogenraw_trend_pos_48h
neutrophilraw_trend_pos_48h
lymphocyteraw_trend_pos_48h
raw_sodiumraw_trend_pos_48h
raw_creatinineraw_trend_pos_48h
raw_bunraw_trend_pos_48h
raw_wbcraw_trend_pos_48h
raw_albuminraw_trend_pos_48h
raw_phraw_trend_pos_48h
raw_bilirubinraw_trend_pos_48h
raw_hctraw_trend_pos_48h
bicarbonate_trend_neg_24h
chloride_trend_neg_24h
calcium_trend_neg_24h
magnesium_trend_neg_24h
pt_inr_trend_neg_24h
hco3_trend_neg_24h
base_excess_trend_neg_24h
ionized_calcium_trend_neg_24h
lactate_trend_neg_24h
troponin_i_trend_neg_24h
troponin_t_trend_neg_24h
total_troponin_trend_neg_24h
amylase_trend_neg_24h
lipase_trend_neg_24h
platelets_trend_neg_24h
hemoglobin_trend_neg_24h
phosphate_trend_neg_24h
pao2_trend_neg_24h
fio2_trend_neg_24h
cpk_trend_neg_24h
bnp_trend_neg_24h
fibrinogen_trend_neg_24h
neutrophil_trend_neg_24h
lymphocyte_trend_neg_24h
raw_sodium_trend_neg_24h
raw_creatinine_trend_neg_24h
raw_bun_trend_neg_24h
raw_wbc_trend_neg_24h
raw_albumin_trend_neg_24h
raw_ph_trend_neg_24h
raw_bilirubin_trend_neg_24h
raw_hct_trend_neg_24h
bicarbonate_trend_neg_48h
chloride_trend_neg_48h
calcium_trend_neg_48h
magnesium_trend_neg_48h
pt_inr_trend_neg_48h
hco3_trend_neg_48h
base_excess_trend_neg_48h
ionized_calcium_trend_neg_48h
lactate_trend_neg_48h
troponin_i_trend_neg_48h
troponin_t_trend_neg_48h
total_troponin_trend_neg_48h
amylase_trend_neg_48h
lipase_trend_neg_48h
platelets_trend_neg_48h
hemoglobin_trend_neg_48h
phosphate_trend_neg_48h
pao2_trend_neg_48h
fio2_trend_neg_48h
cpk_trend_neg_48h
bnp_trend_neg_48h
fibrinogen_trend_neg_48h
neutrophil_trend_neg_48h
lymphocyte_trend_neg_48h
raw_sodium_trend_neg_48h
raw_creatinine_trend_neg_48h
raw_bun_trend_neg_48h
raw_wbc_trend_neg_48h
raw_albumin_trend_neg_48h
raw_ph_trend_neg_48h
raw_bilirubin_trend_neg_48h
raw_hct_trend_neg_48h
bicarbonate_trend_neg_presence_24h
chloride_trend_neg_presence_24h
calcium_trend_neg_presence_24h
magnesium_trend_neg_presence_24h
pt_inr_trend_neg_presence_24h
hco3_trend_neg_presence_24h
base_excess_trend_neg_presence_24h
ionized_calcium_trend_neg_presence_24h
lactate_trend_neg_presence_24h
troponin_i_trend_neg_presence_24h
troponin_t_trend_neg_presence_24h
total_troponin_trend_neg_presence_24h
amylase_trend_neg_presence_24h
lipase_trend_neg_presence_24h
platelets_trend_neg_presence_24h
hemoglobin_trend_neg_presence_24h
phosphate_trend_neg_presence_24h
pao2_trend_neg_presence_24h
fio2_trend_neg_presence_24h
cpk_trend_neg_presence_24h
bnp_trend_neg_presence_24h
fibrinogen_trend_neg_presence_24h
neutrophil_trend_neg_presence_24h
lymphocyte_trend_neg_presence_24h
raw_sodium_trend_neg_presence_24h
raw_creatinine_trend_neg_presence_24h
raw_bun_trend_neg_presence_24h
raw_wbc_trend_neg_presence_24h
raw_albumin_trend_neg_presence_24h
raw_ph_trend_neg_presence_24h
raw_bilirubin_trend_neg_presence_24h
raw_hct_trend_neg_presence_24h
bicarbonate_trend_neg_presence_48h
chloride_trend_neg_presence_48h
calcium_trend_neg_presence_48h
magnesium_trend_neg_presence_48h
pt_inr_trend_neg_presence_48h
hco3_trend_neg_presence_48h
base_excess_trend_neg_presence_48h
ionized_calcium_trend_neg_presence_48h
lactate_trend_neg_presence_48h
troponin_i_trend_neg_presence_48h
troponin_t_trend_neg_presence_48h
total_troponin_trend_neg_presence_48h
amylase_trend_neg_presence_48h
lipase_trend_neg_presence_48h
platelets_trend_neg_presence_48h
hemoglobin_trend_neg_presence_48h
phosphate_trend_neg_presence_48h
pao2_trend_neg_presence_48h
fio2_trend_neg_presence_48h
cpk_trend_neg_presence_48h
bnp_trend_neg_presence_48h
fibrinogen_trend_neg_presence_48h
neutrophil_trend_neg_presence_48h
lymphocyte_trend_neg_presence_48h
raw_sodium_trend_neg_presence_48h
raw_creatinine_trend_neg_presence_48h
raw_bun_trend_neg_presence_48h
raw_wbc_trend_neg_presence_48h
raw_albumin_trend_neg_presence_48h
raw_ph_trend_neg_presence_48h
raw_bilirubin_trend_neg_presence_48h
raw_hct_trend_neg_presence_48h
bicarbonate_trend_pos_24h
chloride_trend_pos_24h
calcium_trend_pos_24h
magnesium_trend_pos_24h
pt_inr_trend_pos_24h
hco3_trend_pos_24h
base_excess_trend_pos_24h
ionized_calcium_trend_pos_24h
lactate_trend_pos_24h
troponin_i_trend_pos_24h
troponin_t_trend_pos_24h
total_troponin_trend_pos_24h
amylase_trend_pos_24h
lipase_trend_pos_24h
platelets_trend_pos_24h
hemoglobin_trend_pos_24h
phosphate_trend_pos_24h
pao2_trend_pos_24h

fio2_trend_pos_24h
cpk_trend_pos_24h
bnp_trend_pos_24h
fibrinogen_trend_pos_24h
neutrophil_trend_pos_24h
lymphocyte_trend_pos_24h
raw_sodium_trend_pos_24h
raw_creatinine_trend_pos_24h
raw_bun_trend_pos_24h
raw_wbc_trend_pos_24h
raw_albumin_trend_pos_24h
raw_ph_trend_pos_24h
raw_bilirubin_trend_pos_24h
raw_hct_trend_pos_24h
bicarbonate_trend_pos_48h
chloride_trend_pos_48h
calcium_trend_pos_48h
magnesium_trend_pos_48h
pt_inr_trend_pos_48h
hco3_trend_pos_48h
base_excess_trend_pos_48h
ionized_calcium_trend_pos_48h
lactate_trend_pos_48h
troponin_i_trend_pos_48h
troponin_t_trend_pos_48h
total_troponin_trend_pos_48h
amylase_trend_pos_48h
lipase_trend_pos_48h
platelets_trend_pos_48h
hemoglobin_trend_pos_48h
phosphate_trend_pos_48h
pao2_trend_pos_48h
fio2_trend_pos_48h
cpk_trend_pos_48h
bnp_trend_pos_48h
fibrinogen_trend_pos_48h
neutrophil_trend_pos_48h
lymphocyte_trend_pos_48h
raw_sodium_trend_pos_48h
raw_creatinine_trend_pos_48h
raw_bun_trend_pos_48h
raw_wbc_trend_pos_48h
raw_albumin_trend_pos_48h
raw_ph_trend_pos_48h
raw_bilirubin_trend_pos_48h
raw_hct_trend_pos_48h
bicarbonate_trend_pos_presence_24h
chloride_trend_pos_presence_24h
calcium_trend_pos_presence_24h
magnesium_trend_pos_presence_24h
pt_inr_trend_pos_presence_24h
hco3_trend_pos_presence_24h
base_excess_trend_pos_presence_24h
ionized_calcium_trend_pos_presence_24h
lactate_trend_pos_presence_24h
troponin_i_trend_pos_presence_24h
troponin_t_trend_pos_presence_24h
total_troponin_trend_pos_presence_24h
amylase_trend_pos_presence_24h
lipase_trend_pos_presence_24h
platelets_trend_pos_presence_24h
hemoglobin_trend_pos_presence_24h
phosphate_trend_pos_presence_24h
pao2_trend_pos_presence_24h
fio2_trend_pos_presence_24h
cpk_trend_pos_presence_24h
bnp_trend_pos_presence_24h
fibrinogen_trend_pos_presence_24h
neutrophil_trend_pos_presence_24h
lymphocyte_trend_pos_presence_24h
raw_sodium_trend_pos_presence_24h
raw_creatinine_trend_pos_presence_24h
raw_bun_trend_pos_presence_24h
raw_wbc_trend_pos_presence_24h
raw_albumin_trend_pos_presence_24h
raw_ph_trend_pos_presence_24h
raw_bilirubin_trend_pos_presence_24h
raw_hct_trend_pos_presence_24h
bicarbonate_trend_pos_presence_48h
chloride_trend_pos_presence_48h
calcium_trend_pos_presence_48h
magnesium_trend_pos_presence_48h
pt_inr_trend_pos_presence_48h
hco3_trend_pos_presence_48h
base_excess_trend_pos_presence_48h
ionized_calcium_trend_pos_presence_48h
lactate_trend_pos_presence_48h
troponin_i_trend_pos_presence_48h
troponin_t_trend_pos_presence_48h
total_troponin_trend_pos_presence_48h
amylase_trend_pos_presence_48h
lipase_trend_pos_presence_48h
platelets_trend_pos_presence_48h
hemoglobin_trend_pos_presence_48h
phosphate_trend_pos_presence_48h
pao2_trend_pos_presence_48h
fio2_trend_pos_presence_48h
cpk_trend_pos_presence_48h
bnp_trend_pos_presence_48h
fibrinogen_trend_pos_presence_48h
neutrophil_trend_pos_presence_48h
lymphocyte_trend_pos_presence_48h
raw_sodium_trend_pos_presence_48h
raw_creatinine_trend_pos_presence_48h
raw_bun_trend_pos_presence_48h
raw_wbc_trend_pos_presence_48h
raw_albumin_trend_pos_presence_48h
raw_ph_trend_pos_presence_48h
raw_bilirubin_trend_pos_presence_48h
raw_hct_trend_pos_presence_48h
bicarbonate_inverse_effect_24h
chloride_inverse_effect_24h
calcium_inverse_effect_24h
magnesium_inverse_effect_24h
pt_inr_inverse_effect_24h
hco3_inverse_effect_24h
base_excess_inverse_effect_24h
ionized_calcium_inverse_effect_24h
lactate_inverse_effect_24h
troponin_i_inverse_effect_24h
troponin_t_inverse_effect_24h
total_troponin_inverse_effect_24h
amylase_inverse_effect_24h
lipase_inverse_effect_24h
platelets_inverse_effect_24h
hemoglobin_inverse_effect_24h
phosphate_inverse_effect_24h
pao2_inverse_effect_24h
fio2_inverse_effect_24h
cpk_inverse_effect_24h
bnp_inverse_effect_24h
fibrinogen_inverse_effect_24h
neutrophil_inverse_effect_24h
lymphocyte_inverse_effect_24h
raw_sodium_inverse_effect_24h
raw_creatinine_inverse_effect_24h
raw_bun_inverse_effect_24h
raw_wbc_inverse_effect_24h
raw_albumin_inverse_effect_24h
raw_ph_inverse_effect_24h
raw_bilirubin_inverse_effect_24h
raw_hct_inverse_effect_24h
bicarbonate_inverse_effect_48h
chloride_inverse_effect_48h
calcium_inverse_effect_48h
magnesium_inverse_effect_48h
pt_inr_inverse_effect_48h
hco3_inverse_effect_48h
base_excess_inverse_effect_48h
ionized_calcium_inverse_effect_48h
lactate_inverse_effect_48h
troponin_i_inverse_effect_48h
troponin_t_inverse_effect_48h
total_troponin_inverse_effect_48h
amylase_inverse_effect_48h
lipase_inverse_effect_48h
platelets_inverse_effect_48h
hemoglobin_inverse_effect_48h
phosphate_inverse_effect_48h
pao2_inverse_effect_48h

fio2_inverse_effect_48h
cpk_inverse_effect_48h
bnp_inverse_effect_48h
fibrinogen_inverse_effect_48h
neutrophil_inverse_effect_48h
lymphocyte_inverse_effect_48h
raw_sodium_inverse_effect_48h
raw_creatinine_inverse_effect_48h
raw_bun_inverse_effect_48h
raw_wbc_inverse_effect_48h
raw_albumin_inverse_effect_48h
raw_ph_inverse_effect_48h
raw_bilirubin_inverse_effect_48h
raw_hct_inverse_effect_48h
bicarbonate_24h_is_abnormal
chloride_24h_is_abnormal
calcium_24h_is_abnormal
magnesium_24h_is_abnormal
pt_inr_24h_is_abnormal
hco3_24h_is_abnormal
base_excess_24h_is_abnormal
ionized_calcium_24h_is_abnormal
lactate_24h_is_abnormal
troponin_i_24h_is_abnormal
troponin_t_24h_is_abnormal
total_troponin_24h_is_abnormal
amylase_24h_is_abnormal
lipase_24h_is_abnormal
platelets_24h_is_abnormal
hemoglobin_24h_is_abnormal
phosphate_24h_is_abnormal
pao2_24h_is_abnormal
fio2_24h_is_abnormal
cpk_24h_is_abnormal
bnp_24h_is_abnormal
fibrinogen_24h_is_abnormal
neutrophil_24h_is_abnormal
lymphocyte_24h_is_abnormal
raw_sodium_24h_is_abnormal
raw_creatinine_24h_is_abnormal
raw_bun_24h_is_abnormal
raw_wbc_24h_is_abnormal
raw_albumin_24h_is_abnormal
raw_ph_24h_is_abnormal
raw_bilirubin_24h_is_abnormal
raw_hct_24h_is_abnormal
bicarbonate_48h_is_abnormal
chloride_48h_is_abnormal
calcium_48h_is_abnormal
magnesium_48h_is_abnormal
pt_inr_48h_is_abnormal
hco3_48h_is_abnormal
base_excess_48h_is_abnormal
ionized_calcium_48h_is_abnormal
lactate_48h_is_abnormal
troponin_i_48h_is_abnormal
troponin_t_48h_is_abnormal
total_troponin_48h_is_abnormal
amylase_48h_is_abnormal
lipase_48h_is_abnormal
platelets_48h_is_abnormal
hemoglobin_48h_is_abnormal
phosphate_48h_is_abnormal
pao2_48h_is_abnormal
fio2_48h_is_abnormal
cpk_48h_is_abnormal
bnp_48h_is_abnormal
fibrinogen_48h_is_abnormal
neutrophil_48h_is_abnormal
lymphocyte_48h_is_abnormal
raw_sodium_48h_is_abnormal
raw_creatinine_48h_is_abnormal
raw_bun_48h_is_abnormal
raw_wbc_48h_is_abnormal
raw_albumin_48h_is_abnormal
raw_ph_48h_is_abnormal
raw_bilirubin_48h_is_abnormal
raw_hct_48h_is_abnormal
bicarbonate_24h_is_low
chloride_24h_is_low
calcium_24h_is_low
magnesium_24h_is_low
pt_inr_24h_is_low
hco3_24h_is_low
base_excess_24h_is_low
ionized_calcium_24h_is_low
lactate_24h_is_low
troponin_i_24h_is_low
troponin_t_24h_is_low
total_troponin_24h_is_low
amylase_24h_is_low
lipase_24h_is_low
platelets_24h_is_low
hemoglobin_24h_is_low
phosphate_24h_is_low
pao2_24h_is_low
fio2_24h_is_low
cpk_24h_is_low
bnp_24h_is_low
fibrinogen_24h_is_low
neutrophil_24h_is_low
lymphocyte_24h_is_low
raw_sodium_24h_is_low
raw_creatinine_24h_is_low
raw_bun_24h_is_low
raw_wbc_24h_is_low
raw_albumin_24h_is_low
raw_ph_24h_is_low
raw_bilirubin_24h_is_low
raw_hct_24h_is_low
bicarbonate_48h_is_low
chloride_48h_is_low
calcium_48h_is_low
magnesium_48h_is_low
pt_inr_48h_is_low
hco3_48h_is_low
base_excess_48h_is_low
ionized_calcium_48h_is_low
lactate_48h_is_low
troponin_i_48h_is_low
troponin_t_48h_is_low
total_troponin_48h_is_low
amylase_48h_is_low
lipase_48h_is_low
platelets_48h_is_low
hemoglobin_48h_is_low
phosphate_48h_is_low
pao2_48h_is_low
fio2_48h_is_low
cpk_48h_is_low
bnp_48h_is_low
fibrinogen_48h_is_low
neutrophil_48h_is_low
lymphocyte_48h_is_low
raw_sodium_48h_is_low
raw_creatinine_48h_is_low
raw_bun_48h_is_low
raw_wbc_48h_is_low
raw_albumin_48h_is_low
raw_ph_48h_is_low
raw_bilirubin_48h_is_low
raw_hct_48h_is_low
bicarbonate_24h_is_low_by
chloride_24h_is_low_by
calcium_24h_is_low_by
magnesium_24h_is_low_by
pt_inr_24h_is_low_by
hco3_24h_is_low_by
base_excess_24h_is_low_by
ionized_calcium_24h_is_low_by
lactate_24h_is_low_by
troponin_i_24h_is_low_by
troponin_t_24h_is_low_by
total_troponin_24h_is_low_by
amylase_24h_is_low_by
lipase_24h_is_low_by
platelets_24h_is_low_by
hemoglobin_24h_is_low_by
phosphate_24h_is_low_by
pao2_24h_is_low_by

fio2_24h_is_low_by
cpk_24h_is_low_by
bnp_24h_is_low_by
fibrinogen_24h_is_low_by
neutrophil_24h_is_low_by
lymphocyte_24h_is_low_by
raw_sodium_24h_is_low_by
raw_creatinine_24h_is_low_by
raw_bun_24h_is_low_by
raw_wbc_24h_is_low_by
raw_albumin_24h_is_low_by
raw_ph_24h_is_low_by
raw_bilirubin_24h_is_low_by
raw_hct_24h_is_low_by
bicarbonate_48h_is_low_by
chloride_48h_is_low_by
calcium_48h_is_low_by
magnesium_48h_is_low_by
pt_inr_48h_is_low_by
hco3_48h_is_low_by
base_excess_48h_is_low_by
ionized_calcium_48h_is_low_by
lactate_48h_is_low_by
troponin_i_48h_is_low_by
troponin_t_48h_is_low_by
total_troponin_48h_is_low_by
amylase_48h_is_low_by
lipase_48h_is_low_by
platelets_48h_is_low_by
hemoglobin_48h_is_low_by
phosphate_48h_is_low_by
pao2_48h_is_low_by
fio2_48h_is_low_by
cpk_48h_is_low_by
bnp_48h_is_low_by
fibrinogen_48h_is_low_by
neutrophil_48h_is_low_by
lymphocyte_48h_is_low_by
raw_sodium_48h_is_low_by
raw_creatinine_48h_is_low_by
raw_bun_48h_is_low_by
raw_wbc_48h_is_low_by
raw_albumin_48h_is_low_by
raw_ph_48h_is_low_by
raw_bilirubin_48h_is_low_by
raw_hct_48h_is_low_by
bicarbonate_24h_is_high
chloride_24h_is_high
calcium_24h_is_high
magnesium_24h_is_high
pt_inr_24h_is_high
hco3_24h_is_high
base_excess_24h_is_high
ionized_calcium_24h_is_high
lactate_24h_is_high
troponin_i_24h_is_high
troponin_t_24h_is_high
total_troponin_24h_is_high
amylase_24h_is_high
lipase_24h_is_high
platelets_24h_is_high
hemoglobin_24h_is_high
phosphate_24h_is_high
pao2_24h_is_high
fio2_24h_is_high
cpk_24h_is_high
bnp_24h_is_high
fibrinogen_24h_is_high
neutrophil_24h_is_high
lymphocyte_24h_is_high
raw_sodium_24h_is_high
raw_creatinine_24h_is_high
raw_bun_24h_is_high
raw_wbc_24h_is_high
raw_albumin_24h_is_high
raw_ph_24h_is_high
raw_bilirubin_24h_is_high
raw_hct_24h_is_high
bicarbonate_48h_is_high
chloride_48h_is_high
calcium_48h_is_high
magnesium_48h_is_high
pt_inr_48h_is_high
hco3_48h_is_high
base_excess_48h_is_high
ionized_calcium_48h_is_high
lactate_48h_is_high
troponin_i_48h_is_high
troponin_t_48h_is_high
total_troponin_48h_is_high
amylase_48h_is_high
lipase_48h_is_high
platelets_48h_is_high
hemoglobin_48h_is_high
phosphate_48h_is_high
pao2_48h_is_high
fio2_48h_is_high
cpk_48h_is_high
bnp_48h_is_high
fibrinogen_48h_is_high
neutrophil_48h_is_high
lymphocyte_48h_is_high
raw_sodium_48h_is_high
raw_creatinine_48h_is_high
raw_bun_48h_is_high
raw_wbc_48h_is_high
raw_albumin_48h_is_high
raw_ph_48h_is_high
raw_bilirubin_48h_is_high
raw_hct_48h_is_high
bicarbonate_24h_is_high_by
chloride_24h_is_high_by
calcium_24h_is_high_by
magnesium_24h_is_high_by
pt_inr_24h_is_high_by
hco3_24h_is_high_by
base_excess_24h_is_high_by
ionized_calcium_24h_is_high_by
lactate_24h_is_high_by
troponin_i_24h_is_high_by
troponin_t_24h_is_high_by
total_troponin_24h_is_high_by
amylase_24h_is_high_by
lipase_24h_is_high_by
platelets_24h_is_high_by
hemoglobin_24h_is_high_by
phosphate_24h_is_high_by
pao2_24h_is_high_by
fio2_24h_is_high_by
cpk_24h_is_high_by
bnp_24h_is_high_by
fibrinogen_24h_is_high_by
neutrophil_24h_is_high_by
lymphocyte_24h_is_high_by
raw_sodium_24h_is_high_by
raw_creatinine_24h_is_high_by
raw_bun_24h_is_high_by
raw_wbc_24h_is_high_by
raw_albumin_24h_is_high_by
raw_ph_24h_is_high_by
raw_bilirubin_24h_is_high_by
raw_hct_24h_is_high_by
bicarbonate_48h_is_high_by
chloride_48h_is_high_by
calcium_48h_is_high_by
magnesium_48h_is_high_by
pt_inr_48h_is_high_by
hco3_48h_is_high_by
base_excess_48h_is_high_by
ionized_calcium_48h_is_high_by
lactate_48h_is_high_by
troponin_i_48h_is_high_by
troponin_t_48h_is_high_by
total_troponin_48h_is_high_by
amylase_48h_is_high_by
lipase_48h_is_high_by
platelets_48h_is_high_by
hemoglobin_48h_is_high_by
phosphate_48h_is_high_by
pao2_48h_is_high_by

fio2_48h_is_high_by
cpk_48h_is_high_by
bnp_48h_is_high_by
fibrinogen_48h_is_high_by
neutrophil_48h_is_high_by
lymphocyte_48h_is_high_by
raw_sodium_48h_is_high_by
raw_creatinine_48h_is_high_by
raw_bun_48h_is_high_by
raw_wbc_48h_is_high_by
raw_albumin_48h_is_high_by
raw_ph_48h_is_high_by
raw_bilirubin_48h_is_high_by
raw_hct_48h_is_high_by
charlson_mi
charlson_chf
charlson_peri
charlson_cvd
charlson_dementia
charlson_pul_dis
charlson_connective
charlson_peptic
charlson_mild_liver
charlson_diabetes_no_dam
charlson_hemiplegia
charlson_renal_disease
charlson_diabetes_dam
charlson_diabetes_dam.1
charlson_tumor_no_meta
charlson_leukemia
charlson_lymphoma
charlson_liv_disease
charlson_metastatic_tumor
charlson_aids
sedatives_bin_24h
vasopressors_bin_24h
antiarrythmics_bin_24h
lasixs_bin_24h
antibiotics_bin_24h
sedatives_bin_48h
vasopressors_bin_48h
antiarrythmics_bin_48h
lasixs_bin_48h
antibiotics_bin_48h
transfusion_24h
transfusion_plasma_24h
transfusion_cryo_24h
transfusion_blood_24h
transfusion_platelets_24h
transfusion_48h
transfusion_plasma_48h
transfusion_cryo_48h
transfusion_blood_48h
transfusion_platelets_48h
fluid_balance_24h
fluid_balance_48h
gender
height
weight
bmi
Med-Surg ICU
MICU
Cardiac ICU
SICU
CCU-CTICU
Neuro ICU
CTICU
Trauma ICU
Floating (Universal) License ICU
CSICU
Mixed Acuity
mv_fio2_24h
mv_fio2_48h
mv_plateau_pressure_24h
mv_plateau_pressure_48h
mv_peep_24h
mv_peep_48h
mv_tidal_volume_24h
mv_tidal_volume_48h
mv_tv_kg_24h
mv_tv_kg_48h
is_mv_24h
is_mv_48h
noninvasive_systolictime_scaled_slope_24h
noninvasive_diastolictime_scaled_slope_24h
noninvasive_systolictime_scaled_slope_48h
noninvasive_diastolictime_scaled_slope_48h
noninvasive_systolicraw_trend_neg_24h
noninvasive_diastolicraw_trend_neg_24h
noninvasive_systolicraw_trend_neg_48h
noninvasive_diastolicraw_trend_neg_48h
noninvasive_systolicraw_trend_pos_24h
noninvasive_diastolicraw_trend_pos_24h
noninvasive_systolicraw_trend_pos_48h
noninvasive_diastolicraw_trend_pos_48h
noninvasive_systolic_trend_neg_24h
noninvasive_diastolic_trend_neg_24h
noninvasive_systolic_trend_neg_48h
noninvasive_diastolic_trend_neg_48h
noninvasive_systolic_trend_neg_presence_24h
noninvasive_diastolic_trend_neg_presence_24h
noninvasive_systolic_trend_neg_presence_48h
noninvasive_diastolic_trend_neg_presence_48h
noninvasive_systolic_trend_pos_24h
noninvasive_diastolic_trend_pos_24h
noninvasive_systolic_trend_pos_48h
noninvasive_diastolic_trend_pos_48h
noninvasive_systolic_trend_pos_presence_24h
noninvasive_diastolic_trend_pos_presence_24h
noninvasive_systolic_trend_pos_presence_48h
noninvasive_diastolic_trend_pos_presence_48h
noninvasive_systolic_inverse_effect_24h
noninvasive_diastolic_inverse_effect_24h
noninvasive_systolic_inverse_effect_48h
noninvasive_diastolic_inverse_effect_48h
noninvasive_systolic_24h
noninvasive_diastolic_24h
noninvasive_systolic_48h
noninvasive_diastolic_48h
invasivesystolictime_scaled_slope_24h
invasivediastolictime_scaled_slope_24h
raw_sao2time_scaled_slope_24h
etco2time_scaled_slope_24h
raw_temperaturetime_scaled_slope_24h
raw_heartratetime_scaled_slope_24h
raw_respratetime_scaled_slope_24h
invasivesystolictime_scaled_slope_48h
invasivediastolictime_scaled_slope_48h
raw_sao2time_scaled_slope_48h
etco2time_scaled_slope_48h
raw_temperaturetime_scaled_slope_48h
raw_heartratetime_scaled_slope_48h
raw_respratetime_scaled_slope_48h
invasivesystolicraw_trend_neg_24h
invasivediastolicraw_trend_neg_24h
raw_sao2raw_trend_neg_24h
etco2raw_trend_neg_24h
raw_temperatureraw_trend_neg_24h
raw_heartrateraw_trend_neg_24h
raw_respraterаw_trend_neg_24h
invasivesystolicraw_trend_neg_48h
invasivediastolicraw_trend_neg_48h
raw_sao2raw_trend_neg_48h
etco2raw_trend_neg_48h
raw_temperatureraw_trend_neg_48h
raw_heartrateraw_trend_neg_48h
raw_respraterаw_trend_neg_48h
invasivesystolicraw_trend_pos_24h
invasivediastolicraw_trend_pos_24h
raw_sao2raw_trend_pos_24h
etco2raw_trend_pos_24h
raw_temperatureraw_trend_pos_24h
raw_heartrateraw_trend_pos_24h
raw_respraterаw_trend_pos_24h
invasivesystolicraw_trend_pos_48h
invasivediastolicraw_trend_pos_48h
raw_sao2raw_trend_pos_48h
etco2raw_trend_pos_48h
raw_temperatureraw_trend_pos_48h
raw_heartrateraw_trend_pos_48h

raw_resprateraw_trend_pos_48h
invasivesystolic_trend_neg_24h
invasivediastolic_trend_neg_24h
raw_sao2_trend_neg_24h
etco2_trend_neg_24h
raw_temperature_trend_neg_24h
raw_heartrate_trend_neg_24h
raw_resprate_trend_neg_24h
invasivesystolic_trend_neg_48h
invasivediastolic_trend_neg_48h
raw_sao2_trend_neg_48h
etco2_trend_neg_48h
raw_temperature_trend_neg_48h
raw_heartrate_trend_neg_48h
raw_resprate_trend_neg_48h
invasivesystolic_trend_neg_presence_24h
invasivediastolic_trend_neg_presence_24h
raw_sao2_trend_neg_presence_24h
etco2_trend_neg_presence_24h
raw_temperature_trend_neg_presence_24h
raw_heartrate_trend_neg_presence_24h
raw_resprate_trend_neg_presence_24h
invasivesystolic_trend_neg_presence_48h
invasivediastolic_trend_neg_presence_48h
raw_sao2_trend_neg_presence_48h
etco2_trend_neg_presence_48h
raw_temperature_trend_neg_presence_48h
raw_heartrate_trend_neg_presence_48h
raw_resprate_trend_neg_presence_48h
invasivesystolic_trend_pos_24h
invasivediastolic_trend_pos_24h
raw_sao2_trend_pos_24h
etco2_trend_pos_24h
raw_temperature_trend_pos_24h
raw_heartrate_trend_pos_24h
raw_resprate_trend_pos_24h
invasivesystolic_trend_pos_48h
invasivediastolic_trend_pos_48h
raw_sao2_trend_pos_48h
etco2_trend_pos_48h
raw_temperature_trend_pos_48h
raw_heartrate_trend_pos_48h
raw_resprate_trend_pos_48h
invasivesystolic_trend_pos_presence_24h
invasivediastolic_trend_pos_presence_24h
raw_sao2_trend_pos_presence_24h
etco2_trend_pos_presence_24h
raw_temperature_trend_pos_presence_24h
raw_heartrate_trend_pos_presence_24h
raw_resprate_trend_pos_presence_24h
invasivesystolic_trend_pos_presence_48h
invasivediastolic_trend_pos_presence_48h
raw_sao2_trend_pos_presence_48h
etco2_trend_pos_presence_48h
raw_temperature_trend_pos_presence_48h
raw_heartrate_trend_pos_presence_48h
raw_resprate_trend_pos_presence_48h
invasivesystolic_inverse_effect_24h
invasivediastolic_inverse_effect_24h
raw_sao2_inverse_effect_24h
etco2_inverse_effect_24h
raw_temperature_inverse_effect_24h
raw_heartrate_inverse_effect_24h
raw_resprate_inverse_effect_24h
invasivesystolic_inverse_effect_48h
invasivediastolic_inverse_effect_48h
raw_sao2_inverse_effect_48h
etco2_inverse_effect_48h
raw_temperature_inverse_effect_48h
raw_heartrate_inverse_effect_48h
raw_resprate_inverse_effect_48h
invasivesystolic_24h
invasivediastolic_24h
raw_sao2_24h
etco2_24h
raw_temperature_24h
raw_heartrate_24h
raw_resprate_24h
invasivesystolic_48h
invasivediastolic_48h
raw_sao2_48h
etco2_48h
raw_temperature_48h
raw_heartrate_48h
raw_resprate_48h

List of All Features Used in 24 Hour Feature Set

diag_AMI
diag_SEPSISPULM
diag_CHF
diag_CVASTROKE
diag_DKA
diag_S-CABG
diag_SEPSISUTI
diag_RHYTHATR
diag_PNEUMBACT
diag_CARDARREST
diag_EMPHYSBRON
diag_UNSTANGINA
diag_UGIBLEED
diag_COMA
diag_M-RESOTHER
diag_SEIZURES
diag_ICH
diag_RESPARREST
diag_SEPSISUNK
diag_LOWGIBLEED
diag_ARENFAIL
diag_UNKGIBLEED
diag_SEPSISGI
diag_HYPERTENS
diag_RHYTHCON
diag_S-CAROTEND
diag_PULMEMBOL
diag_S-VALVAO
diag_ODSEDHYP
diag_TRAUMHEAD
age
aids
hepaticfailure
lymphoma
metastaticcancer
leukemia
immunosuppression
cirrhosis
ventday1
admitsource_0
admitsource_1
admitsource_2
admitsource_3
admitsource_4
admitsource_5
admitsource_6
admitsource_7
admitsource_8
emergencysurg
preiculos
diagnosis
thrombolytics
unable_gcs
adj_gcs
pulse_aps
mabp_aps
temperature_aps
resp_aps
pao2_aps
hematocrit_aps
wbc_aps
creatinine_aps
urine_aps
bun_aps
sodium_aps
albumin_aps
bilirubin_aps
glucose_aps
acid_base_aps
gcs_aps
bicarbonate_24h
chloride_24h
calcium_24h
magnesium_24h
pt_inr_24h
hco3_24h
base_excess_24h
ionized_calcium_24h
lactate_24h
troponin_i_24h
troponin_t_24h
total_troponin_24h
amylase_24h
lipase_24h
platelets_24h
hemoglobin_24h
phosphate_24h
pao2_24h
fio2_24h
cpk_24h
bnp_24h
fibrinogen_24h
neutrophil_24h
lymphocyte_24h
raw_sodium_24h
raw_creatinine_24h
raw_bun_24h
raw_wbc_24h
raw_albumin_24h
raw_ph_24h
raw_bilirubin_24h
raw_hct_24h
bicarbonatetime_scaled_slope_24h
chloridetime_scaled_slope_24h
calciumtime_scaled_slope_24h
magnesiumtime_scaled_slope_24h
pt_inrtime_scaled_slope_24h
hco3time_scaled_slope_24h
base_excesstime_scaled_slope_24h
ionized_calciumtime_scaled_slope_24h
lactatetime_scaled_slope_24h
troponin_itime_scaled_slope_24h
troponin_ttime_scaled_slope_24h
total_troponintime_scaled_slope_24h
amylasetime_scaled_slope_24h
lipasetime_scaled_slope_24h
plateletstime_scaled_slope_24h
hemoglobintime_scaled_slope_24h
phosphatetime_scaled_slope_24h
pao2time_scaled_slope_24h
fio2time_scaled_slope_24h
cpktime_scaled_slope_24h
bnptime_scaled_slope_24h
fibrinogentime_scaled_slope_24h
neutrophiltime_scaled_slope_24h
lymphocytetime_scaled_slope_24h
raw_sodiumtime_scaled_slope_24h
raw_creatininetime_scaled_slope_24h
raw_buntime_scaled_slope_24h
raw_wbctime_scaled_slope_24h
raw_albumintime_scaled_slope_24h
raw_phtime_scaled_slope_24h
raw_bilirubintime_scaled_slope_24h
raw_hcttime_scaled_slope_24h
bicarbonateraw_trend_neg_24h
chlorideraw_trend_neg_24h
calciumraw_trend_neg_24h
magnesiumraw_trend_neg_24h
pt_inrraw_trend_neg_24h
hco3raw_trend_neg_24h
base_excessraw_trend_neg_24h
ionized_calciumraw_trend_neg_24h
lactateraw_trend_neg_24h
troponin_iraw_trend_neg_24h
troponin_traw_trend_neg_24h
total_troponinraw_trend_neg_24h
amylaseraw_trend_neg_24h
lipaseraw_trend_neg_24h
plateletsraw_trend_neg_24h
hemoglobinraw_trend_neg_24h
phosphateraw_trend_neg_24h
pao2raw_trend_neg_24h

fio2raw_trend_neg_24h
cpkraw_trend_neg_24h
bnpraw_trend_neg_24h
fibrinogenraw_trend_neg_24h
neutrophilraw_trend_neg_24h
lymphocyteraw_trend_neg_24h
raw_sodiumraw_trend_neg_24h
raw_creatinineraw_trend_neg_24h
raw_bunraw_trend_neg_24h
raw_wbcraw_trend_neg_24h
raw_albuminraw_trend_neg_24h
raw_phraw_trend_neg_24h
raw_bilirubinraw_trend_neg_24h
raw_hctraw_trend_neg_24h
bicarbonateraw_trend_pos_24h
chlorideraw_trend_pos_24h
calciumraw_trend_pos_24h
magnesiumraw_trend_pos_24h
pt_inrraw_trend_pos_24h
hco3raw_trend_pos_24h
base_excessraw_trend_pos_24h
ionized_calciumraw_trend_pos_24h
lactateraw_trend_pos_24h
troponin_iraw_trend_pos_24h
troponin_traw_trend_pos_24h
total_troponinraw_trend_pos_24h
amylaseraw_trend_pos_24h
lipaseraw_trend_pos_24h
plateletsraw_trend_pos_24h
hemoglobinraw_trend_pos_24h
phosphateraw_trend_pos_24h
pao2raw_trend_pos_24h
fio2raw_trend_pos_24h
cpkraw_trend_pos_24h
bnpraw_trend_pos_24h
fibrinogenraw_trend_pos_24h
neutrophilraw_trend_pos_24h
lymphocyteraw_trend_pos_24h
raw_sodiumraw_trend_pos_24h
raw_creatinineraw_trend_pos_24h
raw_bunraw_trend_pos_24h
raw_wbcraw_trend_pos_24h
raw_albuminraw_trend_pos_24h
raw_phraw_trend_pos_24h
raw_bilirubinraw_trend_pos_24h
raw_hctraw_trend_pos_24h
bicarbonate_trend_neg_24h
chloride_trend_neg_24h
calcium_trend_neg_24h
magnesium_trend_neg_24h
pt_inr_trend_neg_24h
hco3_trend_neg_24h
base_excess_trend_neg_24h
ionized_calcium_trend_neg_24h
lactate_trend_neg_24h
troponin_i_trend_neg_24h
troponin_t_trend_neg_24h
total_troponin_trend_neg_24h
amylase_trend_neg_24h
lipase_trend_neg_24h
platelets_trend_neg_24h
hemoglobin_trend_neg_24h
phosphate_trend_neg_24h
pao2_trend_neg_24h
fio2_trend_neg_24h
cpk_trend_neg_24h
bnp_trend_neg_24h
fibrinogen_trend_neg_24h
neutrophil_trend_neg_24h
lymphocyte_trend_neg_24h
raw_sodium_trend_neg_24h
raw_creatinine_trend_neg_24h
raw_bun_trend_neg_24h
raw_wbc_trend_neg_24h
raw_albumin_trend_neg_24h
raw_ph_trend_neg_24h
raw_bilirubin_trend_neg_24h
raw_hct_trend_neg_24h
bicarbonate_trend_neg_presence_24h
chloride_trend_neg_presence_24h
calcium_trend_neg_presence_24h
magnesium_trend_neg_presence_24h
pt_inr_trend_neg_presence_24h
hco3_trend_neg_presence_24h
base_excess_trend_neg_presence_24h
ionized_calcium_trend_neg_presence_24h
lactate_trend_neg_presence_24h
troponin_i_trend_neg_presence_24h
troponin_t_trend_neg_presence_24h
total_troponin_trend_neg_presence_24h
amylase_trend_neg_presence_24h
lipase_trend_neg_presence_24h
platelets_trend_neg_presence_24h
hemoglobin_trend_neg_presence_24h
phosphate_trend_neg_presence_24h
pao2_trend_neg_presence_24h
fio2_trend_neg_presence_24h
cpk_trend_neg_presence_24h
bnp_trend_neg_presence_24h
fibrinogen_trend_neg_presence_24h
neutrophil_trend_neg_presence_24h
lymphocyte_trend_neg_presence_24h
raw_sodium_trend_neg_presence_24h
raw_creatinine_trend_neg_presence_24h
raw_bun_trend_neg_presence_24h
raw_wbc_trend_neg_presence_24h
raw_albumin_trend_neg_presence_24h
raw_ph_trend_neg_presence_24h
raw_bilirubin_trend_neg_presence_24h
raw_hct_trend_neg_presence_24h
bicarbonate_trend_pos_24h
chloride_trend_pos_24h
calcium_trend_pos_24h
magnesium_trend_pos_24h
pt_inr_trend_pos_24h
hco3_trend_pos_24h
base_excess_trend_pos_24h
ionized_calcium_trend_pos_24h
lactate_trend_pos_24h
troponin_i_trend_pos_24h
troponin_t_trend_pos_24h
total_troponin_trend_pos_24h
amylase_trend_pos_24h
lipase_trend_pos_24h
platelets_trend_pos_24h
hemoglobin_trend_pos_24h
phosphate_trend_pos_24h
pao2_trend_pos_24h
fio2_trend_pos_24h
cpk_trend_pos_24h
bnp_trend_pos_24h
fibrinogen_trend_pos_24h
neutrophil_trend_pos_24h
lymphocyte_trend_pos_24h
raw_sodium_trend_pos_24h
raw_creatinine_trend_pos_24h
raw_bun_trend_pos_24h
raw_wbc_trend_pos_24h
raw_albumin_trend_pos_24h
raw_ph_trend_pos_24h
raw_bilirubin_trend_pos_24h
raw_hct_trend_pos_24h
bicarbonate_trend_pos_presence_24h
chloride_trend_pos_presence_24h
calcium_trend_pos_presence_24h
magnesium_trend_pos_presence_24h
pt_inr_trend_pos_presence_24h
hco3_trend_pos_presence_24h
base_excess_trend_pos_presence_24h
ionized_calcium_trend_pos_presence_24h
lactate_trend_pos_presence_24h
troponin_i_trend_pos_presence_24h
troponin_t_trend_pos_presence_24h
total_troponin_trend_pos_presence_24h
amylase_trend_pos_presence_24h
lipase_trend_pos_presence_24h
platelets_trend_pos_presence_24h
hemoglobin_trend_pos_presence_24h
phosphate_trend_pos_presence_24h
pao2_trend_pos_presence_24h

fio2_trend_pos_presence_24h
cpk_trend_pos_presence_24h
bnp_trend_pos_presence_24h
fibrinogen_trend_pos_presence_24h
neutrophil_trend_pos_presence_24h
lymphocyte_trend_pos_presence_24h
raw_sodium_trend_pos_presence_24h
raw_creatinine_trend_pos_presence_24h
raw_bun_trend_pos_presence_24h
raw_wbc_trend_pos_presence_24h
raw_albumin_trend_pos_presence_24h
raw_ph_trend_pos_presence_24h
raw_bilirubin_trend_pos_presence_24h
raw_hct_trend_pos_presence_24h
bicarbonate_inverse_effect_24h
chloride_inverse_effect_24h
calcium_inverse_effect_24h
magnesium_inverse_effect_24h
pt_inr_inverse_effect_24h
hco3_inverse_effect_24h
base_excess_inverse_effect_24h
ionized_calcium_inverse_effect_24h
lactate_inverse_effect_24h
troponin_i_inverse_effect_24h
troponin_t_inverse_effect_24h
total_troponin_inverse_effect_24h
amylase_inverse_effect_24h
lipase_inverse_effect_24h
platelets_inverse_effect_24h
hemoglobin_inverse_effect_24h
phosphate_inverse_effect_24h
pao2_inverse_effect_24h
fio2_inverse_effect_24h
cpk_inverse_effect_24h
bnp_inverse_effect_24h
fibrinogen_inverse_effect_24h
neutrophil_inverse_effect_24h
lymphocyte_inverse_effect_24h
raw_sodium_inverse_effect_24h
raw_creatinine_inverse_effect_24h
raw_bun_inverse_effect_24h
raw_wbc_inverse_effect_24h
raw_albumin_inverse_effect_24h
raw_ph_inverse_effect_24h
raw_bilirubin_inverse_effect_24h
raw_hct_inverse_effect_24h
bicarbonate_24h_is_abnormal
chloride_24h_is_abnormal
calcium_24h_is_abnormal
magnesium_24h_is_abnormal
pt_inr_24h_is_abnormal
hco3_24h_is_abnormal
base_excess_24h_is_abnormal
ionized_calcium_24h_is_abnormal
lactate_24h_is_abnormal
troponin_i_24h_is_abnormal
troponin_t_24h_is_abnormal
total_troponin_24h_is_abnormal
amylase_24h_is_abnormal
lipase_24h_is_abnormal
platelets_24h_is_abnormal
hemoglobin_24h_is_abnormal
phosphate_24h_is_abnormal
pao2_24h_is_abnormal
fio2_24h_is_abnormal
cpk_24h_is_abnormal
bnp_24h_is_abnormal
fibrinogen_24h_is_abnormal
neutrophil_24h_is_abnormal
lymphocyte_24h_is_abnormal
raw_sodium_24h_is_abnormal
raw_creatinine_24h_is_abnormal
raw_bun_24h_is_abnormal
raw_wbc_24h_is_abnormal
raw_albumin_24h_is_abnormal
raw_ph_24h_is_abnormal
raw_bilirubin_24h_is_abnormal
raw_hct_24h_is_abnormal
bicarbonate_24h_is_low
chloride_24h_is_low
calcium_24h_is_low
magnesium_24h_is_low
pt_inr_24h_is_low
hco3_24h_is_low
base_excess_24h_is_low
ionized_calcium_24h_is_low
lactate_24h_is_low
troponin_i_24h_is_low
troponin_t_24h_is_low
total_troponin_24h_is_low
amylase_24h_is_low
lipase_24h_is_low
platelets_24h_is_low
hemoglobin_24h_is_low
phosphate_24h_is_low
pao2_24h_is_low
fio2_24h_is_low
cpk_24h_is_low
bnp_24h_is_low
fibrinogen_24h_is_low
neutrophil_24h_is_low
lymphocyte_24h_is_low
raw_sodium_24h_is_low
raw_creatinine_24h_is_low
raw_bun_24h_is_low
raw_wbc_24h_is_low
raw_albumin_24h_is_low
raw_ph_24h_is_low
raw_bilirubin_24h_is_low
raw_hct_24h_is_low
bicarbonate_24h_is_low_by
chloride_24h_is_low_by
calcium_24h_is_low_by
magnesium_24h_is_low_by
pt_inr_24h_is_low_by
hco3_24h_is_low_by
base_excess_24h_is_low_by
ionized_calcium_24h_is_low_by
lactate_24h_is_low_by
troponin_i_24h_is_low_by
troponin_t_24h_is_low_by
total_troponin_24h_is_low_by
amylase_24h_is_low_by
lipase_24h_is_low_by
platelets_24h_is_low_by
hemoglobin_24h_is_low_by
phosphate_24h_is_low_by
pao2_24h_is_low_by
fio2_24h_is_low_by
cpk_24h_is_low_by
bnp_24h_is_low_by
fibrinogen_24h_is_low_by
neutrophil_24h_is_low_by
lymphocyte_24h_is_low_by
raw_sodium_24h_is_low_by
raw_creatinine_24h_is_low_by
raw_bun_24h_is_low_by
raw_wbc_24h_is_low_by
raw_albumin_24h_is_low_by
raw_ph_24h_is_low_by
raw_bilirubin_24h_is_low_by
raw_hct_24h_is_low_by
bicarbonate_24h_is_high
chloride_24h_is_high
calcium_24h_is_high
magnesium_24h_is_high
pt_inr_24h_is_high
hco3_24h_is_high
base_excess_24h_is_high
ionized_calcium_24h_is_high
lactate_24h_is_high
troponin_i_24h_is_high
troponin_t_24h_is_high
total_troponin_24h_is_high
amylase_24h_is_high
lipase_24h_is_high
platelets_24h_is_high
hemoglobin_24h_is_high
phosphate_24h_is_high
pao2_24h_is_high

fio2_24h_is_high
cpk_24h_is_high
bnp_24h_is_high
fibrinogen_24h_is_high
neutrophil_24h_is_high
lymphocyte_24h_is_high
raw_sodium_24h_is_high
raw_creatinine_24h_is_high
raw_bun_24h_is_high
raw_wbc_24h_is_high
raw_albumin_24h_is_high
raw_ph_24h_is_high
raw_bilirubin_24h_is_high
raw_hct_24h_is_high
bicarbonate_24h_is_high_by
chloride_24h_is_high_by
calcium_24h_is_high_by
magnesium_24h_is_high_by
pt_inr_24h_is_high_by
hco3_24h_is_high_by
base_excess_24h_is_high_by
ionized_calcium_24h_is_high_by
lactate_24h_is_high_by
troponin_i_24h_is_high_by
troponin_t_24h_is_high_by
total_troponin_24h_is_high_by
amylase_24h_is_high_by
lipase_24h_is_high_by
platelets_24h_is_high_by
hemoglobin_24h_is_high_by
phosphate_24h_is_high_by
pao2_24h_is_high_by
fio2_24h_is_high_by
cpk_24h_is_high_by
bnp_24h_is_high_by
fibrinogen_24h_is_high_by
neutrophil_24h_is_high_by
lymphocyte_24h_is_high_by
raw_sodium_24h_is_high_by
raw_creatinine_24h_is_high_by
raw_bun_24h_is_high_by
raw_wbc_24h_is_high_by
raw_albumin_24h_is_high_by
raw_ph_24h_is_high_by
raw_bilirubin_24h_is_high_by
raw_hct_24h_is_high_by
charlson_mi
charlson_chf
charlson_peri
charlson_mi.1
charlson_chf.1
charlson_peri.1
charlson_cvd
charlson_dementia
charlson_pul_dis
charlson_connective
charlson_peptic
charlson_mild_liver
charlson_diabetes_no_dam
charlson_hemiplegia
charlson_renal_disease
charlson_diabetes_dam
charlson_diabetes_dam.1
charlson_tumor_no_meta
charlson_leukemia
charlson_lymphoma
charlson_liv_disease
charlson_metastatic_tumor
charlson_aids
sedatives_bin_24h
vasopressors_bin_24h
antiarrythmics_bin_24h
lasixs_bin_24h
antibiotics_bin_24h
transfusion_24h
transfusion_plasma_24h
transfusion_cryo_24h
transfusion_blood_24h
transfusion_platelets_24h
fluid_balance_24h
gender
height
weight
bmi
Med-Surg ICU
MICU
Cardiac ICU
SICU
CCU-CTICU
Neuro ICU
CTICU
Trauma ICU
Floating (Universal) License ICU
CSICU
Mixed Acuity
mv_fio2_24h
mv_plateau_pressure_24h
mv_peep_24h
mv_tidal_volume_24h
mv_tv_kg_24h
is_mv_24h
noninvasive_systolictime_scaled_slope_24h
noninvasive_diastolictime_scaled_slope_24h
noninvasive_systolicraw_trend_neg_24h
noninvasive_diastolicraw_trend_neg_24h
noninvasive_systolicraw_trend_pos_24h
noninvasive_diastolicraw_trend_pos_24h
noninvasive_systolic_trend_neg_24h
noninvasive_diastolic_trend_neg_24h
noninvasive_systolic_trend_neg_presence_24h
noninvasive_diastolic_trend_neg_presence_24h
noninvasive_systolic_trend_pos_24h
noninvasive_diastolic_trend_pos_24h
noninvasive_systolic_trend_pos_presence_24h
noninvasive_diastolic_trend_pos_presence_24h
noninvasive_systolic_inverse_effect_24h
noninvasive_diastolic_inverse_effect_24h
noninvasive_systolic_24h
noninvasive_diastolic_24h
invasivesystolictime_scaled_slope_24h
invasivediastolictime_scaled_slope_24h
raw_sao2time_scaled_slope_24h
etco2time_scaled_slope_24h
raw_temperaturetime_scaled_slope_24h
raw_heartratetime_scaled_slope_24h
raw_respratetime_scaled_slope_24h
invasivesystolicraw_trend_neg_24h
invasivediastolicraw_trend_neg_24h
raw_sao2raw_trend_neg_24h
etco2raw_trend_neg_24h
raw_temperatureraw_trend_neg_24h
raw_heartrateraw_trend_neg_24h
raw_resprateraw_trend_neg_24h
invasivesystolicraw_trend_pos_24h
invasivediastolicraw_trend_pos_24h
raw_sao2raw_trend_pos_24h
etco2raw_trend_pos_24h
raw_temperatureraw_trend_pos_24h
raw_heartrateraw_trend_pos_24h
raw_resprateraw_trend_pos_24h
invasivesystolic_trend_neg_24h
invasivediastolic_trend_neg_24h
raw_sao2_trend_neg_24h
etco2_trend_neg_24h
raw_temperature_trend_neg_24h
raw_heartrate_trend_neg_24h
raw_resprate_trend_neg_24h
invasivesystolic_trend_neg_presence_24h
invasivediastolic_trend_neg_presence_24h
raw_sao2_trend_neg_presence_24h
etco2_trend_neg_presence_24h
raw_temperature_trend_neg_presence_24h
raw_heartrate_trend_neg_presence_24h
raw_resprate_trend_neg_presence_24h
invasivesystolic_trend_pos_24h
invasivediastolic_trend_pos_24h
raw_sao2_trend_pos_24h
etco2_trend_pos_24h
raw_temperature_trend_pos_24h
raw_heartrate_trend_pos_24h

raw_resprate_trend_pos_24h
invasivesystolic_trend_pos_presence_24h
invasivediastolic_trend_pos_presence_24h
raw_sao2_trend_pos_presence_24h
etco2_trend_pos_presence_24h
raw_temperature_trend_pos_presence_24h
raw_heartrate_trend_pos_presence_24h
raw_resprate_trend_pos_presence_24h
invasivesystolic_inverse_effect_24h
invasivediastolic_inverse_effect_24h
raw_sao2_inverse_effect_24h
etco2_inverse_effect_24h
raw_temperature_inverse_effect_24h
raw_heartrate_inverse_effect_24h
raw_resprate_inverse_effect_24h
invasivesystolic_24h
invasivediastolic_24h
raw_sao2_24h
etco2_24h
raw_temperature_24h
raw_heartrate_24h
raw_resprate_24h